

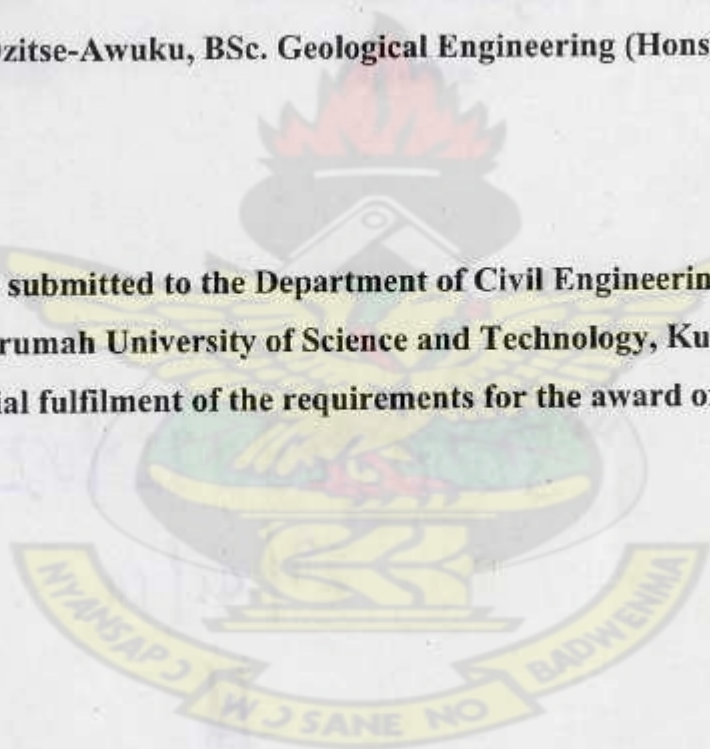
CORRELATION BETWEEN DYNAMIC CONE PENETROMETER (n-VALUE) AND ALLOWABLE BEARING PRESSURE OF SHALLOW FOUNDATION USING MODEL FOOTING

By

KNUST

David Dzitse-Awuku, BSc. Geological Engineering (Hons).

**A Thesis submitted to the Department of Civil Engineering,
Kwame Nkrumah University of Science and Technology, Kumasi
in partial fulfilment of the requirements for the award of**



Master of Philosophy

**Faculty of Civil and Geomatic Engineering
College of Engineering**

May, 2008

DECLARATION

I hereby declare that this submission is my own work towards the MPhil in Civil Engineering and that , to the best of my knowledge, it contains no material previously published by another person nor material which has been accepted for the award of any other degree of the University , except where due acknowledgment has been made in the text.

David Dzitse-Awuku



28/07/2008

INDEX NO. 82001-05

Signature

Date

Certify by:

.....



28/07/2008

Dr. S.I.K. Ampadu

Signature

Date

Certify by:

.....



28/07/2008

Signature

Date

ACKNOWLEDGMENT

and grateful to the LORD ALMIGHTY GOD for making it possible for me to complete this research project in my life.

My sincere appreciation goes to my Lead Supervisor, Dr. S.K. ... and my Second Supervisor Dr. ... for their guidance and cooperation during the project and their support in the successful completion of this work.

DEDICATION

I dedicate this work to my late mother

ESTHER AFI ADEKPO

of blessed memory who can not see the successful end of this work

**L. BRARY
AWAME NKRUMAH UNIVERSITY OF
SCIENCE AND TECHNOLOGY
KUMASI-GHANA**

ACKNOWLEDGMENT

I am grateful to the LORD ALMIGHTY GOD for making it possible for me to complete this landmark project in my life.

My sincere appreciation first and foremost goes to my Lead Supervisor, Dr. S.I.K. Ampadu for his guidance in selection of the topic, assistance and cooperation during difficult times of the project and then to my Second Supervisor Dr. Yaw A. Tuffour for his contribution towards the success of this project.

Secondly, I am grateful to Mr. Edward S. Nyamekye, my Head of Department (Geotechnical) - Architectural & Engineering Services Limited (A.E.S.L.) for not refusing me the opportunity when I decided to pursue this project and then to Joseph K. Oddei, a colleague Engineer at Geotechnical Department of AESL- for his support.

My next thanks goes to Mr. Gilbert Fiadzoc, the Geotechnical Laboratory Assistant, KNUST for his invaluable assistance in the laboratory and many others on campus especially the Second batch students of the Roads and Transportation Engineering Program and the lecturers and Mr. Michael Kwaw Nyarku alias Sir Integral of Materials Engineering Department, KNUST for their various supports accorded me. Also to many others whose names I would not attempt to catalogue here, I say, God Bless you.

Finally, my profound gratitude goes to my dear wife, son and siblings for their numerous help and encouragements.

ABSTRACT

An allowable bearing pressure is one of the most important basic parameters to be determined before the design and construction of foundations for civil engineering structures. The conventional methods of estimating this parameter is becoming relatively expensive and time consuming for small scale projects such as residential buildings.

The DCP is a versatile equipment that may be applied to obtain the bearing capacity. However, currently, there are no reliable correlations between the DCP test results and the bearing capacity. This project was undertaken to develop a reliable correlation between the Dynamic Cone Penetrometer (DCP) n -value (blows/100mm) and the allowable bearing pressure q_{all} (kN/m^2) for shallow foundations using a model footing. In this work, compacted soil sample of different dry densities in a mould was loaded with a model footing until the sample yielded. On the same sample, DCP testing was performed at two locations to determine the average D -value (mm/blow). Triaxial samples were also taken for triaxial test. Results from the triaxial test were used to calculate ultimate bearing capacity using Terzaghi bearing equation. The measured DCP D -value (mm/blow) was processed into n -value (blows/100mm) which is the standard form of recording the DCP test results in the field. The results were analysed and a correlation $q_{all}=48n + 57$, with a coefficient of correlation, $R^2=0.98$ was obtained for the model footing. This correlation was similar to the correlation between the n -value and the allowable bearing pressure computed using the Terzaghi approach, except that the Model underestimated the allowable bearing pressure by a constant value of 165 kN/m^2 for all values of n .

TABLE OF CONTENTS

Content	Page
DECLARATION	ii
DEDICATION	iii
ACKNOWLEDGMENT	iv
ABSTRACT	v
TABLE OF CONTENTS	vi
LIST OF ILLUSTRATIONS	ix
List of Figures	ix
List of Tables	xi
List of Symbols and Abbreviations	xii
 CHAPTER ONE	 1
INTRODUCTION	1
1.1 Background	1
1.2 Objective	2
1.3 Justification	2
1.4 Scope of Work	3
 CHAPTER TWO	 4
LITERATURE REVIEW	4
2.1 Introduction	4
2.2 The Pocket Penetrometer	4
2.3 The Cone Penetrometer Test	5
2.3.1 Applications	7
2.4 The Standard Penetration Test	8
2.4.1 SPT Correlations	10
2.5 Historical Development of DCP	12
2.6 The Dynamic Cone Penetrometer	14

2.6.1	Development of Semi-Empirical Equations	15
2.6.2	Previous Works	18
2.6.3	Empirical DCP Test and Strength Correlations	19
2.6.4	Capabilities of the DCP	20
2.6.5	Limitations of the DCP	21
2.7	Bearing Capacity of Shallow Foundations	22
2.7.1	Factors Affecting Bearing Capacity of Shallow Foundations	22
2.7.2	Terzaghi Ultimate Bearing Capacity Equation	22
2.7.3	Modes of Foundation Failures	25
2.7.4	General Shear Failure	25
2.7.5	Local Shear Failure	26
2.7.6	Punching Shear Failure	27
2.7.7	Scale Effect in Model Test	28
CHAPTER THREE		30
METHODOLOGY		30
3.1	The Fieldwork	30
3.2	The Laboratory Work	30
3.2.1	Sample Preparation	30
3.2.2	Sample Characterisation	30
3.3	Model Test Set-Up	31
3.3.1	The Perspex Mould and Wooden Footing	31
3.3.2	Loading and Measuring System	32
3.4	Model Sample Preparation	33
3.5	The Model Testing Procedure	35
3.6	DCP Test	36
3.6.1	Equipment	36
3.6.2	Test Procedure	37
3.7	Triaxial Test	38

LIBRARY
KWAME NKRUMAH UNIVERSITY OF
SCIENCE AND TECHNOLOGY
KUMASI-SHANA

CHAPTER FOUR	39
RESULTS ANALYSIS AND DISCUSSIONS	39
4.1 Materials Properties	39
4.2 In Mould Model Soil Characteristics	41
4.3 The Loading Test	43
4.3.1 Failure Mode	43
4.3.2 Yield Stress Criterion	43
4.3.3 Model Footing Test Results	44
4.4 DCP Test Results	49
4.5 Allowable Bearing Pressure from Triaxial Test	52
4.5.1 Allowable Bearing Pressure	54
4.6 Correlation between D-value, n-value and Allowable Bearing Pressure	56
4.7 Calibration of the Model	58
4.8 Comparison of the Model to Similar Works	58
CHAPTER FIVE	60
CONCLUSIONS AND RECOMMENDATIONS	60
5.1 Conclusions	60
5.2 Recommendations	61
REFERENCES	62
APPENDICES	
Appendix A: List of Figures	63
Appendix B: List of Tables	64
Appendix C: List of Equations	65
Appendix D: List of Symbols	66
Appendix E: List of Abbreviations	67
Appendix F: List of References	68
Appendix G: List of Figures	69
Appendix H: List of Tables	70
Appendix I: List of Equations	71
Appendix J: List of Symbols	72
Appendix K: List of Abbreviations	73
Appendix L: List of References	74
Appendix M: List of Figures	75
Appendix N: List of Tables	76
Appendix O: List of Equations	77
Appendix P: List of Symbols	78
Appendix Q: List of Abbreviations	79
Appendix R: List of References	80
Appendix S: List of Figures	81
Appendix T: List of Tables	82
Appendix U: List of Equations	83
Appendix V: List of Symbols	84
Appendix W: List of Abbreviations	85
Appendix X: List of References	86
Appendix Y: List of Figures	87
Appendix Z: List of Tables	88

LIST OF ILLUSTRATIONS

List of Figures

Figure 2.1	Pocket Penetrometer	5
Figure 2.2	Cone Penetration Tip	6
Figure 2.3	Typical Operation of the SPT	9
Figure 2.4	Split Spoon Sampler	9
Figure 2.5	Relationship between ϕ , N_q and N_γ with SPT N-values	10
Figure 2.6	Relationship between SPT N-values and Allowable Bearing Pressure	11
Figure 2.7	Correlations between Unconfined Compressive Strength and SPT N-values, for clays	12
Figure 2.8	General Shear Failure Pattern	23
Figure 2.9	Failure Mode Chart	25
Figure 2.10a	General Shear Failure of Soil	26
Figure 2.10b	Typical Stress-Settlement Graph of General Shear Failure	26
Figure 2.11a	Local shear Failure of Soil	27
Figure 2.11b	Typical Stress-Settlement Graph of Local Shear Failure	27
Figure 2.12a	Punching Shear Failure	28
Figure 2.12b	Typical Stress-Settlement Graph of Punching Shear Failure	28
Figure 2.13	Variation of N_γ with Footing Width	28
Figure 3.1	The Perspex Mould Used for Model Footing Test	31
Figure 3.2	Wooden Footing with 60-Grade Sand Paper glued to the Base	32
Figure 3.3	Picture of Triaxial Frame Used for the Loading Test	33
Figure 3.4	Wooden Rammer Used for the Model Compaction	34
Figure 3.5	Plan of location of tests positions	35
Figure 3.6	The Loading test Set-Up with Mould Filled in Section	36
Figure 3.7	Dynamic Cone Penetrometer	37
Figure 3.8	Triaxial Test Set Up Used	38
Figure 3.9	Confining Pressure Unit	38

LIBRARY
KWAME NKRUMAH UNIVERSITY OF
SCIENCE AND TECHNOLOGY
KUMASI-GHANA

Figure 4.1	Particle Size Distribution Curve of Test Soil	40
Figure 4.2	Compaction Characteristic Curve of the Test Sample	40
Figure 4.3	Moisture Content Variation of the Model Sample	42
Figure 4.4	Starting Condition of the Test Sample	42
Figure 4.5	Definition of Yield Pressure	44
Figure 4.6	Load-Settlement Curve for Experiment BC-15	45
Figure 4.7	Load-Settlement Curve for Experiment BC-20	45
Figure 4.8	Load-Settlement Curve for Experiment BC-30	46
Figure 4.9	Load-Settlement Curve for Experiment BC-35	46
Figure 4.10	Load-Settlement Curve for Experiment BC-100	47
Figure 4.11	Load-Settlement Curve for Experiment BC-150	47
Figure 4.12	Yield Stress against Dry Density	48
Figure 4.13	Variation of Initial Slope of Load-Settlement Curve with Dry Density	49
Figure 4.14	Plot of Average Penetration against Cumulative Blows	50
Figure 4.15	Plot of level of compaction (LC) against D-value	51
Figure 4.16	Variation of Stiffness with Dry Density	54
Figure 4.17	Correlation between Allowable Bearing Pressure and D-value for the Model and Terzaghi Approach	57
Figure 4.18	Correlation between Allowable Bearing Pressure and n-value for Model and Terzaghi Approach	57
Figure 4.19	Comparisons between Ampadu (2005), Sanglerat (1972), and the Model	59

LIST OF SYMBOLS AND ABBREVIATIONS

List of Tables

Table 2.1	Correlation between SPT N-value and Point Resistance of Cone Penetrometer for Various Soil Materials	10
Table 2.2	Some versions of the DCP	14
Table 2.3	Comparison between STP and DCPT Used	15
Table 2.4	Some Relationships between D-value and CBR	20
Table 2.5	Some Relationships between D-value and CBR (after Amini,2003)	20
Table 2.6	Correction Factors for Footing Shape	24
Table 2.7	Some Model Footing Used in Various Studies	29
Table 4.1	Summary of Materials Properties	39
Table 4.2	Summary of Moisture Content Variation across the Model Sample	41
Table 4.3	Summary of Loading Test Results	44
Table 4.4	Summary of DCP Test Results	51
Table 4.5	Summary of the Triaxial Results	52
Table 4.6	Stress-Strain Analysis of the Triaxial Results	53
Table 4.7	Computation of Allowable Bearing Pressure	56
Table 4.8	Summary of Allowable Bearing Pressures, D-value and n-value	57

LIST OF SYMBOLS AND ABBREVIATIONS

A	= Cross-Sectional Area of Cone Base
ASTM	= America Society of Testing and Materials
b	= Mould Width
B	= Footing Width
B	= Skin Resistance Reduction Factor
BC-15	= Name of the Test for 15 rammer blow on Model Sample
BS	= British Standard
CBR	= California Bearing Ratio
CPT	= Cone Penetrometer Test
c_u	= Undrained Coefficient of Cohesion
D	= Penetration per Blow
DCP	= Dynamic Cone Penetrometer
D_f	= Foundation Depth
E_{50}	= Stiffness of Triaxial Sample at Half the Maximum Deviator Stress
EMC	= Existing Moisture Content
ϵ_{50}	= Strain at Half the Maximum Deviator Stress
FS	= Factor of Safety
g	= Acceleration due to Gravity
h	= Mould Height
H	= Height of Hammer Fall
k_o	= Plane Strain
λ	= Tip Resistance Reduction Factor
l	= Mould Length
L	= Footing Length
LL	= Liquid Limit
M	= Mass of the Hammer

MDD = Maximum Dry Density

M_R = Resilient Modulus,

M_s = Mass of Sample

n-value = Number of DCP test Blows per 100mm Penetration

N-value = Number of SPT Blows per 300mm Penetration

N_c = Bearing Capacity Factor due to Contribution of Cohesion

N_{lc} = Bearing Capacity Factor due to Contribution of Cohesion for Local Shear Failure

N_γ = Bearing Capacity Factor due to Contribution of Unit weight

$N_{l\gamma}$ = Bearing Capacity Factor due to Contribution of Unit weight for Local Shear Failure

N_q = Bearing Capacity Factor due to Contribution of Overburden Pressure

N_{lq} = Bearing Capacity Factor due to Contribution of Overburden Pressure for Local Shear Failure

OMC = Optimum Moisture Content

*p = Average Confining Pressure at Failure during the Triaxial Test

P = Mass of the Penetrometer without the Sliding Hammer

PCPT = Piezocone Cone Penetrometer Test

PL = Plastic Limit

PI = Plasticity Index

ϕ_u = Undrained Internal Angle of Friction

ϕ_l = Transformed internal friction angle for local shear failure

Q = Load

q_{all} = Allowable Bearing Pressure,

q_c = Static Cone Penetration Resistance of Soil

q_f = Ultimate Failure Pressure using Model Footing

$q_{f(1)}$ = First-Failure Pressure

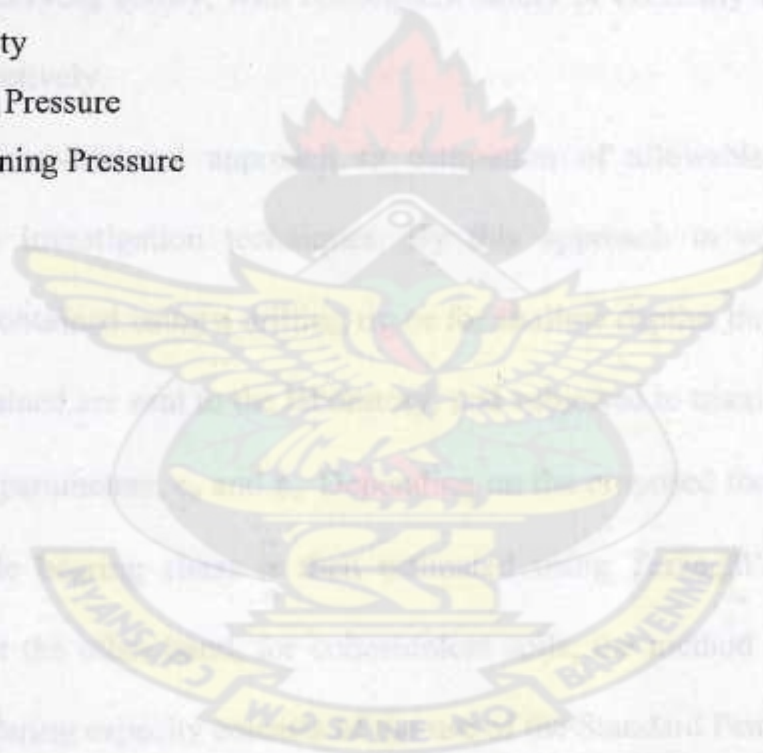
q_{ult} = Ultimate Bearing Capacity by Terzaghi Approach

$Q_{uh(1)}$ = First-Failure Load

q_y = Yield Stress

R_d = Dynamic Resistance of Soil

- s = Skin (rods) Resistance
 s_c = Bearing Capacity Shape Factor for Cohesion Component
 S_r = Maximum Deviator Stress
 s_γ = Bearing Capacity Shape Factor for Unit Weight Component
 s_q = Bearing Capacity Shape Factor for Surcharge Component
 S_y = Yield settlement
 t = Tip (cone) Resistance
 U_{100} = Undisturbed 100mm Diameter Sample
 UCS = Unconfined Compression Strength
 V = Yield Stiffness
 ρ = Density
 σ_1 = Axial Pressure
 σ_3 = Confining Pressure



CHAPTER ONE

INTRODUCTION

1.1 Background

One important objective in site investigation for the design and construction of foundations for civil engineering structures is the estimation of the allowable bearing stress for the foundation system proposed. Improper estimation of the allowable bearing stress leads to either overestimation or underestimation of the soil's load carrying ability, with consequent safety or economy implications on the project respectively.

The conventional approach to estimation of allowable bearing stress is through site investigation techniques. By this approach in cohesive soils, U_{100} samples are obtained using a drilling rig or for shallow depths, through trial pits. The samples obtained are sent to the laboratory, and subjected to triaxial test to determine the strength parameters, c_u and ϕ_u . Depending on the proposed footing configuration, the allowable bearing stress is then estimated using Terzaghi's bearing capacity equation. On the other hand, for cohesionless soils, the method of determining the allowable bearing capacity consists of the use of the Standard Penetration Test (SPT) which is an in-situ test. The SPT, however, is performed as part of site investigations using the percussion drilling rig whose cost do not make it any more economical than the use of samples. For example, a typical site investigation within Accra, for simple structure such as 4 bedroom single-storey house will cost about GH¢ 3,000.00 for 3 boreholes not exceeding 10.0m deep and will require at least 8 days for the fieldwork alone. This cost is considered too high for average developers of these types of buildings with estimated total project cost of about GH¢30,000.00 (The site

investigation cost therefore represent about 10% of the total project cost). In the light of these challenges, there is the need to find cost effective ways of undertaking site investigation for these categories of simple structures. The potentials of the DCP are therefore being explored for evolving allowable bearing capacity for shallow foundations. The dynamic cone penetrometer (DCP) is simple and versatile equipment which in combination with other methods has the potential of simplifying site investigations.

1.2 Objective

The objective of the study was to establish a correlation between the Dynamic Cone Penetrometer Test n-value (number of blows per 100mm) and allowable bearing stress for shallow foundations using a laboratory model footing and a sandy *CLAY* material.

1.3 Justification

The DCP is simple and cost effective equipment and has been recommended to be an appropriate technology for use in developing countries (Sanglerat, 1972). However, up to date, not much research has been conducted into the use of DCP in general and its use in estimating of allowable bearing pressure for shallow foundation design in particular. Even of the few works done regarding the DCP, the focus has been on its use in pavement design and in agricultural engineering for the determination of the consistency of potential cultivatable land and grazing fields (Amini, 2003; Burham and Johnson 1993 ; Edil and Benson, 2004; Gabr et al., 2000; Karunaprema and Edirisinghe, 2002; Singh et al., 1973; Uddin, 2002; Vanagas et al. 2004;). In spite of the very limited research on DCP test for estimating allowable

bearing stress for shallow foundations design and construction, Sowers and Hedges (1966), Sanglerat (1972), Cearns and McKenzie (1988) and Ampadu (2005) have made significant strides in that respect.

Notwithstanding the few attempts to find suitable ways of using the DCP testing effectively for the estimation of allowable bearing stress, the absence of a credible correlation is leading to a situation where some practitioners in the country are attempting to use any kind of DCP specification to estimate the allowable bearing stress of foundation system basing the analyses mainly on the works of Sanglerat (1972). These weaknesses are leading to inconsistent outputs for the users of the DCP testing for estimating allowable bearing stress. This study, however, sought to correlate the DCP n-values with directly measured allowable bearing stress using a laboratory model footing on a sandy *CLAY* material.

1.4 Scope of Work

The scope of work was limited to:

- (i) field work which consisted of manual excavation of test pit to recover sample for the tests and logging the test pit;
- (ii) laboratory work consisting of the characterisation of the test material and performance of unconsolidated-undrained triaxial test to derive the undrained strength parameters , c_u and ϕ_u
- (iii) The laboratory work also covered a model footing test on compacted sample and DCP testing of the model ground.

CHAPTER TWO

LITERATURE REVIEW

2.1 Introduction

The use of penetrometers in geotechnical site investigation is widespread (Harison, 1987). Different types of penetrometers are used for site investigation in response to varying needs. Usually, during the initial exploration stage, penetration tests are employed to determine the stratigraphy, thickness, the soil type in terms of consistency, and the lateral extent of the lithologies. At the detailed site investigation stage, penetration tests are still employed to determine some geotechnical design parameters (Mayne et al, 1995). In general, there are two categories of penetrometers; static and dynamic penetrometers. Available literature indicates that, the use of static penetrometers have been extensively researched into far more than the dynamic penetrometers.

2.2 The Pocket Penetrometer

This is a static cone penetrometer. It is commonly used on split spoon and thin walled tube samples to evaluate consistency and approximate unconfined compressive strength of saturated cohesive soils. It is also used for the same purpose in freshly excavated test pits and trenches. The pocket penetrometer, Figure 2.1 is extremely small and portable; typically weighing less than 300g and approximately 15cm long. It is a spring-loaded penetrometer. The spring is calibrated against unconfined compressive strength (in kg/cm^2). Prior to testing, the indicator ring is positioned at the top of the barrel. Next, the probe is slowly inserted into the soil until the calibration mark is levelled with the soil surface. The movement of the

indicator ring corresponds to the spring compression. The chamber is marked with unconfined compressive strengths that have been calibrated with the internal compression of the spring. The mark at which the indicator ring is located is taken as the unconfined compressive strength of the soil. It must however, be noted that, the readings obtained from the Penetrometer should not replace laboratory test results due to the fact that a small area of penetration test could give misleading results. The instrument should not be used for obtaining final foundation design data. It should be noted that pocket penetrometer readings are only approximations of actual strengths and accuracy of about 1/2 division is possible (Humboldt Manufacturing Company, 2002). One 8- mm interval on the scale is equivalent to $1\text{kg/cm}^2=98.1\text{kN/m}^2$ unconfined compressive strength



Figure 2.1 Pocket Penetrometer (after Humboldt Manufacturing Company, 2002)

2.3 The Cone Penetrometer Test

The Cone Penetration Test (CPT) is traditionally used by most European and American geotechnical engineers. Original specification for its use has been designated ASTM D3441 and was adopted in 1974 by the American Society of Testing and Materials. In this test, a small cone is attached to a rod and pushed steadily into the ground at a rate of 20.32mm of displacement per second. The penetrometer is attached to a vehicle that provides the large jacking forces required

during testing. The 60° apex angle cone has a base area of 1032mm^2 , with a diameter of 35.56mm and a height of 30.48mm . The cone is attached to a friction sleeve having a diameter of approximately 35.6mm as in Figure 2.2. The CPT equipment is steadily pushed into the ground and has been used to characterize soils to depths of 30m below the ground surface. The tip of the cone is typically instrumented to measure the tip resistance using strain gauges, while the sleeve above the cone is instrumented to measure the sleeve friction. These parameters are used to obtain a profile of the variation of soil strength and soil type with depth (Brouwer, 2002). An improvement over the original CPT in 1995, led to the new electronic CPT called Piezocone Cone Penetrometer Test (PCPT) which has been produced and its operation outlined in ASTM D-5778. The PCPT combines both electronic friction cone and piezocone penetrometers. This device produces computerized log of tip and sleeve resistance, induced pore pressure just behind the cone tip, pore pressure ratio (change in pore pressure divided by measured pressure) and lithologic interpretation of each 2 cm intervals of subsoil. The data acquisition systems typically include a portable computer, analog-digital converter, storage media (hard drive, floppy drives), and strip chart recorder or printer and printed out (Mayen et al, 1995).

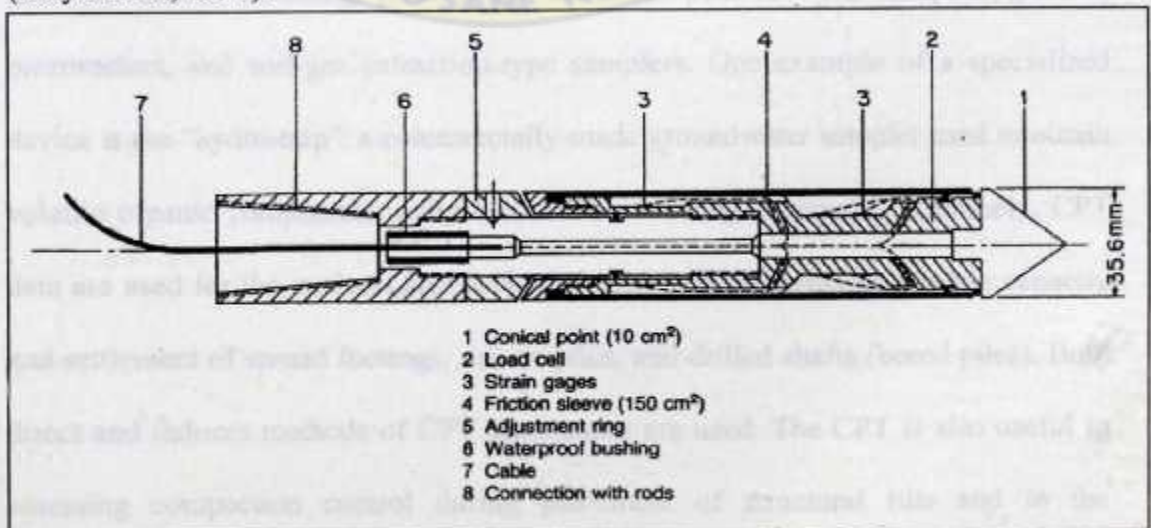


Figure 2.2 Cone Penetration Tip (after D5778)

2.3.1 Applications

The results of the PCPT are used for delineating soil strata and for evaluating the geotechnical engineering parameters of the subsurface layers. Its exceptional resolution makes the detection of thin seams and lenses possible, particularly via the pore pressure channel. This facet is very important and is used in slope stability evaluations. Considerable effort has been made to derive soil engineering properties from the results of cone and piezocone data. Methodologies have been developed using empirical and statistical methods, back-calculations, analytical studies, and numerical simulation (Mayen et al, 1995). Mayen et al, (1995) report that many recent developments in CPT have centered on its use for geo-environmental concerns. The incorporation of additional sensors within the penetrometer to instantaneously and continuously monitor phenomena offers significant potential for evaluating subsurface chemical and biological conditions. For example, cone data are used to infer or detect the presence of anomalies such as contaminants in the pore fluid. In addition, modifications and add-on modules to the standard cone penetrometer, such as, direct-push technology has led to other specialized probes for sampling and testing groundwater and soil during environmental site characterization, including: push-in soil samplers, push-in water samplers, push-in piezometers, and soil-gas extraction-type samplers. One example of a specialized device is the "hydro-trap", a commercially-made groundwater sampler used to obtain volatile organic compounds under controlled confining pressures. Routinely, CPT data are used for the analysis and design of foundations, including bearing capacity and settlement of spread footings, driven piles, and drilled shafts (bored piles). Both direct and indirect methods of CPT assessment are used. The CPT is also useful in assessing compaction control during placement of structural fills and in the

evaluation of effectiveness of ground modification techniques (e.g., vibroflotation, dynamic compaction) and site improvement works (Mitchell, 1986).

2.4 The Standard Penetration Test

This is a dynamic cone penetrometer designed to provide information on the engineering properties of soils. The test procedure is described in the British Standard BS 1377: Part 9:1990. A typical test operation is as shown in Figure 2.3. The test uses a split thick-walled sample tube, with an outside diameter of 51mm and an inside diameter of 35mm and a minimum length of 457mm, Figure 2.4. This is driven into the ground at the bottom of a borehole by blows from 63.5kg hammer falling through a distance of 760mm. The sample tube is initially driven 150mm into the ground (seat-in-drive) and then the number of blows needed to further penetrate each of 75mm of the tube markings to a depth of 300mm is recorded. The total number of blows for the 300mm penetration is the standard penetration resistance N-value. In cases where 50 blows are insufficient to advance the tube through the 300mm interval, the penetration after 50 blows is recorded and indicated as refusal. The main purpose of the test is to provide an indication of the relative density of granular deposits, such as sand and gravels from which it is virtually impossible to obtain undisturbed samples for strength testing. The great merit of the test and the main reason for its widespread use is that, it is simple and relatively inexpensive. It has been observed that interpretation of the SPT results depends on the soil type, with fine-grained sands giving the most useful results, with coarser sands and silty sands giving reasonably useful results, and clays and gravelly soils yielding results which may be very poorly representative of the true soil conditions.

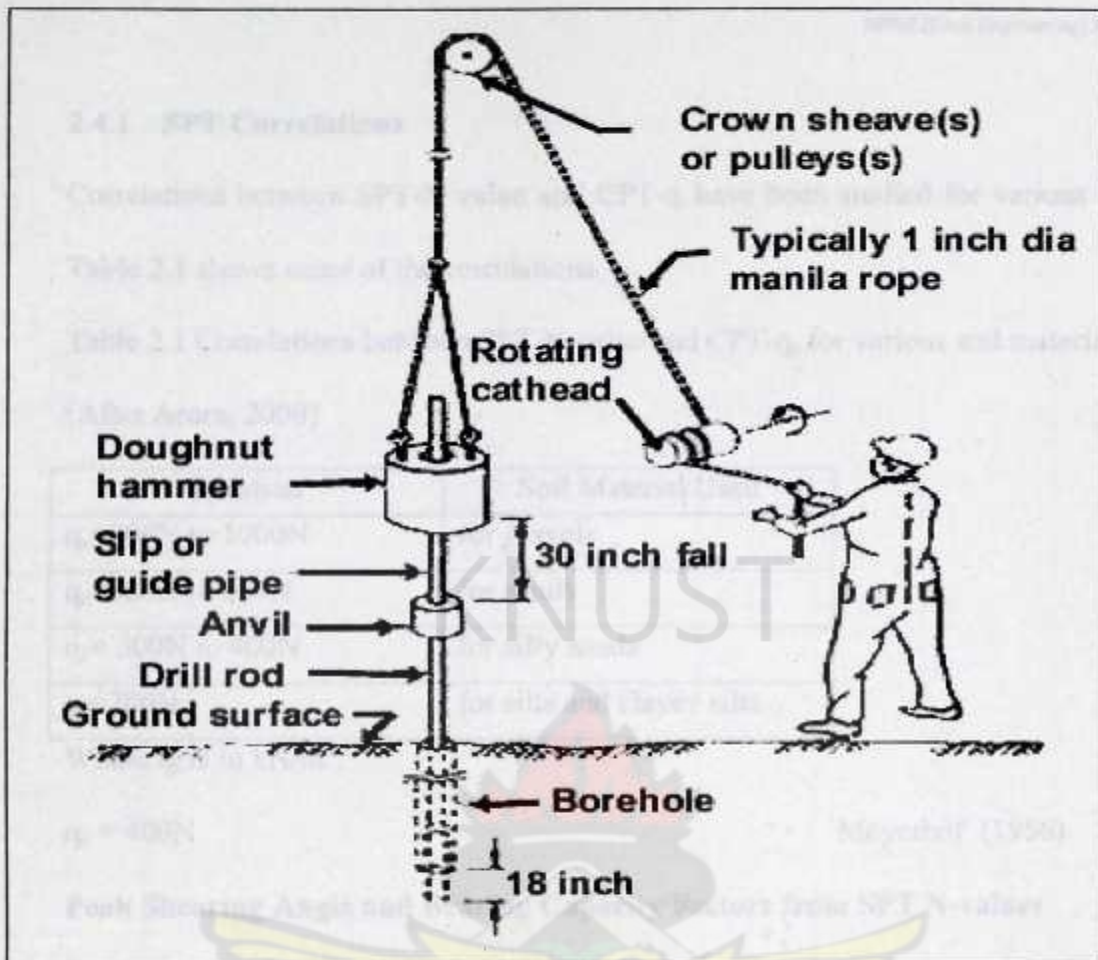


Figure 2.3 Typical Operation of the SPT (after www.en.wikipedia.org)

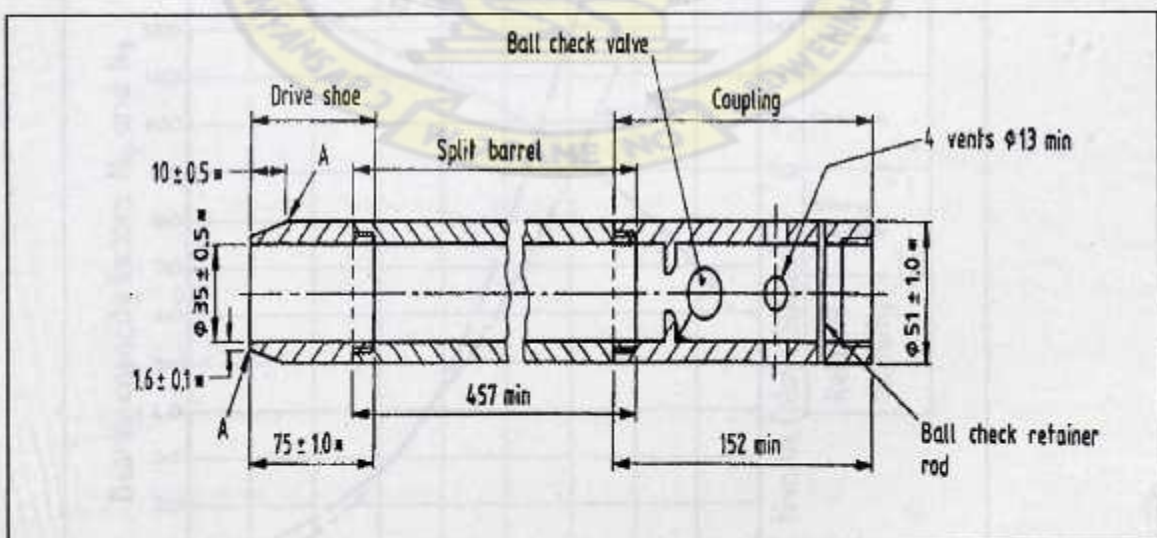


Figure 2.4 Split Spoon Sampler, dimensions in mm (after BS 1377: Part 9: 1990)

2.4.1 SPT Correlations

Correlations between SPT-N value and CPT- q_c have been studied for various soils.

Table 2.1 shows some of the correlations.

Table 2.1 Correlations between SPT N-value and CPT- q_c for various soil materials

(After Arora, 2000)

Relation	Soil Material Used
$q_c=800N$ to $1000N$	for gravels
$q_c=500N$ to $600N$	for sands
$q_c=300N$ to $400N$	for silty sands
$q_c=200N$	for silts and clayey silts ,

Where q_c is in kN/m^2 ,

$$q_c = 400N$$

Meyerhof (1956)

Peak Shearing Angle and Bearing Capacity Factors from SPT N-values

Figure 2.5 shows the chart for estimating internal friction angle and bearing capacity factors of a cohesionless soil from SPT N-values.

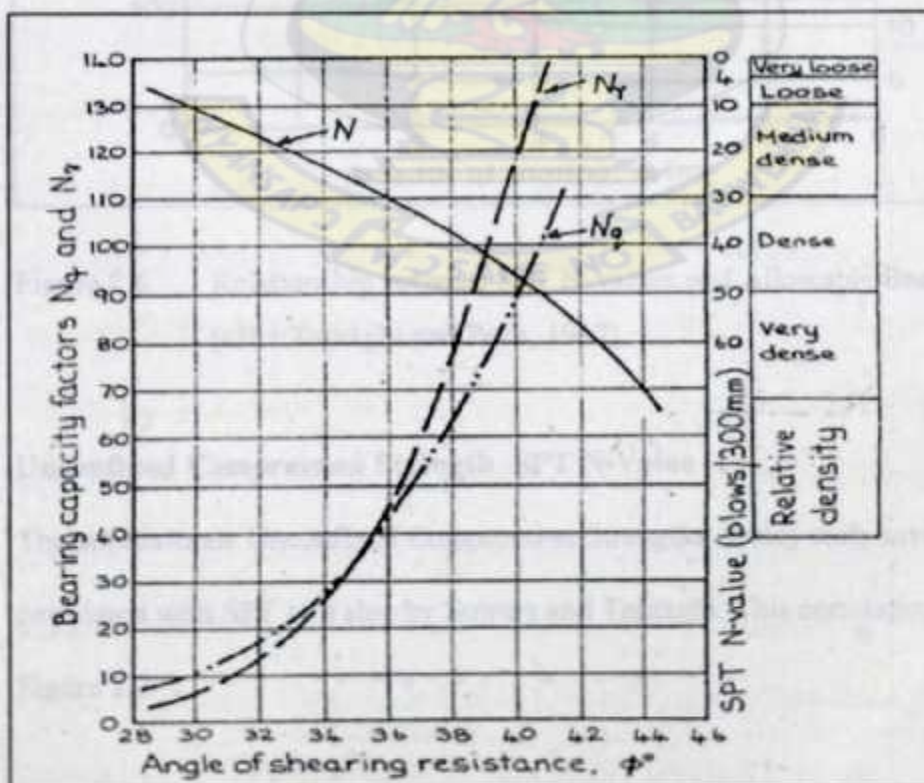


Figure 2.5 Relationship between ϕ , N_q and N_y with SPT N-values
(After Peck, Hanson & Thornburn, 1973)

Allowable Bearing Pressure- SPT N-Values

Figure 2.6 is a chart for estimating allowable bearing capacity of sand based on SPT N-values

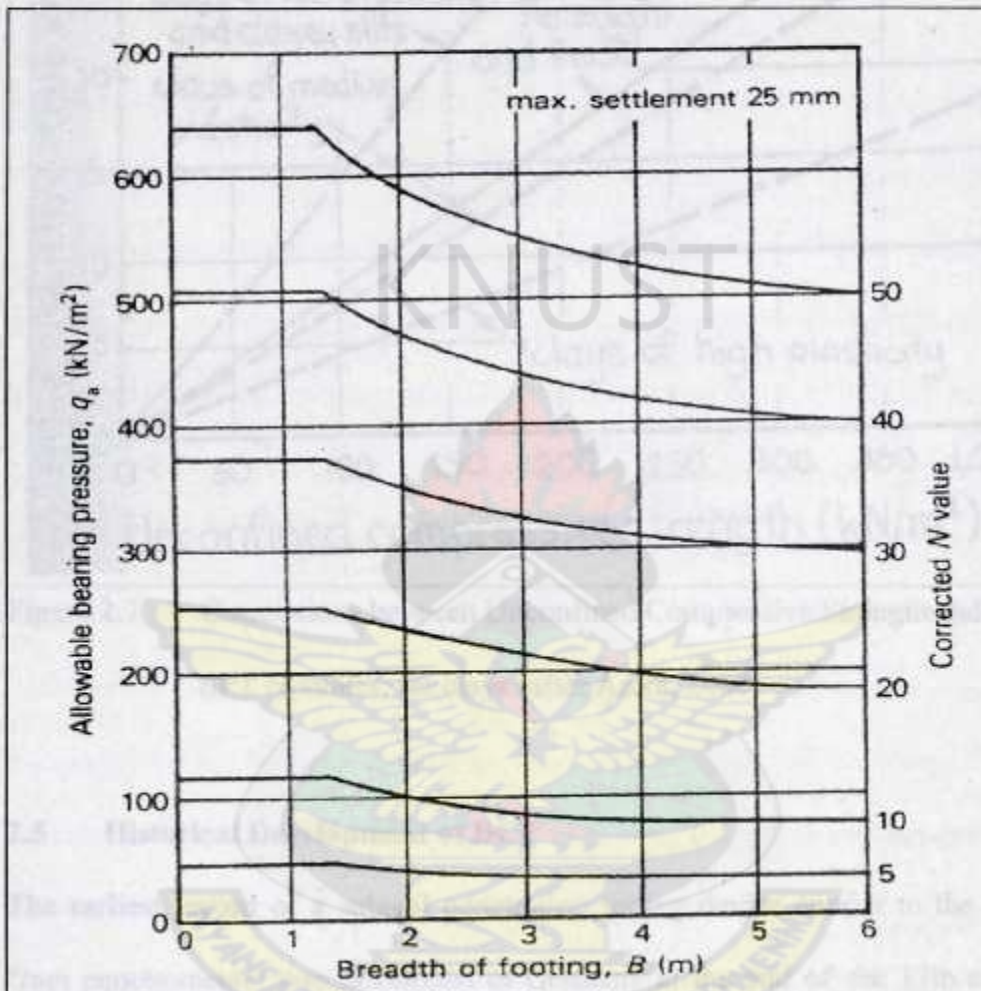


Figure 2.6 Relationship between SPT N-values and Allowable Bearing Pressure (after Terzaghi and Peck, 1967)

Unconfined Compression Strength -SPT N-Value

The approximate Unconfined Compression Strengths of clay soils have been correlated with SPT N-Value by Sowers and Terzaghi. This correlation is shown in Figure 2.7

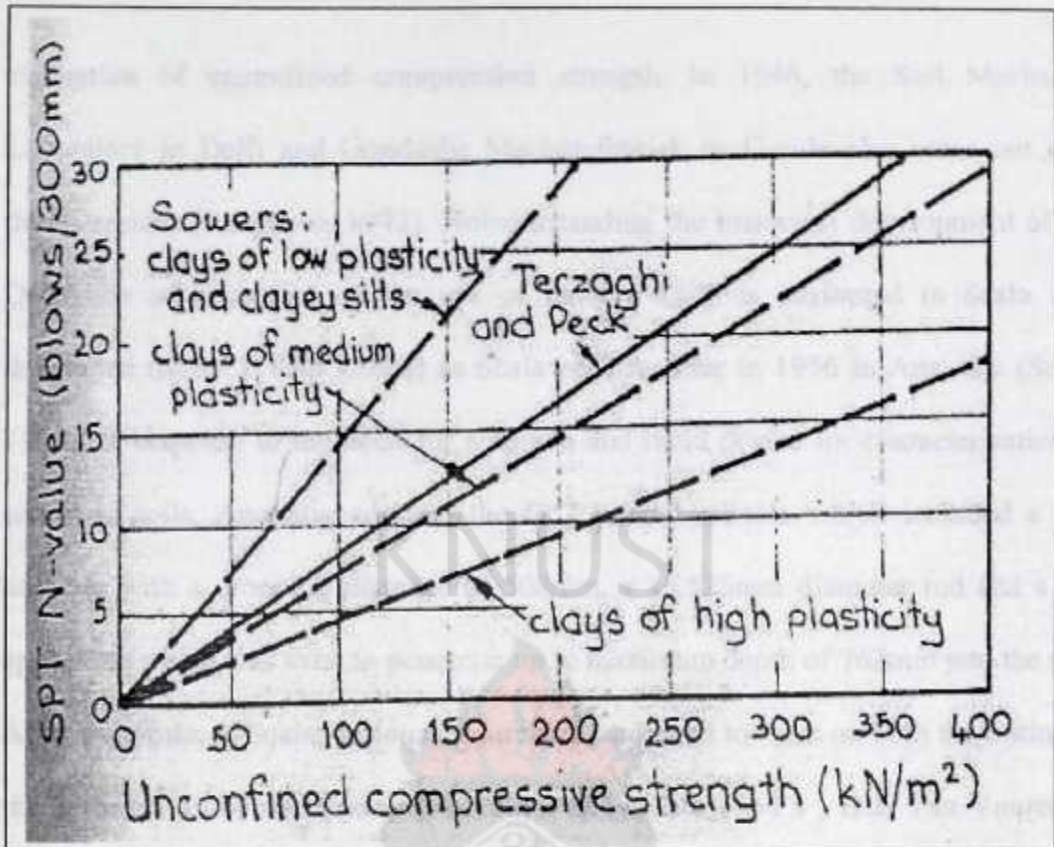


Figure 2.7 Correlations between Unconfined Compressive Strength and SPT N-values, for clays (after Arora, 2000)

2.5 Historical Development of DCP

The earliest record of a subsoil penetration testing device similar to the DCP, the "ram penetrometer" was developed in Germany at the end of the 17th century by Nicholas Goldmann (Burham and Johnson, 1993). The next major development again came from Germany, when, Kunzel in 1936 developed what was known as "Prufstab". This device was later used by Paproth in 1943 and eventually became standardized in 1964 as the "Light penetrometer", the German Standard DIN 4094. Concurrent with the German standardization of the "Light Penetrometer", several other countries and individuals developed their own penetration devices, such as : Collin of France in 1846; the Swedish Railroads standardized theirs in 1917, Danish Railroads in 1931 came out with the pocket penetrometer used for approximate

evaluation of unconfined compression strength. In 1946, the Soil Mechanics Laboratory in Delft and Gondsche Machinefabriek oa Gouda also came out with their versions (Sanglerat, 1972). Notwithstanding the historical development of the DCP, the advancement of the use of modern DCP is attributed to Scala who developed the DCP also known as Scala penetrometer in 1956 in Australia (Scala, 1956). In response to the need for a simple and rapid device for characterization of subgrade soils. Australia adopted the DCP used by Scala which included a 9kg hammer with a dropping distance of 508mm, a 15.875mm diameter rod and a 30° apex cone which was used to penetrate up to maximum depth of 762mm into the soil. After the works of Scala, various researchers continued to work on both the testing of the instrument and the testing procedure. In the late 1960's , D.J. Van Vuuren in Zimbabwe continued with the development of the DCP(Van Vuuree, 1969). He used a similar device as Scala, except for some differences in dimensions: a 10kg hammer was dropped from a height of 460mm, forcing a 30° apex cone connected to a 16mm diameter rod into the soil for a maximum depth of 1000mm (Burnham and Johnson, 1993). Kleyn (1982) contribution to the development of DCP was in the area of its application to determine in-situ properties of road pavement layers and subgrade in South Africa. Other applications included identification of potential collapsible soils, compaction construction especially when high lift rates render normal compaction control techniques to time be consuming to be effective. He further considered the use of DCP in pavement evaluation and monitoring in terms of structural evaluation of pavement, comparing in-situ CBR and structural monitoring. Some of the many versions of the DCP used by various people are tabulated in Table 2.2.

Table 2.2 Some Versions of the DCP (adapted from Ampadu, 2005)

Type	Cone Diameter (mm)	Mass of Hammer (Kg)	Height of Fall (mm)	Energy per Blow per Cone Area (KN-m/m ²)
Sowers & Hedges (1966)	38	6.8	508	30
Scala (1956)	20	9.08	508	144
Kleyn (1975)	20	8	575	144
Borros Penetrometer	50	63	750	231
Singh (1973)	35	10	500	51
Ampadu (2005)	20	10	460	144
This Study	20	8	578	144

2.6 The Dynamic Cone Penetrometer

The dynamic cone penetrometer in operation consists of a drop weight, an anvil, rods and a cone. It is traditionally used in testing of subgrade soils for road projects. It is also used during reconnaissance exploration of soils at shallow depths for other civil engineering projects. The consistency of cultivatable lands is determined using DCP testing prior to ploughing. During testing, the drop weight is allowed to fall through a specified height. As the drop weight hits the anvil, kinetic energy is imparted into the DCP system and the cone is driven into the ground. The depth of penetration with each blow is measured or derived as the D-value. The soil layering profile and strength are interpreted from the D-values. The test procedure is described in the ASTM D6951-03, The Transport Research Laboratory(TRL) Research Report 361(2004) and in the recommendations of the study group created in 1957 by committee of the International Society for soil Mechanics and foundation engineering to analyse test methods involving the dynamic and static penetrometers (Sanglerat 1972).

A comparison of the main features of SPT and DCPT is shown in table 2.3.

Table 2.3 comparison between SPT and DCPT Used

SPT	DCPT
Dynamic Impact	Dynamic Impact
Open Cone(occasionally solid cone)	Solid cone
Weight of hammer is 63.5kg	Weight of hammer is 8kg
Height of hammer fall is 760mm	Height of hammer fall is 578mm
Diameter of cone 51mm	Diameter of cone 20mm
Energy per blow 232kN-m/m ²	Energy per blow 144kN-m/m ²

2.6.1 Development of Semi Empirical Equations

The principle of the dynamic cone penetrometer test is based on dynamic resistance offered by soil to deformation caused by dynamic penetrometer. The degree of the resistance is a measure of the soil's shear strength and hence its bearing capacity. Thus a penetrometer of constant energy (blow) would develop higher D-value in a soil layer of low shear strength as compared to a soil layer of higher shear strength (Sanglerat, 1972; Singh et al., 1973; Peck et al., 1973 and Braja, 1985). The theory of dynamic cone penetrometer however can be attributed to Aimé Nadal, a French civil engineer of "Ponts et Chaussées" in Paris and the Dutch. The work of Aimé Nadal was based on empirical evidence gathered over many years of working on penetrometer tests and driving of piles. It was observed that the dynamic resistance of soil, R_d to advancement of penetrometer was a function of the shear strength of the soil by the dynamic expression;

$$R_d = \lambda \cdot t(c, \phi) + B s(c, \phi) \dots \dots \dots (2.1)$$

Where t and s are the tip(cone) and skin(rods) resistances respectively; ϕ and c are angle of internal friction and cohesion factors respectively, while λ and B are

reduction factors whose values depend on the nature of the soil into which the penetrometer is being driven; and the design of the penetrometer.

Because the design of the DCP used in this study is such that, the diameter of the cone base (20mm) is larger than the diameter of the rod behind it (16mm), the total resistance is theoretically provided by the cone resistance only.

Hence, $\lambda = 1$ and $\beta = 0$

$$\Rightarrow R_d = t(c, \phi) \dots \dots \dots (2.2)$$

The Dutch Formula is a dynamic formula which is based on the assumption that the kinetic energy delivered by the hammer during penetration by a dynamic penetrometer is equal to work done by the entire penetrometer system. It is founded on the Newton's principle of energy and impact motion. Upon releasing the hammer, the mobilized maximum potential energy is progressively transferred into kinetic energy which attains maximum value just at the point of striking the anvil. At point of strike, most of the kinetic energy is transferred from the hammer to the anvil which in turn is transmitted to the lower rods and finally to the cone. Theoretically, when the cone eventually comes to rest, the total kinetic energy imparted has been dissipated in the soil. Therefore by the law of conservation of energy, the total work done by the soil to stop the advancing cone and wasted (lost) energy to environment such as sound and wave energy equals the maximum potential energy attained by the hammer at the highest point, neglecting sliding friction and air resistance of the hammer. The main components of energy losses in DCP operation are; sound energy, heat energy generated, wave energy propagated through the soil and skin friction energy of the rod.

The Dutch formula is hence expressed as;

$$R_d = \frac{M^2 g H}{[AD(M + P)]} \quad \dots\dots\dots (2.3)$$

Where R_d = dynamic resistance in kN/m^2

M =mass of the hammer in kg;

H = height of hammer fall in mm;

A = cross-sectional area of the cone base in m^2

D =penetration per blow in mm;

g = acceleration due to gravity, in ms^{-2}

P =mass of the penetrometer (without the sliding hammer) in kg; (Sanglerat, 1972).

It should be noted that for a particular dynamic penetrometer, all the parameters in equation (2.3) are constant except D =penetration per blow which is a variable dependent on the shear strength of the soil being tested.

Substituting the following specifications of the dynamic cone penetrometer used,

$M = 8\text{kg}$, $H=578\text{mm}$, $A = 3.142 \times 10^{-4} \text{ m}^2$, $P= 3.864\text{kg}$, D =penetration in mm per blow;

equation 2.3 reduces to

$$R_d = \frac{97351}{D} \text{ kN / m}^2$$

Sanglerat (1972) recommends that for shallow foundations, the allowable bearing pressure, q_{all} , may be estimated by dividing R_d by a factor of 20,

$$\text{Thus, } q_{all} = \frac{R_d}{20}$$

$$q_{all} = \frac{4867.55}{D} \text{ kN/m}^2, \text{ For } n\text{-value}=100\text{mm/D}$$

$$\Rightarrow q_{all} = 48.7n \quad \dots\dots\dots (2.4)$$

2.6.2 Previous Works

Previous attempts to establish relation between n -value and allowable bearing pressure for the design and construction of shallow foundations includes, Sowers and Hedges (1966), Sanglerat (1972), Cearns and McKenzie (1988) and Ampadu (2005). It must however be noted that, the DCP penetration increment of the Sowers and Hedges(1966) study was only 44 mm instead of the standard 100mm and also the energy per blow per unit area of cone was only 21% of that used in used in this work. Virgin Piedmont soil was used for the research. The Sanglerat (1972) work involved the use of the Dutch formula for the dynamic resistance, R_d . The obtained R_d was divided a factor of 20 to obtain the allowable bearing pressure in a cohesionless soils. Based on the specifications of the DCP used in this work, as shown in Table 2.2, Sanglerat (1972) correlates q_{all} with n -value as in equation (2.4).

The Cearns and McKenzie (1988) on the other hand, used the Borros penetrometer that had energy per blow per unit area of cone of about double of that used in this study. The Ampadu (2005), work involved establishing a correlation between n -value and allowable bearing capacity. He estimated the allowable bearing capacity from the strength parameters c_u and ϕ_u obtained from triaxial test and then used Terzaghi bearing capacity formula. The n -values of DCP testing were correlated with an allowable bearing stresses obtained. He used sandy to silty *CLAY* material in his work to obtain the correlation equation (2.5);

$$q_{all} = 164n - 504, \text{ for } n > 6 \dots\dots\dots(2.5)$$

2.6.3 Empirical DCP Test and Strength Correlations

Relationship between D-value and other soil parameters have been established by many researchers on empirical basis. Below are some of the correlations.

Relationship between D-value and unconfined compression strength (UCS) in kN/m^2 have been studied in the laboratory for lime stabilised soil and relation below has been established;

$$\text{Log (UCS)} = 3.21 - 0.809 \log D \quad (\text{after McElaveney and Djatnika, 1991})$$

Many studies have been conducted to formulate correlation between D-value and resilient modulus, M_R . The results of George and Uddin (2000) shows that;

$$\begin{aligned} M_R (\text{MN/m}^2) &= 235.3 D^{-0.475} && \text{for coarse-grained soil} \\ M_R (\text{MN/m}^2) &= 532.1 D^{-0.492} && \text{for fine-grained soils} \end{aligned}$$

Allowable Bearing Pressure - n-value

The relationship between n-value and allowable bearing pressure shown below has been derived by Ampadu (2005) from ultimate bearing capacity calculated using Terzaghi's bearing capacity equation for sandy to silty *CLAY* materials.

$$q_{all} (\text{kN/m}^2) = 164n - 504 \quad \text{for } n\text{-value (blows/100mm.)} > 6$$

DCP and CBR

Correlations between D-value and California bearing ratio (CBR) have been investigated by many researchers using various materials. The Table 2.4 and Table 2.5 show some of the correlations between D-value and California Bearing Ratio and the materials used.

Table 2.4 Some Relationships between D-value and CBR

	Correlation	Material	Investigator
1	$\log(CBR) = 1.145 - 0.336 \log D$	disturbed soaked CBR	Karunaprema and Edirisinghe (2002) (7 < D < 75)
2	$\log(CBR) = 1.671 - 0.577 \log D$	Undisturbed- unsoaked clayey or silty sand	
3	$\log(CBR) = 2.182 - 0.872 \log D$	disturbed unsoaked CBR	
4	$\log(CBR) = 2.56 - 1.16 \log D$	Claylike soils	Harison(1987)
5	$\log(CBR) = 2.81 - 1.32 \log D$	Claylike-Well graded Gravels	

Table 2.5 Some Relationships between D-value and CBR (after Amini, 2003)

	Correlation	Material	Investigator
1	$\log(CBR) = 2.45 - 1.12 \log D$	Granular and cohesive	Livneh et al. (1992)
2	$\log(CBR) = 2.46 - 1.12 \log D$	Various soil types	Webster et al. (1992)
3	$\log(CBR) = 2.62 - 1.27 \log D$	Unknown	Kleyn (1975)
4	$\log(CBR) = 2.44 - 1.07 \log D$	Aggregate base course	Ese et al. (1995)
5	$\log(CBR) = 2.60 - 1.07 \log D$	Aggregate base course and cohesive	NCDOT (Pavement, 1998)
6	$\log(CBR) = 2.53 - 1.14 \log D$	Piedmont residual soil	Coonse (1999)

2.6.4 Capabilities of the DCP

The DCP has many capabilities, the following are some of them:

- (i) It is not expensive to acquire and can be manufactured in-house; it is costing about \$1,400.00 from Salem Tool Company, USA as compared to Forager-55 Cable Percussion Rigs cost £14,192.00 (Consallen Group Sales Ltd, 2008). Locally, the DCP is costing about GH¢1,000.00.
- (ii) It is portable and suitable when access and space become a constraint especially in confined areas such as inside buildings to be rehabilitated or

- at congested sites that would prevent the use of traditional boring equipment;
- (iii) It is easy to learn how to operate it in matter of minutes;
- (iv) It is a simple device to operate, requiring 3 people for its efficient operation;
- (v) It is fast to conduct, leading to large amounts of data over an area;
- (vi) Its data are easy to process, especially when used with appropriate software;
- (vii) The test results have been correlated to other soil parameters (CBR, unconfined compressive strength, shear strength and SPT N-values) by various researchers ;
- (viii) It is cost-effective to operate, especially when compared with other traditional site characterization methods (borings and laboratory/field tests).

2.6.5 Limitations of the DCP

In spite of the many advantages of the DCPT, there are some associated limitations that have been identified. For example:

- (i) It does not permit groundwater conditions to be readily evaluated;
- (ii) No samples are obtained for either visual inspection or further analysis; and
- (iii) It is not suitable for gravel soils and hard formations such as highly weathered and fresh rock formations. This is because, the DCP rod may bend.

2.7 Bearing Capacity of Shallow Foundations

The ultimate bearing capacity of a soil, q_{ult} is classically defined as the value of bearing pressure that will cause a large increase in settlement of the foundation without further increase in bearing pressure, resulting in shear failure. The ultimate bearing capacity of shallow foundations is usually calculated from the Terzaghi bearing capacity equation by incorporating appropriate soil parameters (cohesion, internal friction and unit weight), footing details and foundation depth. The allowable bearing pressure (q_{all}) is the maximum bearing pressures that can safely be applied to a foundation such that, it is safe against instability due to shear failure and maximum tolerable settlement. The allowable bearing pressure is normally calculated from the ultimate bearing capacity by using appropriate factor of safety, F_s . Typical value of factor of safety for shallow foundation is 3.0.

2.7.1 Factors Affecting Bearing Capacity of Shallow Foundations

A number of factors have been studied and found to affect the bearing capacity of shallow foundations. Some of these factors are;

- i. The unit weight, shear strength and deformation characteristics of the soil.
- ii. The size, shape, depth and roughness of the footing.
- iii. Groundwater level and initial stresses in the foundation soil (Dunn et al., 1980).

2.7.2 Terzaghi Ultimate Bearing Capacity Equation

The present Terzaghi formula which is a modified form of Prandtl (1921) plastic failure theory (Radhakrishnan and Ramanathan, 1965) is used for evaluation of the ultimate bearing capacity of shallow foundations. Terzaghi's theory is based

surface. In the theory, the angles α between the footing base and the sides of the triangular zone were taken to be equal to the soil internal friction angle, ϕ .

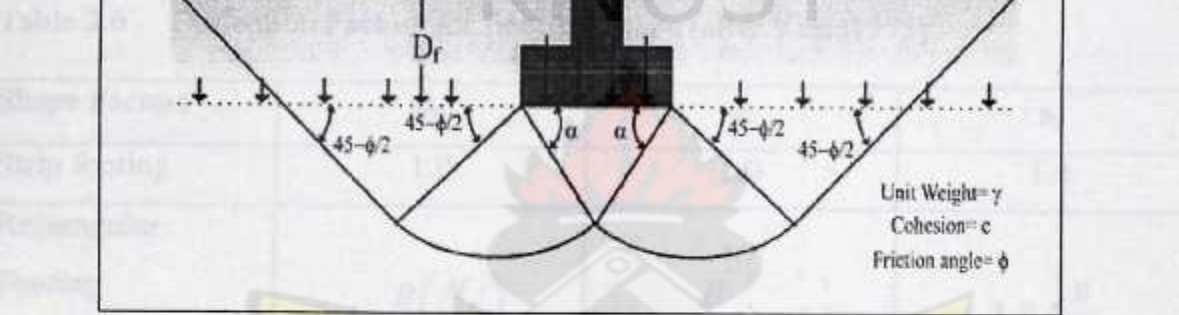


Figure 2.8 General Shear Failure Pattern (after Terzaghi Analysis)

Using the equilibrium analysis, Terzaghi expressed the ultimate bearing capacity for shallow strip foundation in its simplest form as;

$$q_{ult} = cN_c + \gamma D_f N_q + \frac{1}{2} \gamma B N_\gamma \quad (2.6)$$

Where N_c , N_q and N_γ are the Terzaghi bearing capacity factors.

Equation (2.6) is subject to the following conditions:

- general shear failure ;
- strip (continuous) footing for which $L > 5B$;
- rough foundation base ; and
- shallow foundation ($D_f < 4B$).

On the basis of comparative loading tests with footings of different shapes, equation (2.6) has been modified into equation (2.7) by incorporating correction factors for footing shape configuration (Vesic,1973).

$$q_{ult} = cN_c s_c + \gamma D_f N_q s_q + \frac{1}{2} \gamma B N_\gamma s_\gamma \quad \dots\dots\dots(2.7)$$

Where s_c , s_q and s_γ are shape factors

Table 2.6 gives the correction factors for footing shape configuration for shallow foundations.

Table 2.6 Correction Factors for Footing Shape (after Vesic1973)

Shape Factors	s_c	s_q	s_γ
Strip footing	1.0	1.0	1.0
Rectangular Footing Limitation $B \leq L$	$1 + \frac{B}{L} \left(\frac{N_q}{N_c} \right)$	$1 + \frac{B}{L} \tan \phi$	$1 - 0.4 \frac{B}{L}$
Circle and square	$1 + \frac{N_q}{N_c}$	$1 + \tan \phi$	0.60

L and B are length and breadth of the footing.

For foundations that exhibit local shear failure, equation (2.6) is modified into;

$$q_{ult} = \frac{2}{3} c N_{1c} s_c + q N_{1q} s_q + \frac{1}{2} \gamma B N_{1\gamma} s_\gamma \quad \dots\dots\dots(2.8)$$

where the values of N_{1c} , N_{1q} and $N_{1\gamma}$ are bearing capacity factors obtained after modifying ϕ using equation (2.8).

$$\phi_1 = \tan^{-1} (2/3 \tan \phi) \quad \dots\dots\dots(2.9)$$

2.7.3 Modes of Foundation Failures

According to experimental results of foundations resting on sands, the mode of failure likely to occur in any situation depends on the size of the footing relative to the foundation depth and the relative density of the soil (Vesic, 1973). It must be stated that while the above stated factors have been observed to be responsible for a particular mode of failure, there is at present no general numerical criteria that can be used to predict a particular failure mode. An attempt by Vesic (1973) to link relative density and depth of foundation relative to footing width to failure mode is shown in Figure 2.9.

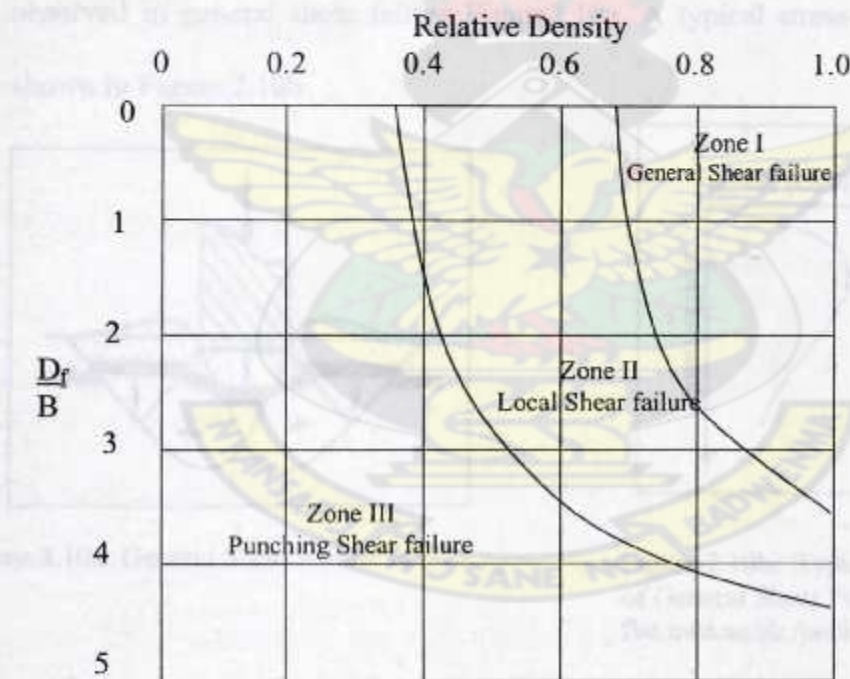


Figure 2.9 Failure Mode Chart (after Vesic, 1973)

Vesic (1973) classified bearing capacity failures into three main categories for shallow foundations depending on how the yield surface developed as explained below.

2.7.4 General Shear Failure

When a load (Q) is gradually applied to a foundation, settlement occurs which is almost elastic to begin with. At the ultimate load, general shear failure occurs when a plastic yield surface develops under the footing, extending outward and upward to the ground surface and catastrophic settlement and/or rotation of the foundation occurs. The load per unit area at the point of failure is the ultimate bearing capacity, q_f for foundation using model footing. This type of failure has been noted to be common in highly incompressible soils of definite shear strength such as very dense sand and hard overconsolidated clays. A heave on the side is always observed in general shear failure Figure 2.10a. A typical stress-settlement graph is shown in Figure 2.10b

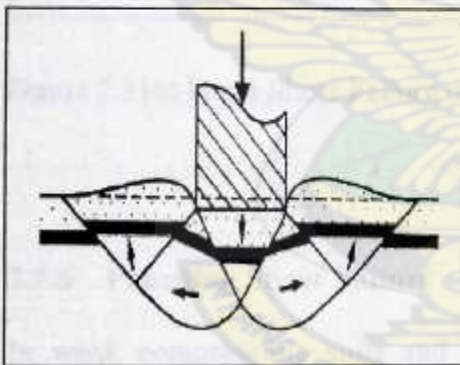


Figure 2.10a: General Shear Failure of Soil

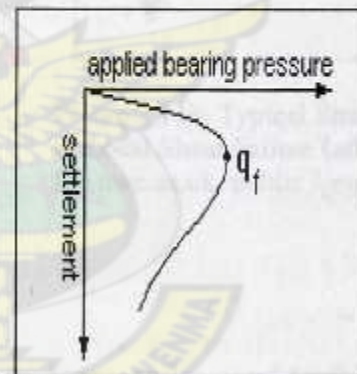


Figure 2.10b: Typical Stress-Settlement Graph of General Shear Failure (after www.fbe.uwe.ac.uk/public/geocal/foundations)

2.7.5 Local Shear Failure

In medium dense sand and clays of medium consistency, significant vertical settlement may take place due to local shear failure. The local shear results from partial development of the state of plastic equilibrium close to the lower edges of the footing. The yield surfaces often do not reach the ground surface and may only slightly heave Figure 2.11a. Several yield developments may occur accompanied by

settlement in a series of jerks. The bearing pressure at which the first yield takes place is referred to as the first-failure pressure, $q_{f(1)}$ Figure 2.11b-the. The term first-failure load $Q_{f(1)}$ is also used (Malandraki and Toll, 1996). Local shear is characterised by relatively large settlements and the ultimate bearing capacity is not clearly defined (www.fbe.uwe.ac.uk/public/geocal/foundations), in these cases settlement is the major factor in the foundation design.

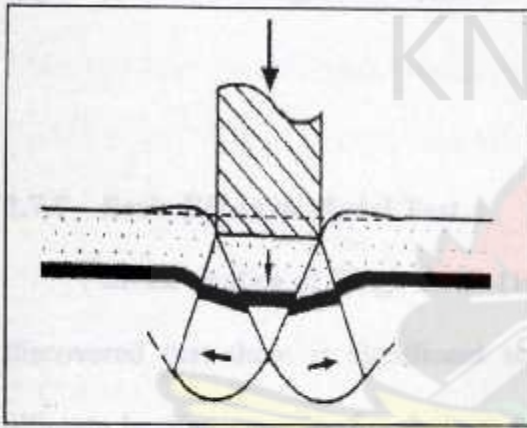


Figure 2.11a: Local Shear Failure of Soil

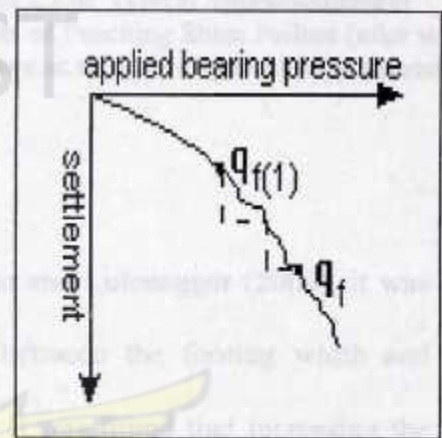


Figure 2.11b: Typical Stress-Settlement Graph of Local Shear Failure (after www.fbe.uwe.ac.uk/public/geocal/foundations)

2.7.6 Punching Shear Failure

In weak compressible soils and very loose to loose soils, considerable vertical settlement may take place with the yield surfaces restricted to vertical planes immediately adjacent to the sides of the foundation; The ground surface may be dragged down, Figure 2.12a. There is no heaving of the ground surface away from the edges and no tilting of the footing occurs. After the first yield has occurred, the stress - settlement curve will become slightly steep, but remain fairly flat Figure 2.12b. This is referred to as a punching shear failure.

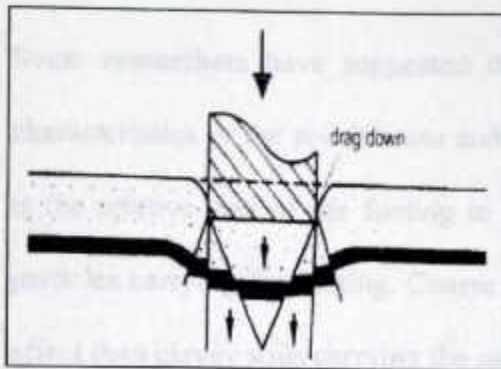
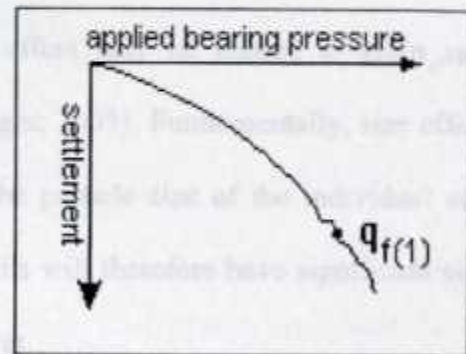
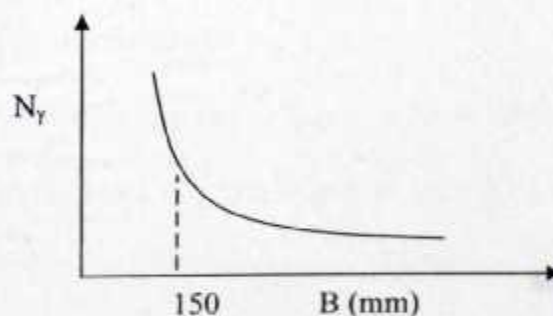


Figure 2.12a: Punching Shear Failure

Figure 2.12b: Typical Stress-Settlement Graph of Punching Shear Failure (after www.fbe.uwe.ac.uk/public/geocal/foundations)

2.7.7 Scale Effect in Model Test

In the studies of Singh et al. (1973), Cerato and Lutenecker (2003), it was discovered that there is significant scale effect between the footing width and ultimate bearing capacity for shallow foundations. It was found that increasing the footing width results in higher ultimate bearing stress for the same soil material. Similarly, in the works of De Beer (1965) and Vesic (1973), it was realised that model footings used for bearing capacity studies of width, B less than 150mm gave results that were higher. This was due to the fact that, the magnitude of N_γ decreased significantly with B until $B \geq 150$ mm when N_γ becomes fairly constant as illustrated in Figure 2.13. By this, a condition of lower limit on footing size to use in model footing experiments is suggested.

Figure 2.13: Variation of N_γ with Footing Width (after Das and Omar 1993)

Some researchers have suggested the scale effect may be related to grain size characteristics of the soil (Cerato and Lutenecker, 2003). Fundamentally, size effect is the relative size of the footing to that of the particle size of the individual soil particles carrying the footing. Coarse sandy soils will therefore have significant size effect than clayey soils carrying the same footing.

Model footing sizes used in previous model footing studies are shown in Table 2.7.

Table 2.7 Some Model Footings Used in Various Studies

Authors	Mould Dimension l x b x h (mm ³)	Footing Dimension L x B (mm ²)	Footing Clearance from Mould Edge	Soil Material Used
Patra et al (2005)	800 x 365 x 700	360 x 80	1.8B	Geogrid Re- inforced SAND
Shin et al (1999)	1000 x 175 x 800	175 x 70	0.8B	Crude oil con- terminated SAND
Das & Omar (1994)	1960 x 305 x 914	304.8 x 127	0.7B	SAND
Das & Maji (1994)	610x 610 x 610	76.2 x 76.2	3.5B	Geogrid Re- inforced SAND
Ko & Davidson(1973)	1540x102x 480	100 x 76	0.2B	SAND
This Study	609 x 300 x 376	300 x 150	0.5B	Sandy CLAY

CHAPTER THREE

METHODOLOGY

3.1 The Fieldwork

The fieldwork was carried out near the College of Engineering within the site earmarked for KNUST/DFR collaborative pavement engineering studies on KNUST Campus, Kumasi. The work involved manual excavation of a test pit using pick axe and shovel and then recovery of sample from the test pit. Samples were recovered from a depth of 0.30m to 0.80m. Two samples were taken, a bulk sample and then a small sample in an airtight plastic sample bag for the determination of natural moisture content. The test pit was then logged, after which the samples were taken to the laboratory for further works.

3.2 The Laboratory Work

3.2.1 Sample Preparation

The bulk sample was air dried for about 72 hours to almost constant moisture content. It was then sieved through 19mm aperture sieve to remove cobble materials. Index property and compaction tests were then performed on a representative sample. The remaining sample was bagged into five sacks for storage awaiting the model tests.

3.2.2 Sample Characterisation

1. The sample for the natural moisture content was taken directly from the test pit in an air tight plastic bag in accordance with BS 1377: Part 2:1990.
2. The particle size analysis was performed in accordance with BS 1377: Part 2:1990 but first, the sample was sieved through a 19mm aperture sieve in order

to remove cobble sized particles. Sedimentation by the hydrometer method was used for the fines.

3. Atterberg limits test was performed on the bulk sample according to BS 1377: Part 2:1990. The Casagrande method was used for the determination of the liquid limit.
4. Compaction characteristics were determined according to BS 1377: Part 4:1990 using 2.5kg rammer (Standard Proctor).

3.3 Model Test Set-Up

3.3.1 The Perspex Mould and Wooden Footing

The mould consisted of 16mm thick perspex of internal dimensions, 609mm (length) x 300mm (width) x 376mm (height). To minimise lateral yielding during model soil compaction and to ensure plane strain (k_0) condition during the loading test, the mould was braced on the outside by three (3no.) 5mm thick by 25mm wide steel as shown in Figure 3.1.

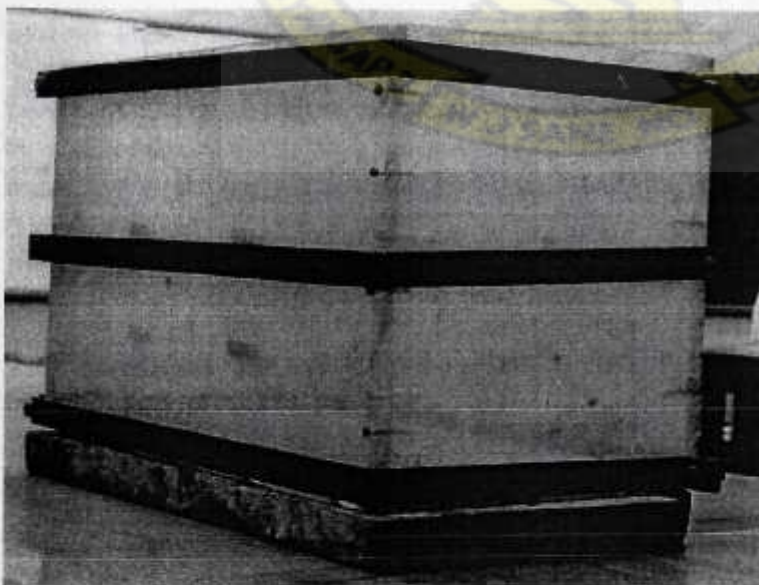


Figure 3.1 The Perspex Mould used for the Footing Model Test

The model footing was made of wooden block of dimensions, 300mm (length) x 150mm (width) and 50mm thick. The base of the model footing was made rough by gluing 60-grade sandpaper onto it as shown in Figure 3.2, to satisfy the rough footing base condition of Terzaghi's bearing capacity formula derivation.



Figure 3.2 Wooden Footing with 60-Grade Sandpaper glued to the Base

3.3.2 Loading and Measuring System

The loading system used was strain controlled set to a rate of 0.375mm penetration per minute (resulting in approximately 2 hours per loading test). The loading system consisted of a system of gears that push up the loading system. This system raised the whole loading platform against the fixed frame Figure 3.3. The proving ring readings at 0.5mm penetration intervals were taken. Prior to the start of the test, the proving ring was calibrated. The details of the calibration are presented in Appendix III.

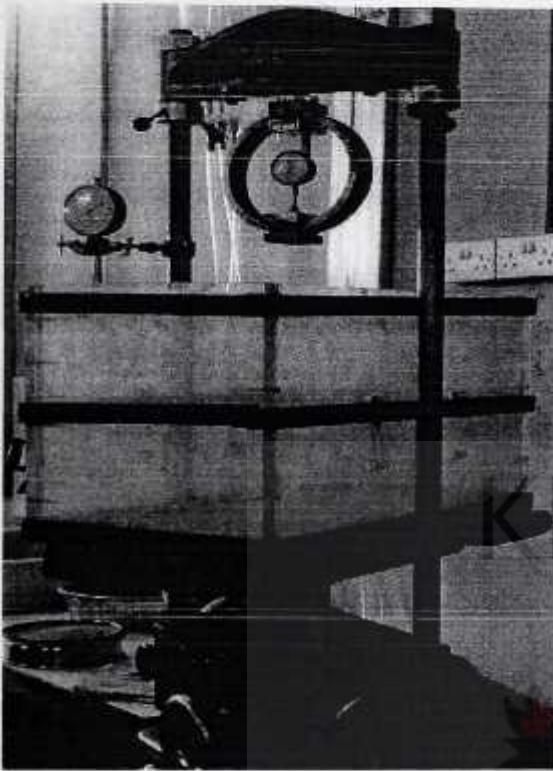


Figure 3.3 Picture of Triaxial Frame Used for loading test with the Mould in it

3.4 Model Sample Preparation

1. The existing moisture content (EMC) of the sample for each run of the model compaction was determined. The amount of water to be added to achieve optimum moisture content was computed from;

$$\text{Amount of water added} = \frac{OMC - EMC}{100 + EMC} \times M_s$$

where; OMC-Optimum moisture content,

EMC- Existing moisture content,

M_s - Mass of sample used.

The following procedure was followed for the model compaction;

2. About 120 kg of the stored sample was weighed and divided into four parts of about 30kg per part.

3. The amount of water required to achieve OMC was added to each part and mixed thoroughly in a large pan.
4. After mixing all the four parts, the mixture was heaped together in a large pan and covered with polythene sheet for about 16 hours for curing in order to equilibrate the moisture content.
5. The sample was then compacted in 6-layers in the perspex mould with each layer receiving 20 blows of the rammer, dropping through approximately 0.50m height.
6. The rammer consists of 190mm x 190mm square base wooden hammer with 1.36m long handle, weighing 6.06kg.
7. Steps 1-6 were repeated for 15, 30, 35, 100 and 150 blows respectively.

Figure 3.4 shows details of the wooden rammer used for the model's compaction.

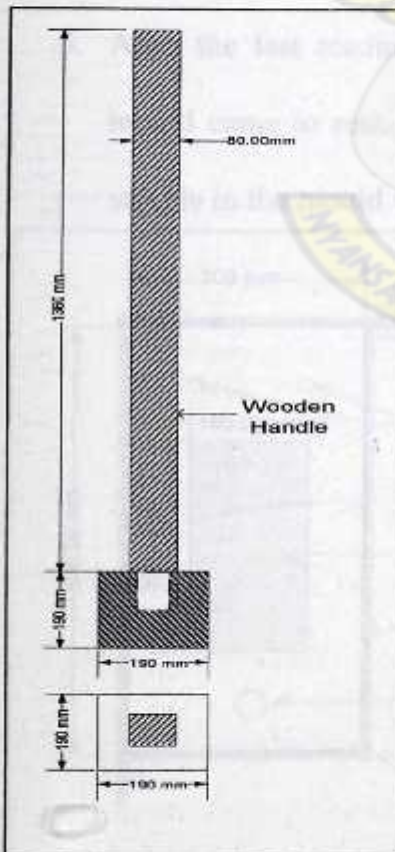


Figure 3.4 Wooden Rammer Used for the Model Compaction in Section and Plan

3.5 The Model Testing Procedure

1. The compacted sample in the mould was placed in the triaxial frame. The wooden footing was centrally positioned on the compacted sample as shown in Figure 3.5. and Figure 3.6.
2. The proving ring was lowered to make contact with the footing and the dial gauge was set fixed to the triaxial frame and making contact with the mould.
3. The loading system was then engaged and maintained at a rate of 0.375mm penetration per minute for the loading test until a settlement of at least 25% of the footing width (37.5mm) was attained.
4. The proving ring readings were taken at 0.0mm, 0.5mm, 1.0mm, 1.5mm, 2.0mm, until minimum penetration of 37.5mm was achieved. The dial gauge readings for the corresponding settlement were taken and recorded.
5. After the last readings were taken, the loading action was reversed until the mould came to rest. It was then lowered to the floor using manual crane. The sample in the mould was then used for the subsequent tests.

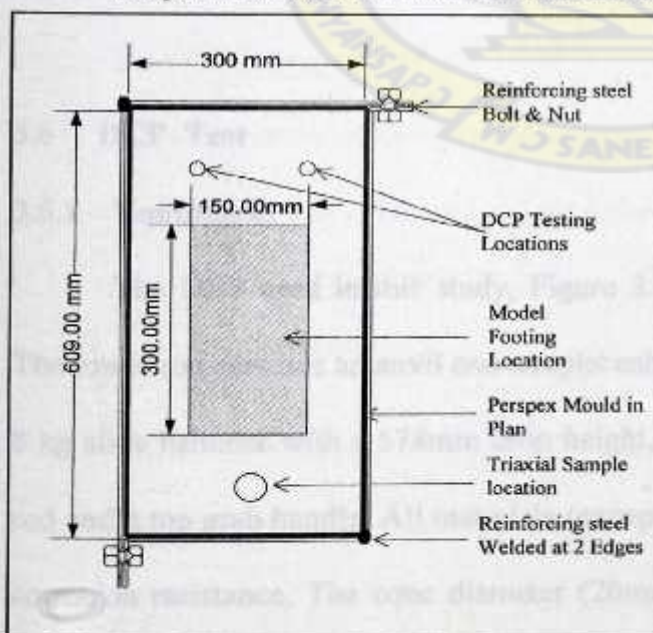


Figure 3.5 Plan of location of tests positions

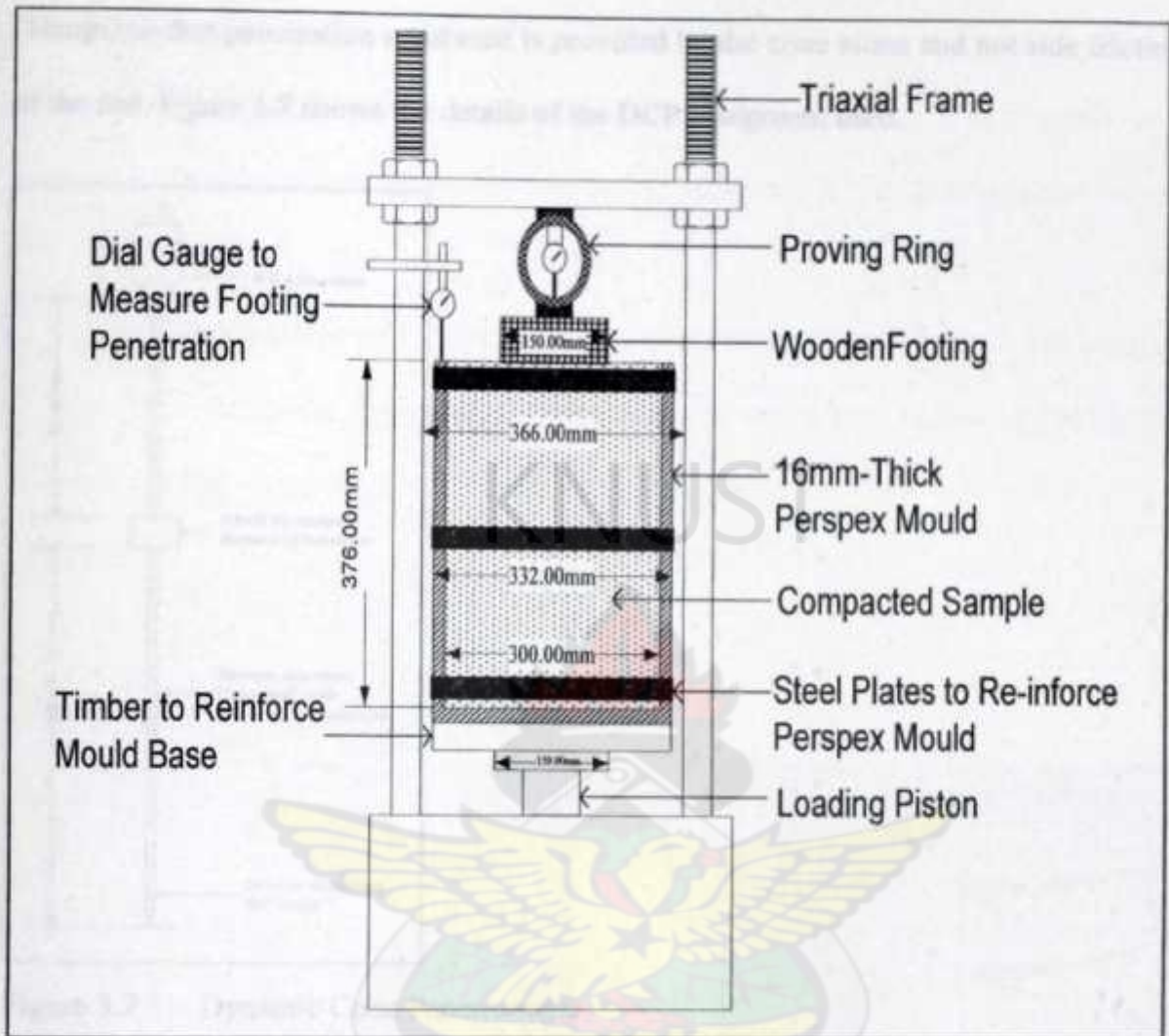


Figure 3.6 The Loading Test Set-Up with Mould filled in Section

3.6 DCP Test

3.6.1 Equipment

The DCP used in this study, Figure 3.7, consists of two 16mm diameter rods. The lower rod contains an anvil and a replaceable 60° apex cone. The upper rod contains 8 kg slide hammer with a 578mm drop height, an end plug for connection to the lower rod and a top grab handle. All materials (except the drop hammer) are stainless steel for corrosion resistance. The cone diameter (20mm) is made wider than the rod diameter

(16mm) so that penetration resistance is provided by the cone alone and not side friction of the rod. Figure 3.7 shows the details of the DCP equipment used.

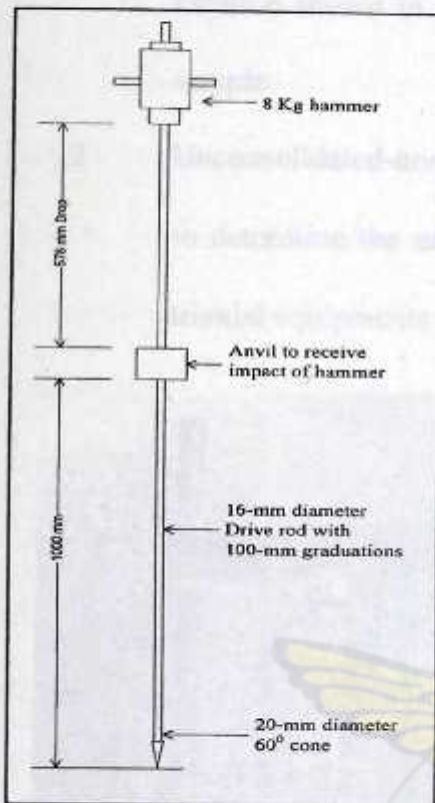


Figure 3.7 Dynamic Cone Penetrometer

3.6.2 Test Procedure

1. The DCP set up was held vertically and position at the desired test location.
2. The hammer was lifted and dropped from the specified height to initiate the test.
3. Following each blow of the hammer, the depth of penetration was measured and recorded as the D-value (mm/blow).
4. Steps 2 and 3 were continued until the desired depth of testing was reached.

After the testing was completed, a special adapted jack was used to extract the device.

3.7 Triaxial Test

- 1 A 38mm x 76mm sampling thin tube was pushed into the sample at a location shown in plan in Figure 3.5 in the mould, to obtain a triaxial test sample.
- 2 Unconsolidated-undrained triaxial tests were conducted on the cored samples to determine the undrained shear strength parameters (c_u and ϕ_u) using the triaxial equipments in Figure 3.8 and Figure 3.9.



Figure 3.8 Triaxial Test Set Up Used



Figure 3.9 Confining Pressure Unit

CHAPTER FOUR

RESULTS ANALYSIS AND DISCUSSIONS

4.1 Material Properties

The formation from which the sample was obtained for this investigation was reddish brown, sandy *CLAY* with some silt and muscovite mica. The log of the test pit is presented in Appendix I. The index properties and compaction characteristics of the sample tested in the laboratory are summarised in the Table 4.1 below and the details in Appendix II. Figure 4.1 and Figure 4.2 show the grading curve and compaction characteristics of the test sample respectively.

Figure 4.1 Particle Size Distribution on Test Sample

Table 4.1: Summary of Materials Properties

Clay	46%
Silt	12%
Sand	39%
Gravel	3%
% passing 75 μ m sieve	58%
Liquid limit (LL)	56%
Plastic limit (PL)	29%
Plasticity Index (PI)	27%
Specific gravity	2.65
Maximum Dry Density (MDD) (Standard Proctor)	1.68Mg/m ³
Optimum Moisture Content(OMC)	19%

Based on the unified soil classification system (ASTM D2487-60), the soil is classified as inorganic sandy *CLAY* with high plasticity (CH).

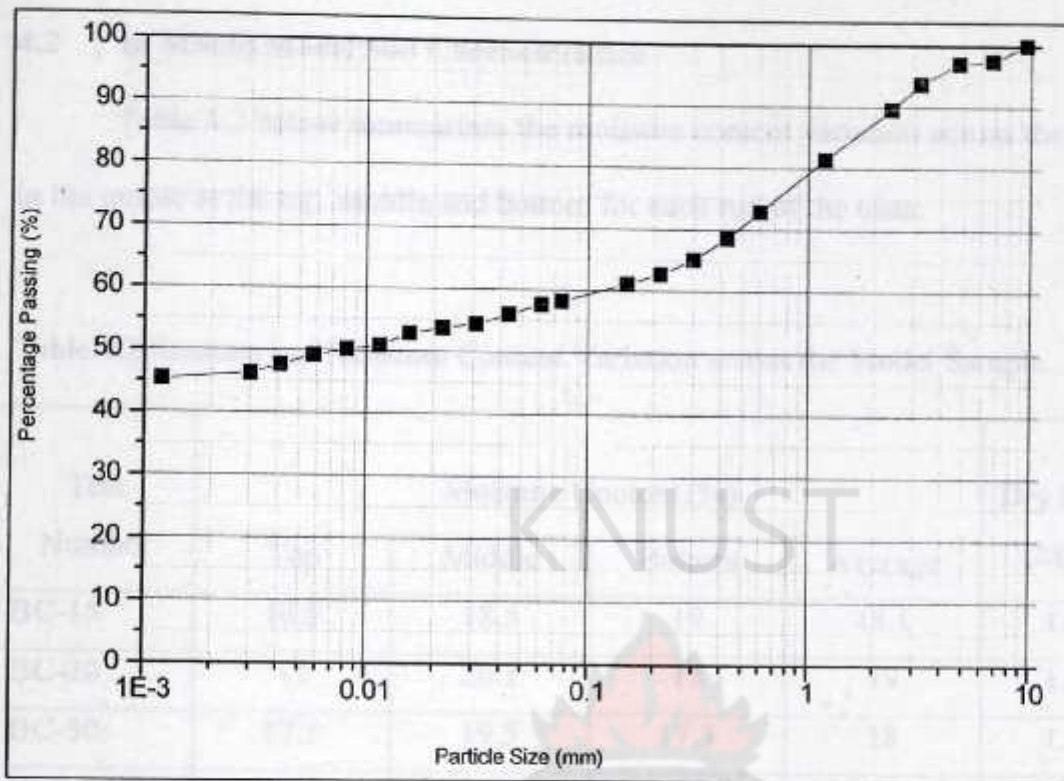


Figure 4.1 Particle Size Distribution Curve of the Test Sample

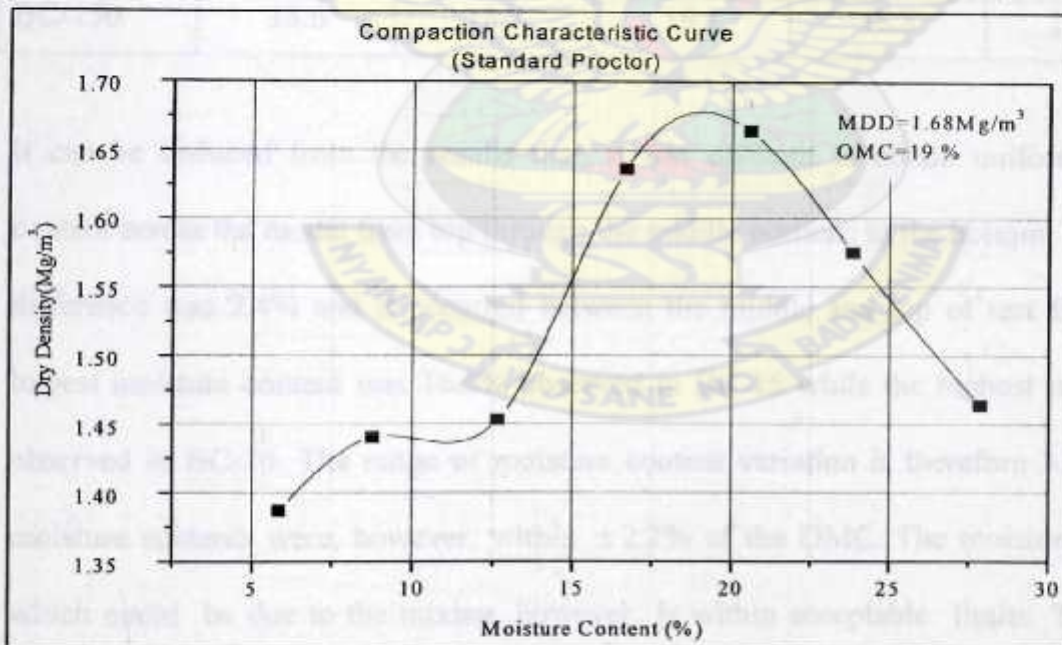


Figure 4.2 Compaction Characteristic Curve of the Test Sample

Based on the unified soil classification system (ASTM D2487-00), the soil is classified as inorganic sandy *CLAY* with high plasticity (CH).

4.2 In Mould Model Soil Characteristics

Table 4.2 below summarises the moisture content variation across the model soil in the mould at the top, middle and bottom for each run of the tests.

Table 4.2 Summary of Moisture Content Variation across the Model Sample

Test Number	Moisture Content (%)				Dry Density (Mg/m ³)
	Top	Middle	Bottom	Average	
BC-15	16.8	18.5	19	18.1	1.326
BC-20	19	20.1	18	19	1.345
BC-30	17.1	19.5	17.3	18	1.451
BC-35	18.8	18.9	18	18.5	1.500
BC-100	19.7	19.5	19.1	19.4	1.648
BC-150	18.6	18.7	19.1	18.8	1.775

It can be deduced from the results that, it was difficult to obtain uniform moisture content across the model from top through the middle portions to the bottom. The largest difference was 2.4% and it occurred between the middle and top of test BC-30. The lowest moisture content was 16.8% observed in BC-15 while the highest was 20.1 % observed in BC-20. The range of moisture content variation is therefore 3.3 %. The moisture contents were, however, within $\pm 2.2\%$ of the OMC. The moisture variation which could be due to the mixing, however is within acceptable limits. The sample may therefore be said to have been prepared at the OMC. Figure 4.3 shows the moisture content variation across the in mould sample.

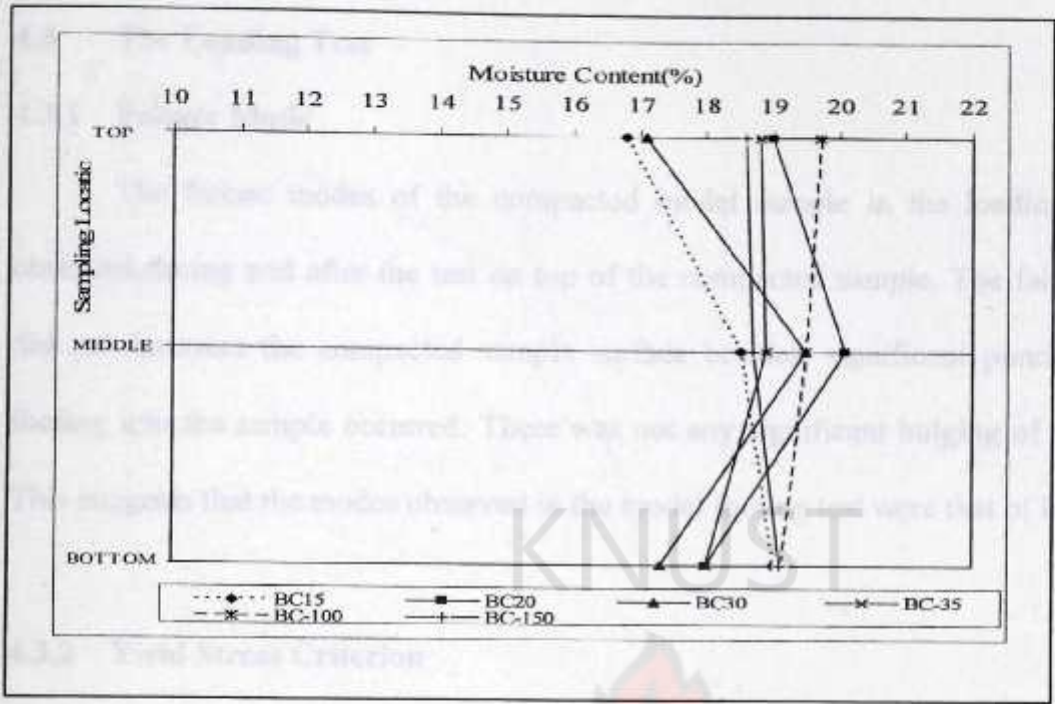


Figure 4.3 Mositure Content variation of the Model Sample

Figure 4.4 shows a plot of the dry density and average moisture content across the sample on the compaction curve. Figure 4.4 shows that, the objective of the model sample preparation for this study, which was to produce samples of different dry densities, was achieved within the range of 1.326 Mg/m^3 to 1.775 Mg/m^3 . These correspond to relative compaction of between 79% and 106%.

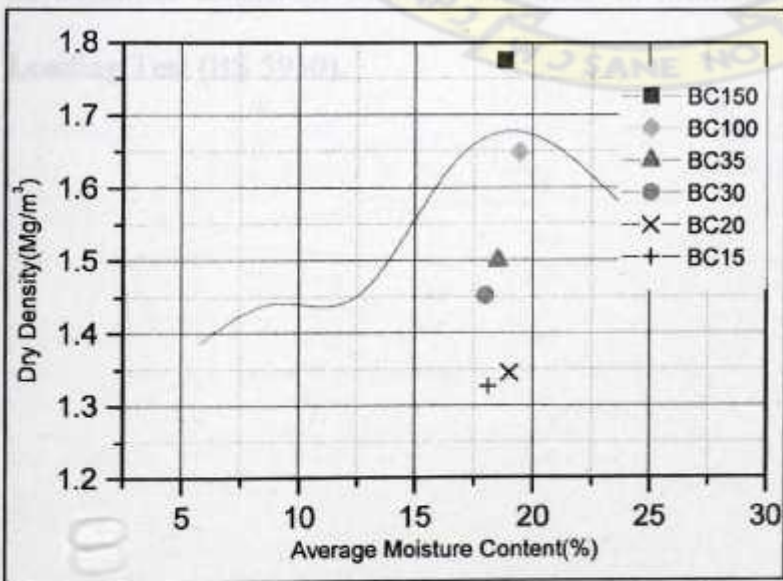


Figure 4.4 Starting Condition of the Test Sample

4.3 The Loading Test

4.3.1 Failure Mode

The failure modes of the compacted model sample in the loading test were observed during and after the test on top of the compacted sample. The failure surface did not intersect the compacted sample surface besides, significant punching of the footing into the sample occurred. There was not any significant bulging of the surface. This suggests that the modes observed in the model footing test were that of local shear.

4.3.2 Yield Stress Criterion

For local shear failures, the ultimate load is not well defined, it therefore becomes difficult to establish the ultimate load. In this study, the concept of yield stress, Q_Y criterion is used to define the limit of safe contact pressure at which the creeping settlement curve increases considerably with the corresponding yield settlement, S_Y . This pressure is the intersection point of the two slopes illustrated in the Figure 4.5 below. This pressure is also considered the allowable bearing pressure in this study. This definition is consistent with the definition of ultimate load in the evaluation of Plate Loading Test (BS 5930).

Sample Number	Density (ton/m ³)	Moisture Content (%)	Yield bearing stress q_Y (kN/m ²)	Yield settlement S_Y (mm)	Yield settlement ratio S_Y/q_Y (mm/kN/m ²)
BC-150	1.326	18.1	41	7.1	0.17
BC-200	1.345	19.0	83	12.6	0.15
BC-300	1.451	18.0	122	8.6	0.07
BC-350	1.500	18.5	143	8.6	0.06
BC-1000	1.642	19.4	266	7.1	0.03
BC-1500	1.725	18.9	394	8.1	0.02

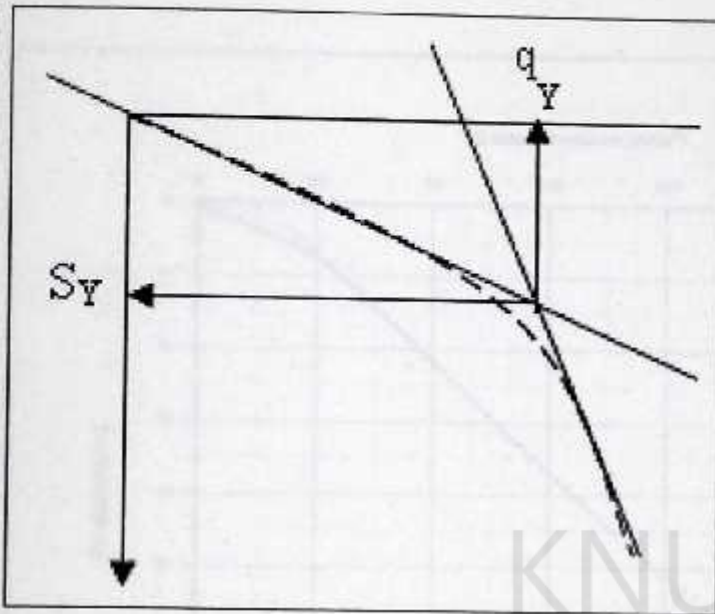


Figure 4.5 Definition of Yield Pressure

4.3.3 Model Footing Test Results

Six successful set of tests were conducted. For each set of tests, different compaction energy was used resulting in different dry density. A summary of the load test results is given in Table 4.3. Figure 4.6 to Figure 4.11 show the load- settlement curves for the various model tests with the details given included in Appendix IV.

Table 4.3: Summary of Loading Test Results

Test Number	Dry Density $\rho_{dry}(Mg/m^3)$	Average Moisture Content (%)	Yield Bearing stress $q_Y(kN/m^2)$	Yield settlement $s_Y(mm)$	Yield Stiffness $v = \frac{q_Y}{s_Y}$ ($kN/m^2/mm$)
BC-15/1	1.326	18.1	41	7.3	5.6
BC-20/1	1.345	19.0	83	12.6	6.6
BC-30/1	1.451	18.0	178	8.6	20.7
BC-35/1	1.500	18.5	183	8.6	21.3
BC-100/1	1.648	19.4	266	7.1	37.5
BC-150/1	1.775	18.8	331	8.1	40.9

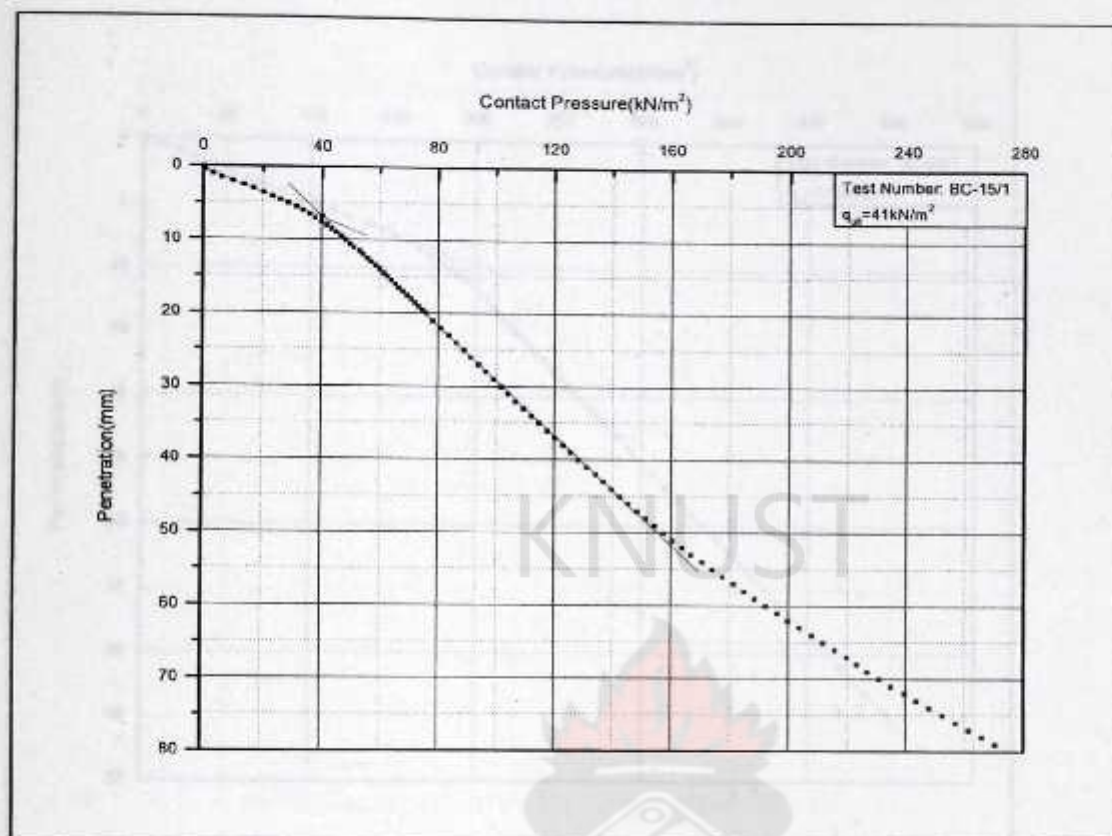


Figure 4.6 Load-Settlement Curve for Experiment BC-15

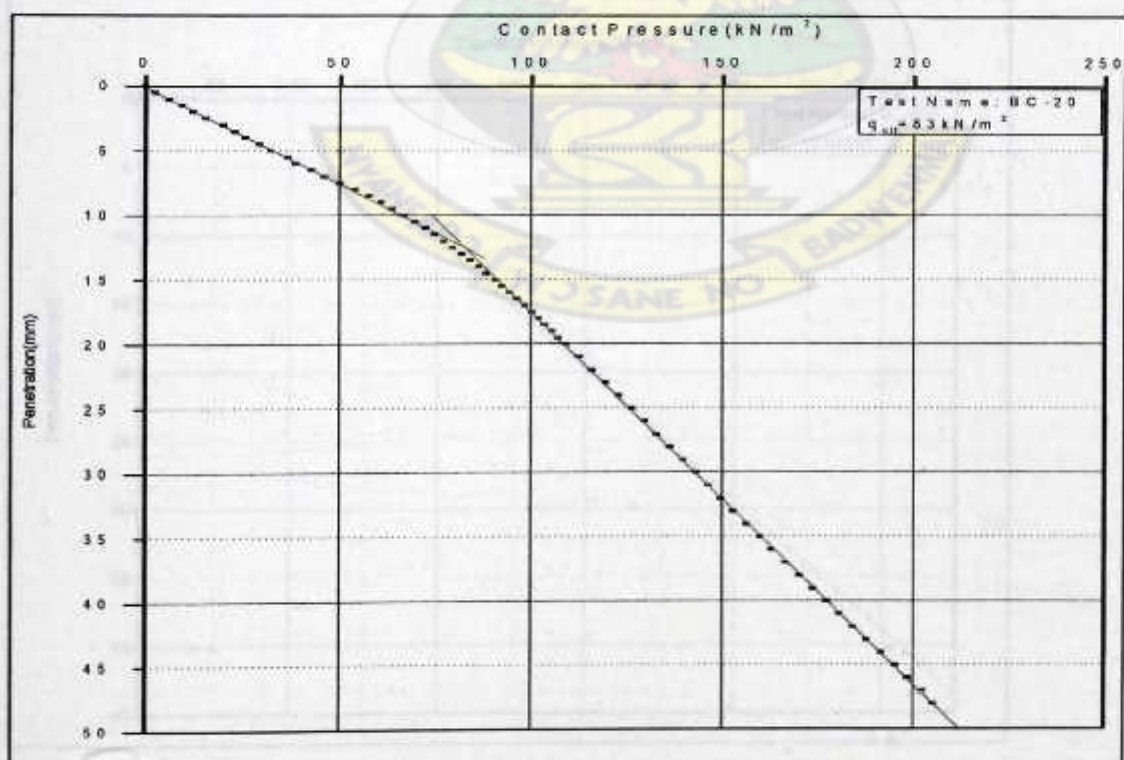


Figure 4.7 Load-Settlement Curve for Experiment BC-20

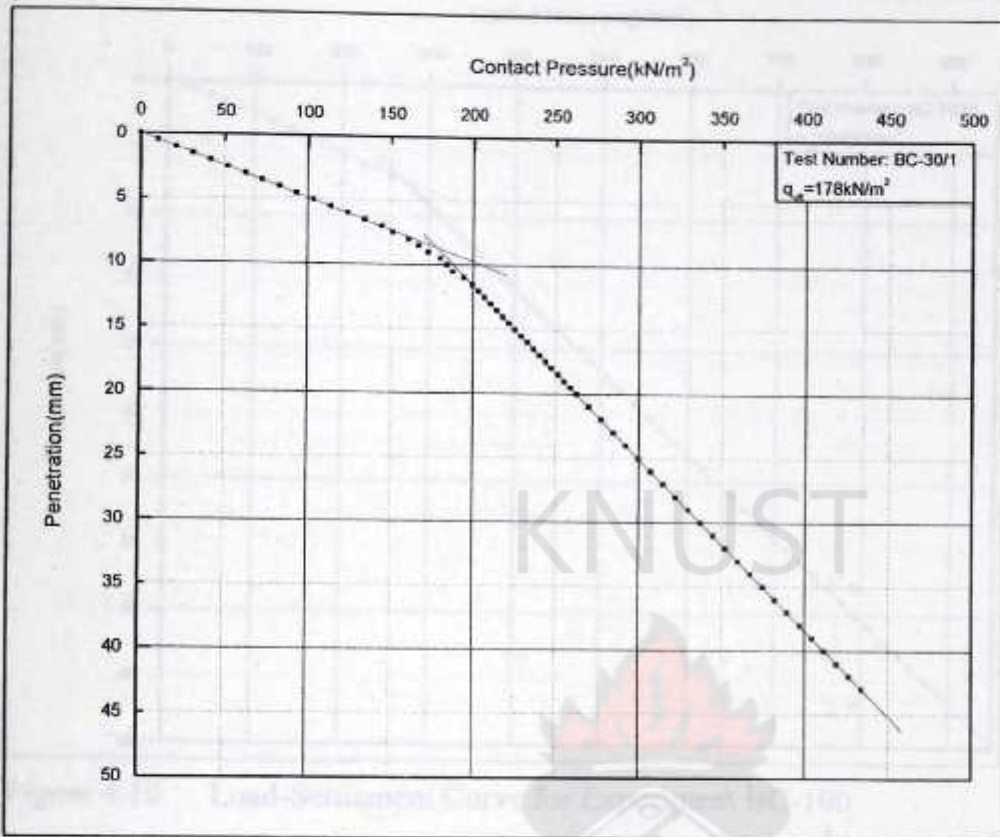


Figure 4.8 Load-Settlement Curve for Experiment BC-30

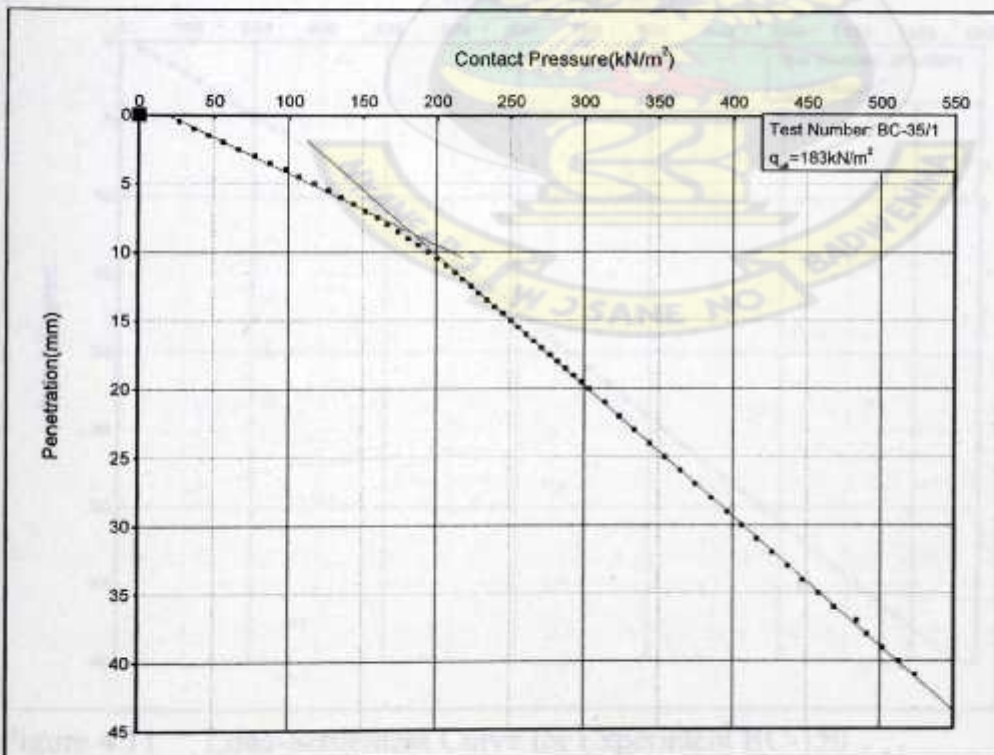


Figure 4.9 Load-Settlement Curve for Experiment BC-35

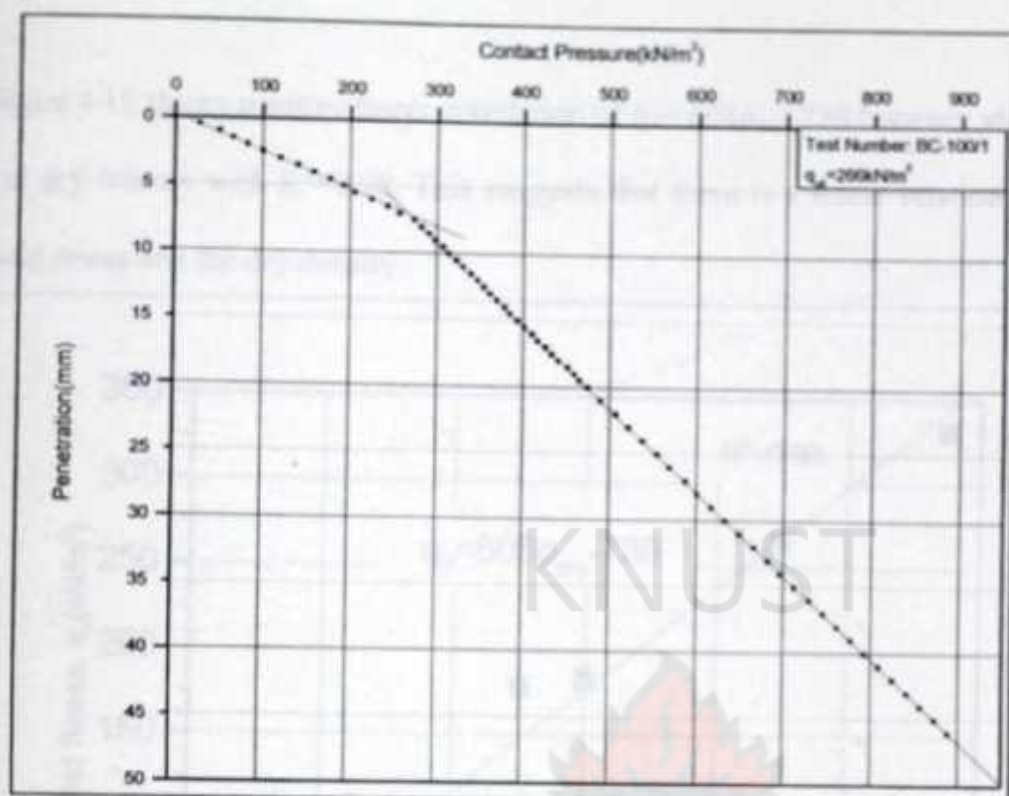


Figure 4.10 Load-Settlement Curve for Experiment BC-100

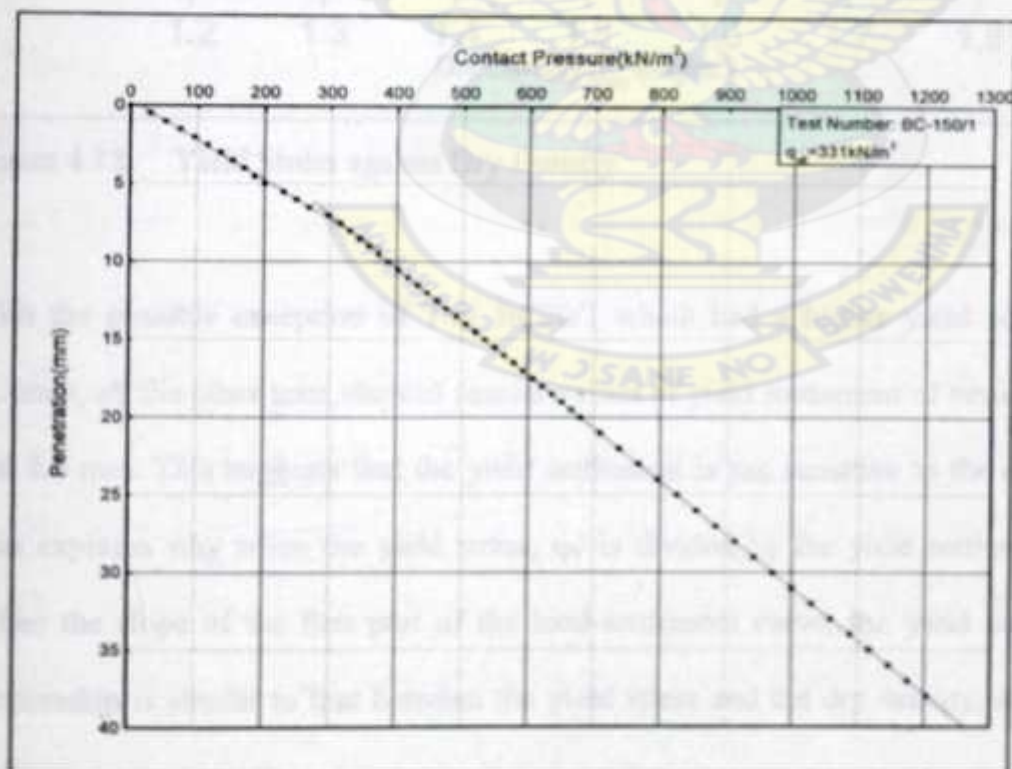


Figure 4.11 Load-Settlement Curve for Experiment BC-150

Figure 4.12 shows positive linear correlation of $q_Y = 608\rho_{dry} - 736$ between yield stress, q_Y and dry density with $R^2=0.98$. This suggests that there is a linear relation between the yield stress and the dry density.

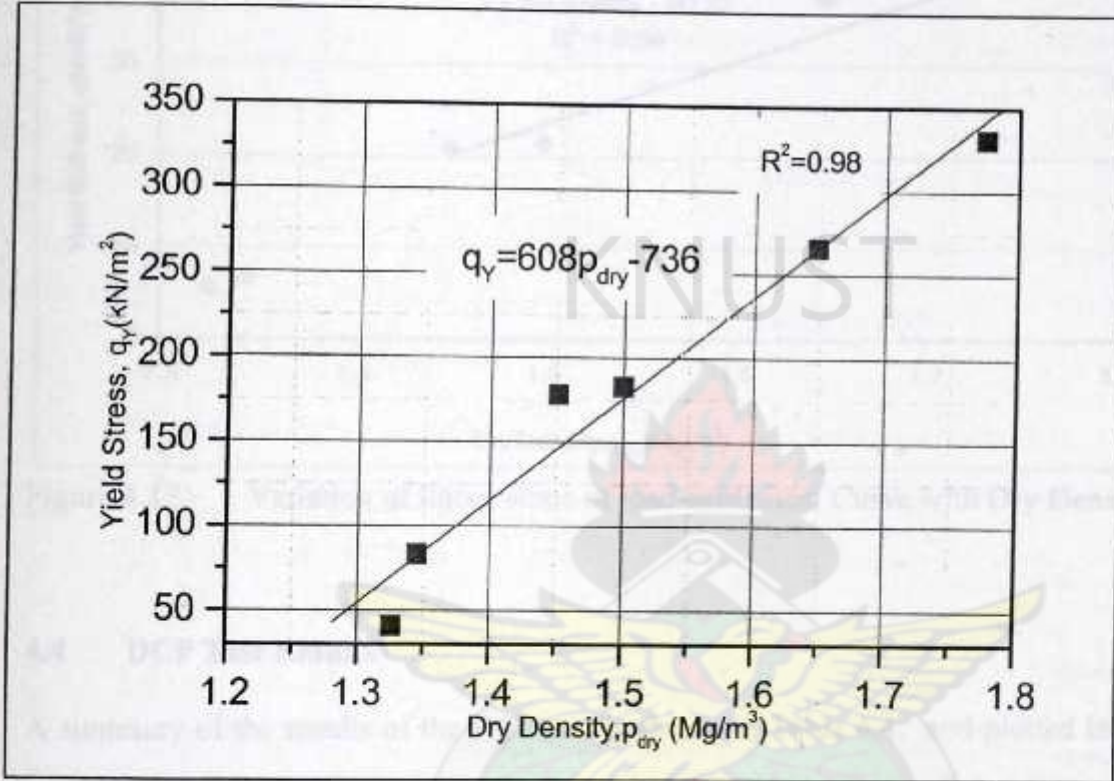


Figure 4.12 Yield Stress against Dry Density

With the possible exception of Test BC20/1 which had a higher yield settlement of 12.6mm, all the other tests showed similar values of yield settlement of between 7.1mm and 8.6 mm. This suggests that the yield settlement is not sensitive to the dry density. This explains why when the yield stress, q_Y is divided by the yield settlement, S_Y to define the slope of the first part of the load-settlement curve, the yield stiffness, the relationship is similar to that between the yield stress and the dry density, as in Figure 4.13

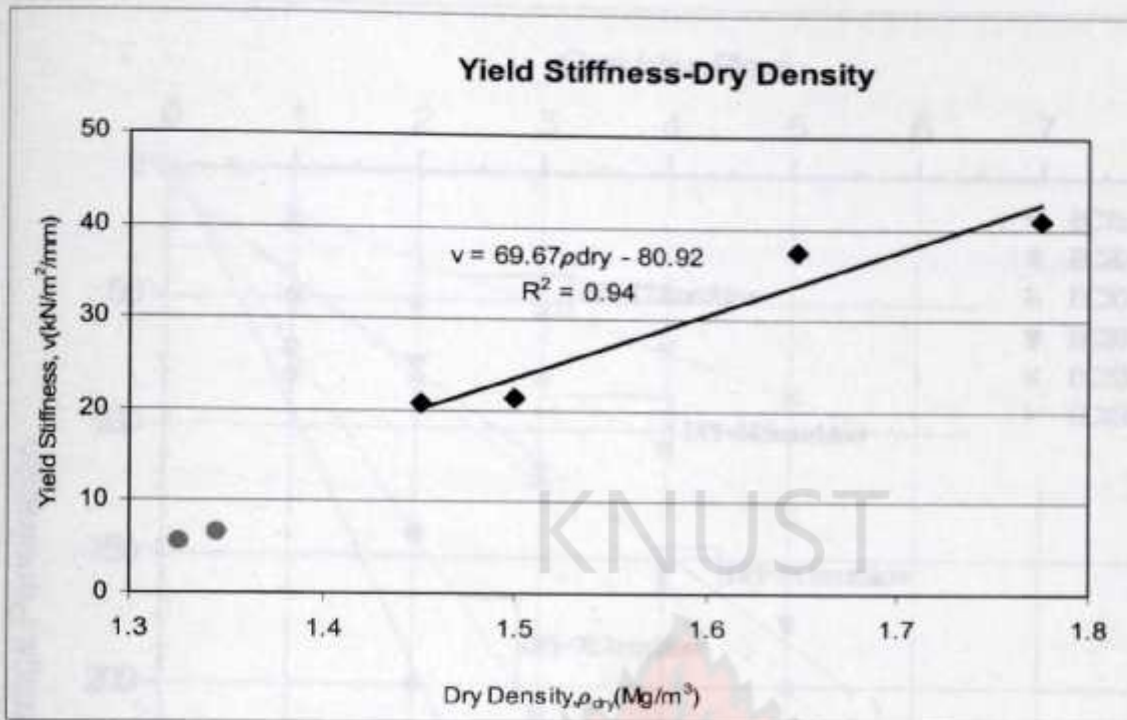


Figure 4.13 Variation of Initial slope of load-settlement Curve with Dry Density

4.4 DCP Test Results

A summary of the results of the DCP test is shown in Table 4.4. and plotted in Figure 4.14. Each DCP penetration value is the average of two readings taken from adjacent test locations. The average D-values also known as the Dynamic Penetration Index (DPI), is the penetration produced by one drop of the sliding hammer and it is obtained as the gradient of the line of best fit of the graph of cumulative blows against penetration in mm as shown Figure 4.14. In field, however, the number of blows required to advance the cone by 100mm into the soil is what is measured and recorded as the n-value. The n-values (blows/100mm) in this study were derived from the D-values by dividing 100mm by the D-values. The details of the DCP test results are presented in Appendix V.

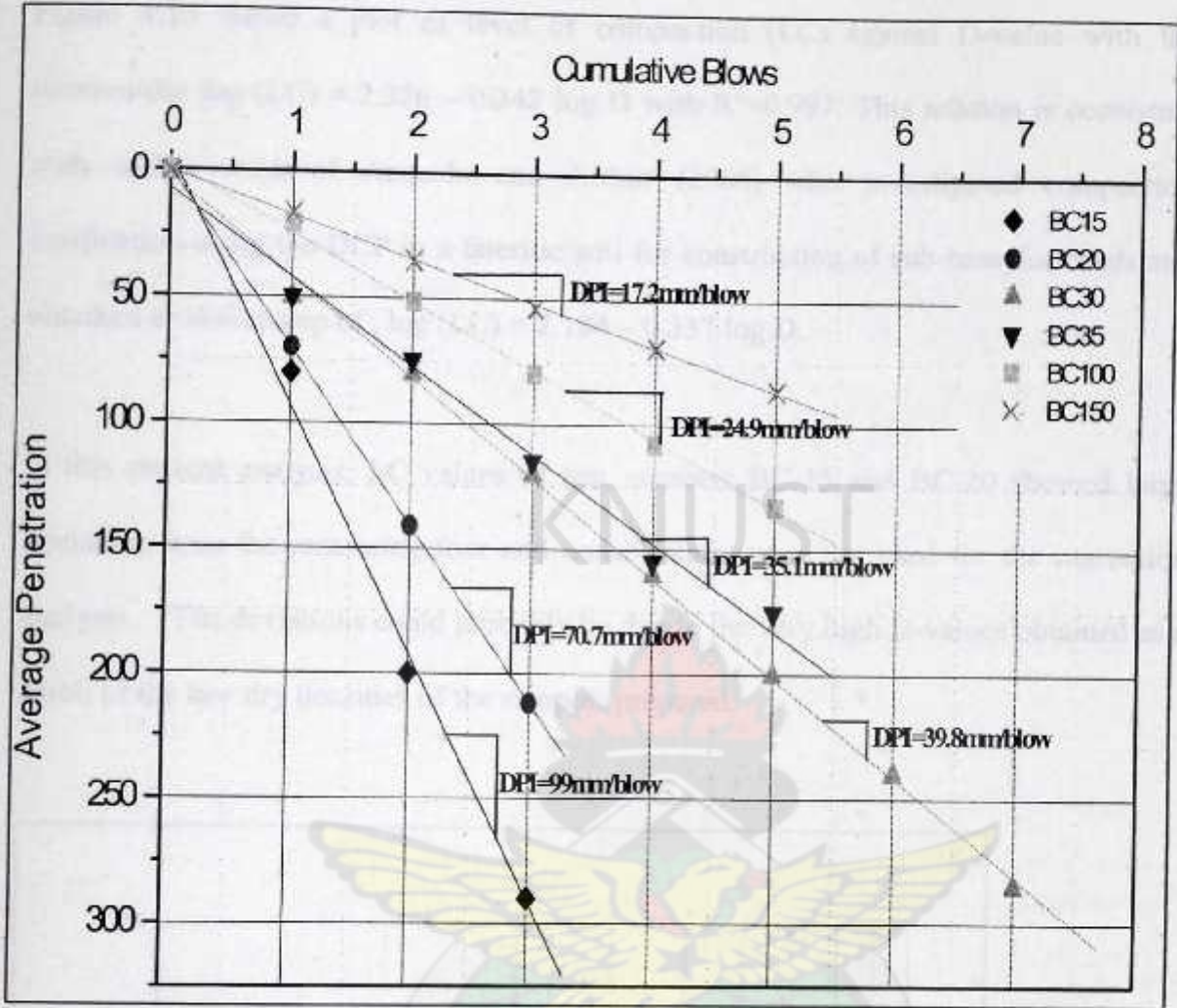


Figure 4.14 Plot of Average DCP Penetration against Cumulative No. of Blows

Table 4.4: Summary of DCP Test Results

Test Number	D-value (mm / blow)	Moulding Water Content (%)	Dry Density, $\rho_{dry}(Mg/m^3)$	Level of Compaction, LC (%)
BC-15	99	18.1	1.326	79
BC-20	70.7	19	1.345	80
BC-30	39.8	18	1.451	86
BC-35	35.1	18.5	1.500	89
BC-100	24.9	19.4	1.648	98
BC-150	17.2	18.8	1.775	106

Figure 4.15 shows a plot of level of compaction (LC) against D-value with the relationship $\log (LC) = 2.326 - 0.242 \log D$ with $R^2=0.997$. This relation is consistent with earlier work of Ampadu and Arthur (2006) who investigated compaction verification using the DCP in a lateritic soil for construction of sub-base for roads and obtained a relationship of , $\log (LC) = 2.184 - 0.337 \log D$.

In this present analysis, LC values of test numbers BC-15 and BC-20 showed large deviation from the remaining four and consequently were not used for the regression analysis. . The deviations could probably be due to the very high D-values obtained as a result of the low dry densities of the samples prepared.

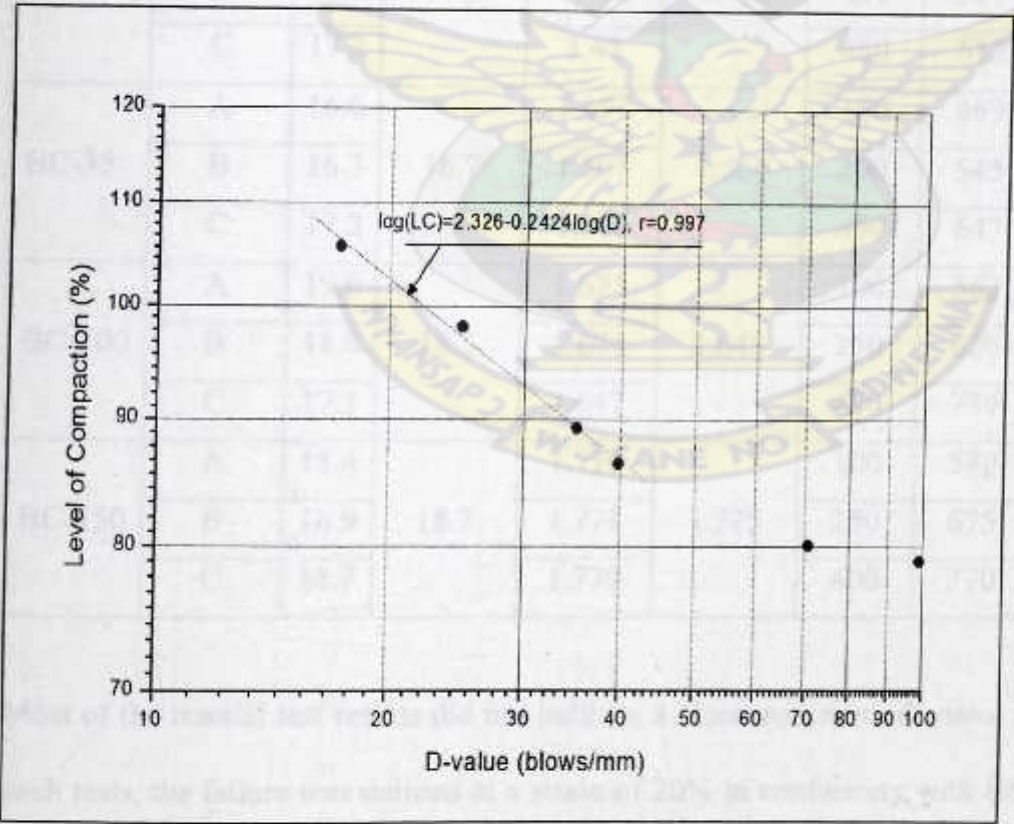


Figure 4.15 Plot of level of compaction (LC) against D-value

4.5 Allowable Bearing Pressure from the Triaxial Test

A summary of the triaxial tests results is shown in Table 4.5 below. The detailed triaxial tests data and graphs are shown in Appendix VI.

Table 4.5 Summary of the Triaxial Results

TEST NO.	Sample Number	Moisture Content (%)		Dry Density (Mg/m ³)		σ_3 (kPa)	$\sigma_1 - \sigma_3$ (kPa)	C_u (kN/m ²)	ϕ (°)
			Average		Average				
BC-15	A	16.1	16.3	1.325	1.326	150	372	126	11
	B	16.5		1.327		300	469		
	C	16.2		1.326		450	517		
BC-20	A	16.2	16.5	1.348	1.345	150	420	135	13
	B	16.8		1.342		300	504		
	C	15.1	15.1	1.367	1.367	450	533		
BC-30	A	16	17.1	1.461	1.451	150	448	144	13
	B	17.9		1.442		300	524		
	C	17.3		1.45		450	618		
BC-35	A	16.6	16.7	1.497	1.500	150	469	149	13
	B	16.3		1.503		300	545		
	C	17.2		1.501		450	647		
BC-100	A	19.6	18.5	1.623	1.648	100	567	199	13
	B	18.8		1.674		250	624		
	C	17.1		1.647		400	739		
BC-150	A	18.4	18.7	1.776	1.775	100	589	208	13
	B	18.9		1.771		250	675		
	C	18.7		1.779		400	770		

Most of the triaxial test results did not indicate a clear maximum deviator stress, S_f . For such tests, the failure was defined at a strain of 20% in conformity with BS 1377 part 7. The triaxial test result of sample BC-20 C was not used in the analysis. This was due to drastic loss of moisture prior to the triaxial test. From the stress – strain graphs of the

triaxial test, the deviator stresses at failure, S_f and confining pressures were used to plot Mohr circles. From the Mohr circles, the undrained cohesion intercept, c_u and angle of internal friction ϕ_u were deduced, and used to calculate the allowable bearing pressure.

The stiffness of the samples tested is defined in terms of the E_{50} which is the stiffness at half the deviator stress. In order to take into account the effect of confining pressure, the stiffness values have been divided by the mean pressure, p . These values have been plotted against the dry density in Figure 4.16. From the graph, there seems to be no correlation between the two parameters in this work.

Table 4.6 Stress-Strain Analysis of the Triaxial Results

Test Number	Moisture Content (%)	Dry Density, (Mg/m ³)	σ_3 (kN/m ²)	*p (kN/m ²)	S_f (kN/m ²)	ϵ_{50} (%)	E_{50} (kN/m ²)	$\frac{E_{50}}{p}$
BC-15-150	16.1	1.325	150	274	372	7.5	2,480	9.1
BC-15-300	16.5	1.327	300	456	469	7.4	3,169	6.9
BC-15-450	16.2	1.326	450	622	517	6.8	3,801	6.1
BC-20-150	16.2	1.348	150	290	420	2.9	7,241	25.0
BC-20-300	16.8	1.342	300	468	504	2.3	10,957	23.4
BC-30-150	16.0	1.461	150	299	448	2.5	8,960	29.9
BC-30-300	17.9	1.442	300	475	524	1.9	13,789	29.1
BC-30-450	17.3	1.45	450	656	618	1.1	28,091	42.8
BC-35-150	16.6	1.497	150	306	469	1.8	13,028	42.5
BC-35-300	16.3	1.503	300	482	545	1.7	16,029	33.3
BC-35-450	17.2	1.501	450	666	647	1.4	23,107	34.7
BC-100-100	19.6	1.623	100	289	567	4.5	6,300	21.8
BC-100-250	18.8	1.674	250	458	624	3.1	10,065	22.0
BC-100-400	17.1	1.647	400	646	739	3.1	11,919	18.4
BC-150-100	18.4	1.776	100	296	589	4.3	6,849	23.1
BC-150-250	18.9	1.771	250	475	675	2.3	14,674	30.9
BC-150-400	18.7	1.779	400	657	770	1.7	22,647	34.5

$$*p = \frac{\sigma_1 + 2\sigma_3}{3}$$

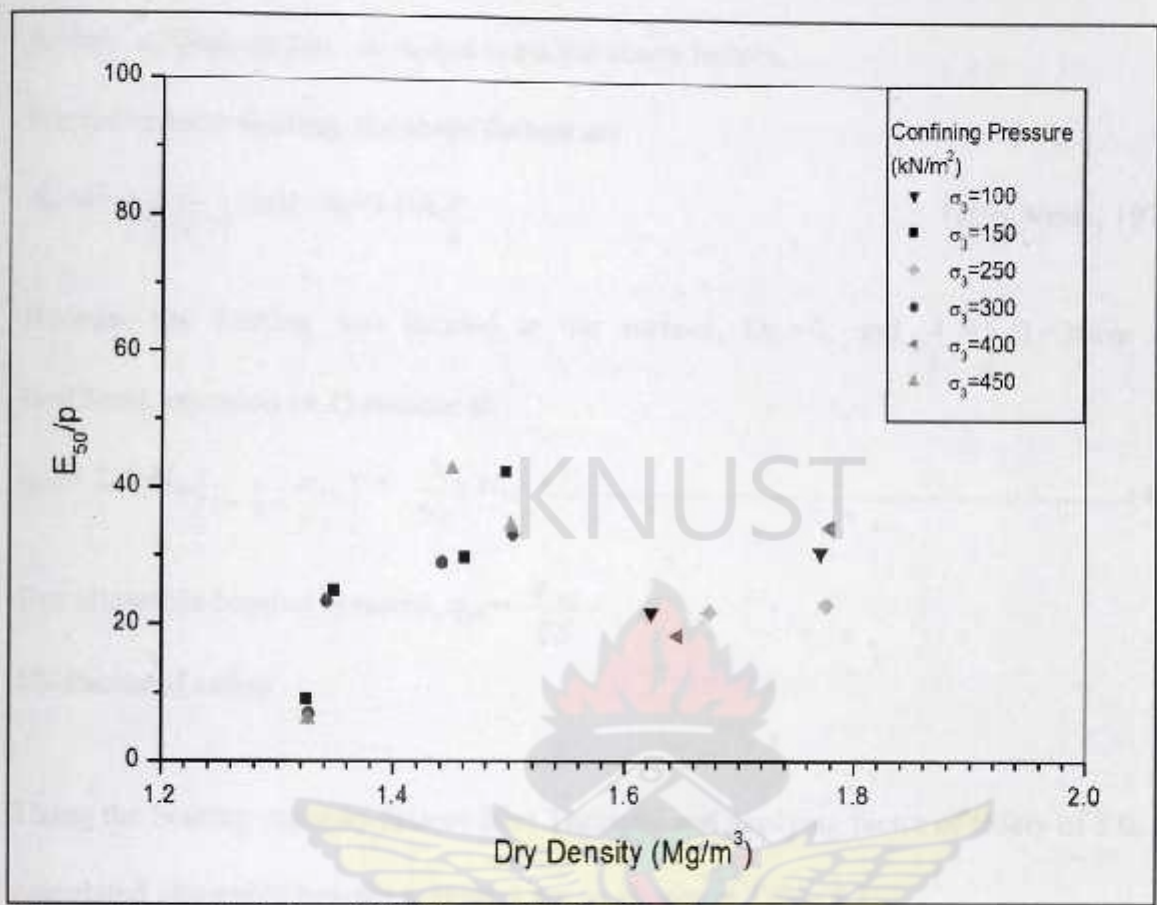


Figure 4.16 Variation of Stiffness with Dry Density

4.5.1 Allowable Bearing Pressure

The allowable bearing pressure from the triaxial results was calculated using the Terzaghi bearing capacity equation for local shear failure, taking the footing shape factors into consideration and applying a factor of safety to the ultimate bearing capacity, q_{ult} to obtain q_{all} .

$q_{ult} = 2/3c N_{lc} s_c + \gamma D_f N_{lq} s_q + 1/2 \gamma B N_{ly} s_\gamma$ (4.1)

where the values of N_{lc} , N_{lq} and N_{ly} are obtained by replacing ϕ by ϕ_1 and reading the bearing capacity factors from Terzaghi bearing capacity chart.

Being a local shear failure mode,

$\phi_1 = \tan^{-1} (2/3 \tan \phi)$ and s_c, s_q and s_γ are the shape factors.

For rectangular footing, the shape factors are

$$S_c = 1 + \frac{B}{L} \left(\frac{N_q}{N_c} \right) \text{ and } S_\gamma = 1 - 0.4 \frac{B}{L} \quad (\text{after Vesic, 1973})$$

Because the footing was located at the surface, $D_f = 0$, and $\frac{B}{L} = \frac{1}{2}$ ($L=30\text{cm}$ and $B=15\text{cm}$), equation (4.1) reduces to

$$q_{ult} = 2/3 c N_{1c} \left(1 + \frac{1}{2} \times \frac{N_{1q}}{N_{1c}} \right) + \frac{3}{50} \gamma N_{1\gamma} \quad (4.2)$$

But allowable bearing pressure, $q_{all} = \frac{q_{ult}}{FS}$,

FS-Factor of safety

Using the bearing capacity factors after Terzaghi and applying factor of safety of 3.0, the calculated allowable bearing pressures are as shown in Table 4.7.

Table 4.7 Computation of Allowable Bearing Pressure.

Test Number	c_u	ϕ (°)	ϕ_1 (°)	N_{1c}	N_{1q}	$N_{1\gamma}$	γ_{bulk} kN/m ³	q_{ult} (kN/m ²)	q_{all} (kN/m ²)
BC-15	126	11	7	8	1.8	0.9	15.1	748	249
BC-20	135	13	9	9	2.4	1	15.4	918	306
BC-30	144	13	9	9	2.4	1	16.7	979	326
BC-35	149	13	9	9	2.4	1	17.2	1013	338
BC-100	199	13	9	9	2.4	1	19.2	1353	451
BC-150	208	13	9	9	2.4	1	20.7	1415	472

4.6 Correlation between D-value, n-value and Allowable Bearing Pressure, q_{all}

A summary of model yield stress, allowable bearing pressure by Terzaghi approach, the D-value and n-values have been presented in Table 4.8. The model yield stress is take to be the allowable bearing pressure for the model

Table 4.8 Summary of the Allowable Bearing pressures, D-value and n-value.

Test Number	Allowable Bearing Pressure (kN/m ²)		D-value (Mm/blow)	n-Value (blows/100mm)
	Model	Terzaghi Approach		
BC-15	41	249	99	1.0
BC-20	83	306	70.7	1.4
BC-30	178	326	39.8	2.5
BC-35	183	338	35.1	2.8
BC-100	266	451	24.9	4.0
BC-150	331	472	17.2	5.8

In order to establish the relevant correlations, the allowable bearing pressures have been plotted against the D-values and n-values in Figure 4.18 and Figure 4.19 respectively.

The regressions for the correlation equations did not include the two data points for the very soft samples. The regression analysis of the data points gave the following correlations;

$$q_{all(model)} = 48.3n + 57.3,$$

$$R^2=0.988$$

$$q_{all(model)} = 881-443.9\log_{10}(D),$$

$$R^2=0.993, \text{ by model footing, and}$$

$$q_{all(Terzaghi)} = 46.4n + 222$$

$$R^2=0.921,$$

$$q_{all(Terzaghi)} = 1030-439.1\log_{10}(D),$$

$$R^2=0.953 \text{ by Terzaghi approach.}$$

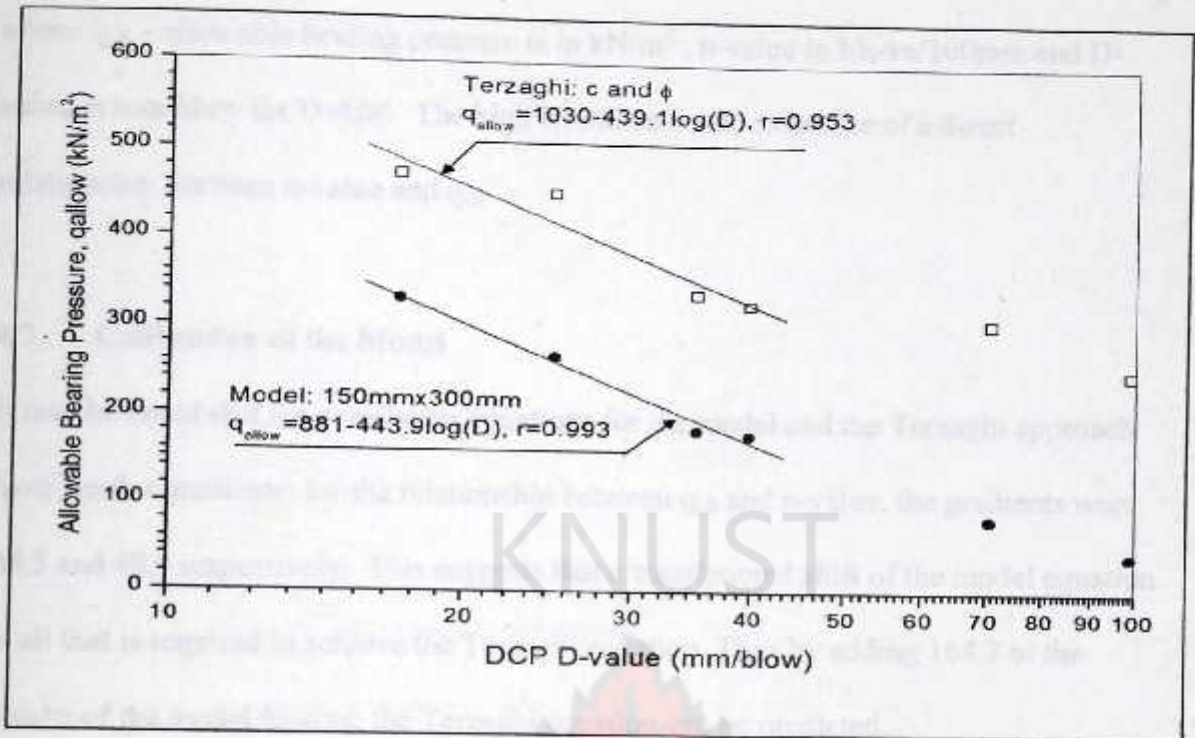


Figure 4.17 Correlation between Allowable Bearing Pressure and D-value for the Model and Terzaghi Approach

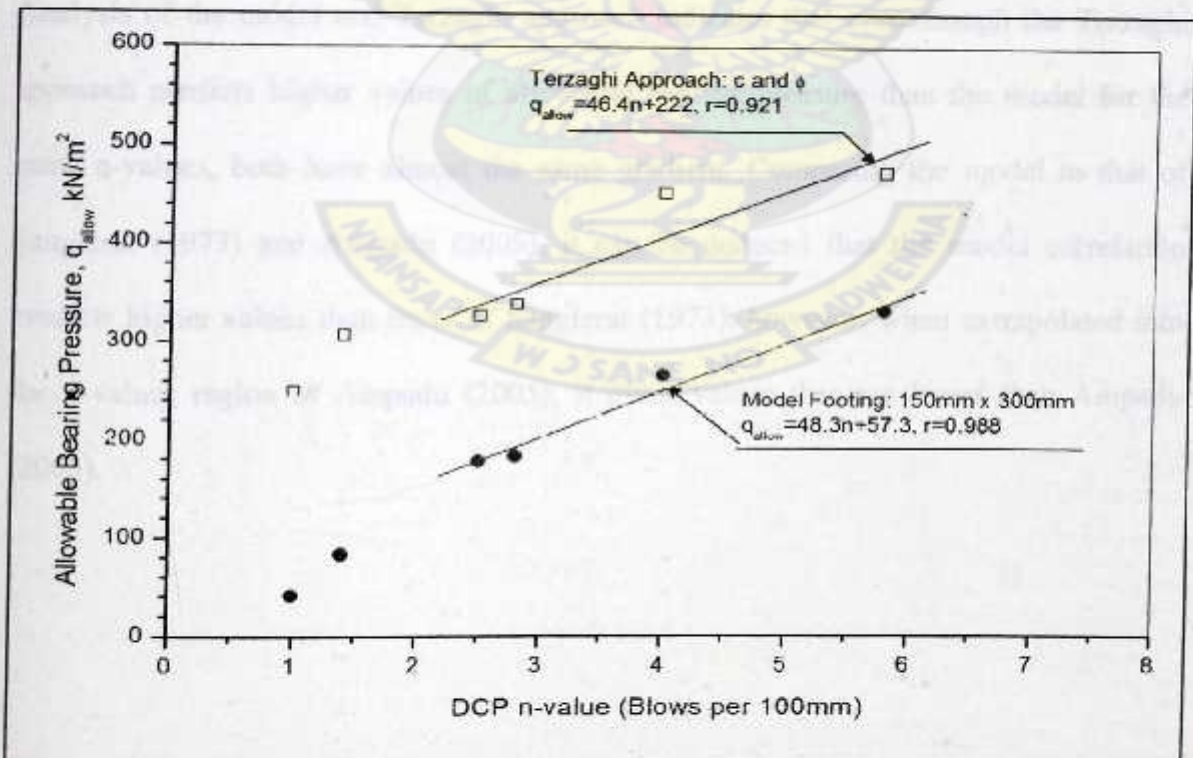


Figure 4.18 Correlation between Allowable Bearing Pressure and n-value for Model and Terzaghi Approach

where q_{all} – allowable bearing pressure is in kN/m^2 , n -value in blows/100mm and D -value in mm/blow for $D \leq 100$. The high R^2 indicates the existence of a direct relationship between n -value and q_{all} .

4.7 Calibration of the Model

It may be noted that the correlation equations for the model and the Terzaghi approach have similar gradients; for the relationship between q_{all} and n -value, the gradients were 48.3 and 46.4 respectively. This suggests that a translational shift of the model equation is all that is required to achieve the Terzaghi equation. Thus by adding 164.7 to the results of the model footing, the Terzaghi equation can be predicted.

4.8 Comparison of the Model to Similar Works

Analysis of the model and Terzaghi approach indicates that even though the Terzaghi approach predicts higher values of allowable bearing pressure than the model for the same n -values, both have almost the same gradient. Comparing the model to that of Sanglerat (1973) and Ampadu (2005), it can be deduced that the model correlation predicts higher values than those of Sanglerat (1973), however, when extrapolated into the n -values region of Ampadu (2005), it gives values that are lower than Ampadu (2005).

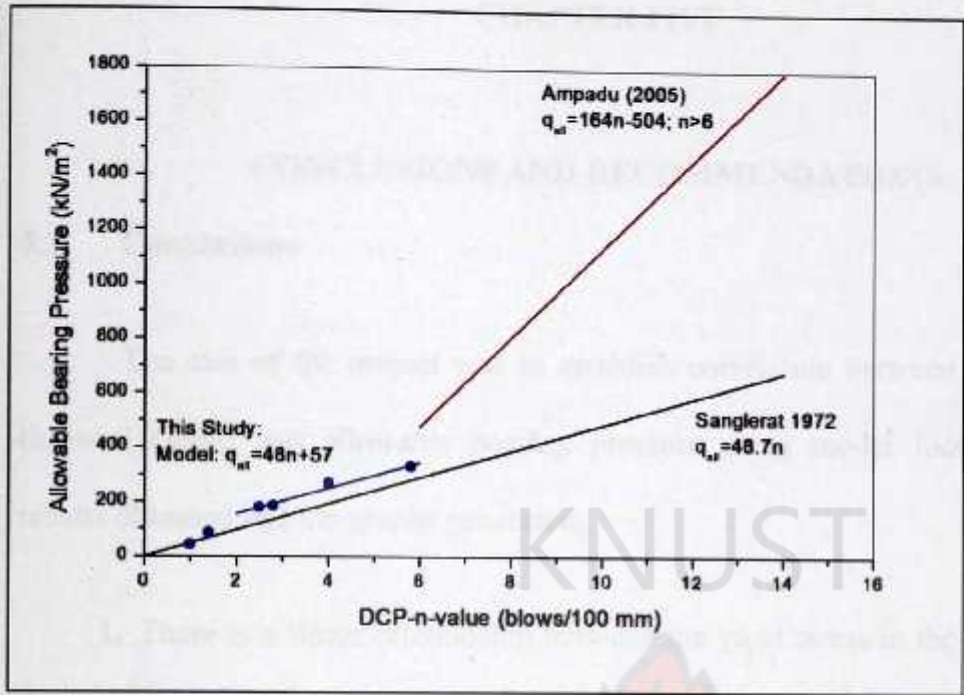


Figure 4.19 Comparisons between Ampadu (2005), Sanglerat (1972), and the Model



CHAPTER FIVE

CONCLUSIONS AND RECOMMENDATIONS

5.1 Conclusions

The aim of the project was to establish correlation between DCPT n-value (blows/100mm) and allowable bearing pressure using model footing. From the results obtained and the graphs generated,

1. There is a linear relationship between the yield stress in the model test and the dry density of the model ground given by $q_Y = 608\rho_{dry} - 736$ with $R^2 = 0.98$.
2. There is a log – log relationship between the level of compaction of the model ground and the DCP D-value given by $\log(LC) = 2.326 - 0.242 \log(D)$ with $R^2 = 0.997$.
3. The stiffness of the model ground normalized by the mean pressure as measured in the triaxial test appears insensitive to the dry density.
4. There is a linear relationship between the allowable bearing pressure and the DCP n-value and this equation has similar gradient for allowable bearing pressure obtained by both the model footing and by the Terzaghi approach.
5. The relationship between n-value and allowable bearing pressure for the calibrated model is given by $q_{all} = 48n + 57$, for $2 < n < 6$

This relationship predicts marginal higher allowable bearing pressure values than that of Sanglerat (1972).

5.2 Recommendations

It is recommended that;

- A simple loading system should be procured for this type of work in the future. The existing loading system makes the work too cumbersome requiring a lot of physical strength.
- Additional works should be done with higher n -values for similar sandy Clay material so as to validate the established correlation over wider range.



REFERENCES

America Society of Testing and Materials D2487-00(USC), D3441-03(CPT), D6951-03(DCPT). *Annual Book of Standards*.

Amini, F., (2003). "*Potential Application of Dynamic and Static Cone Penetrometers in Mississippi Department of Transportation Pavement Design and Construction*", Final Report ,Mississippi Department of Transportation-USA.

Ampadu, S.I.K., (2005). "*A Correlation between the Dynamic Cone Penetrometer and Bearing Capacity of a Local Soil Formation*", 16th ICSMGE, Osaka, Japan, pp655-659.

Arora, K.,R.(2000). "*Soil Mechanics and Foundation Engineering*", 4th Edition, New Delhi

Braja, M.D.,(1985). "*Principles of Foundation Engineering*", PWS Publishers Boston.

British Standard 1377 Part 2: 1990, BS1377 Part4:1990, BS1377 Part 7: 1990, BS1377 Part 9: 1990, BS 5930.

Brouwer, J.J. M., (2002). "*Guide to Cone Penetration Testing*" First Edition www.concpenetration.com.

Burnham, T., and Johnson, D., (1993). "*In- situ Foundation Characterization using the Dynamic Cone Penetrometer*", Study Report No. 9PR 3001, Minnesota Department of Transportation-USA.

Cearns, P.,J., and McKenzie, A.,(1988). "*Application of Dynamic Cone Penetrometer Testing in East Anglia*" Symposium on Penetration Testing in UK, Thomas Telford, London , pp123-137.

Cerato, A.B., and Lutenecker, A. J., (2003). "Scale Effects of Shallow Foundation Bearing Capacity on Granular Materials", Proceedings of the British Geotechnical Association international conference on foundations pp217-225.

Consallan Group Sales Ltd (2008). "Proforma Invoice to Architectural and Engineering Services Limited, Accra", Sudbury-UK.

Das, B. M., and Maji, A., (1994). "Transient Loading Related Settlement of A Square Foundation on Geogrid-Reinforced Sand", Geotechnical and Geological Engineering 12, pp241-251

Das, B. M., and Omar, M.T., (1994). "The Effect of Foundation Width on Model Tests for Bearing Capacity of Sand with Geogrid Reinforcement", Geotechnical and Geological Engineering 12, pp133-141

DeBeer, E.,E.,(1965). "Bearing Capacity and Settlement of Shallow Foundations on Sand", Proceedings of Bearing Capacity and Settlement of Foundations, Duke University Durham NC, USA, pp15-34.

Dunn, D.I., Anderson, L.R., and Kier, F.W., (1980). "Fundamentals of Geotechnical Analysis", Wiley, New York.

Edil, T., B. and Benson, C.,H.(2004). "Investigation of Soil Stiffness Gauge and DCP for Earth Work Property Evaluation", Wisconsin Department of Transportation, USA.

Gabr, M.A., Hopkins, K., Coonse, J., and Hearne,T.(2000). "DCP Criteria for Performance Evaluation of Pavement Layers" Journal of Performance of Constructed Facilities pp.141-148.

George, K. P., and Uddin, W. (2000). "Subgrade Characterization for Highway Pavement Design, Final Report", Mississippi Department of Transportation, Jackson, MS.

Harrison, J.A., (1987). "Correlation Between California Bearing Ratio and Dynamic Cone Penetrometer Strength Measurement of Soils", Proceedings of Institution of Civil Engineers, London, Part 2, Technical Note 463, pp833-844.

Humboldt Manufacturing Company (2002). "Instruction Manual Soil Penetrometer, Pocket Type" www.humboldtmfg.com.

Jones, C., (2004). "Dynamic Cone Penetrometer Tests and Analysis", Technical Information Note, Department for International Development.

Karunaprema, K.A.K., and Edirisinghe, A.G.H.J., (2002). "A Laboratory Study to Establish Some Useful Relationships for the Use of Dynamic Cone Penetrometer", Department of Civil Engineering, University of Peradeniya, Peradeniya, Sri Lanka.

Kleyn, E.G., Maree, J.H., and Savage, F.(1982). "The Application of a Potable Pavement Dynamic Cone Penetrometer to Determine In- Situ Bearing Properties of Road Pavement Layers and Subgrades in South Africa", Proceedings of the Second European Symposium on Penetration Testing, Amsterdam, pp 277-282".

Ko, H., and Davidson, L.W., (1973). "Bearing Capacity of Footing in Plain Strain", Journal of the Soil Mechanics and Foundations Division, ASCE Volume 99 No.SM1 pp1-23.

Malandraki, V., and Toll, D.G., (1996). "The Definition of Yield for Bonded Materials", Geotechnical and Geological Engineering, volume 14 pp67-82.

Mayne, P., W., Auxt, J., A., Mitchell, J., K., and Yilmaz, R., (1995). "Proceedings of International Symposium on Cone Penetration Testing", Linköping, Sweden Vol. 1 pp 263-276.

McElvaney, J., and Djatnika, I. (1991). "Strength Evaluation of Lime-Stabilized Pavement Foundations Using the Dynamic Cone Penetrometer", Australian Road Res., Volume 21, No. 1, pp 40-52.

- Meyerhof, G.,G., (1956). "Penetration Tests and Bearing Capacity of Cohesionless Soils", Proceedings ASCE, Volume 82, No. SM1, Paper 866, pp. 1-19.
- Mitchell, J.K. (1986). "Ground Improvement Evaluation by In-Situ Tests", Use of In-Situ Tests in Geotechnical Engineering, ASCE, GSP 6, pp 221-236.
- Patra, C.R., Das, B.M., and Atalar, C (2005). "Bearing Capacity of Embedded Strip Foundation on Geogrid-Reinforced Sand", Geotextiles and Geomembranes, Volume 23, Issue5 pp454-462.
- Peck R.B, Hanson W.E. and Thornburn, T.H., (1973). "Foundation Engineering", 2nd edition Wiley, New York.
- Prandtl, L. (1921). "On the Penetrating Strength) of Plastic Construction Materials and the Strength of Cutting Edges), Zeit. Angew. Math. Mechanics1, No.1, pp.15-20.
- Radhakrishnan, S., and Ramanathan, B.,(1965). "A Critical Study on Estimation of Bearing Capacity of Soils" Journal of the Indian Roads Congress, Vol. 29-2, No. 2 pp 256-283.
- Sanglerat, G., (1972). "The Penetrometer and Soil Exploration. Developments in Geotechnical Engineering", Elsevier Publishing: New York.
- Scala, A.,J., (1956) "Simple Methods of Flexible Pavement Design using Dynamic Cone Penetrometer" New Zealand Engineer, Volume 11 No.2, pp33-44.
- Shin, E.C., Lee J.B., Das, B.M., (1999). "Bearing Capacity of a Model Scale Footing on Crude Oil-Contaminated Sand", Geotechnical and Geological Engineering 17 pp 123-132.

Singh, A., Sharma, D. and Sharma, B. (1973). "*Some Experiments with a Light Dynamic Penetrometer with a View to Assess Its Suitability for Exploring Subgrades and Foundations*", Journal of the Indian Roads Congress, Vol. 35-1, No. 1 pp.155 - 172

Sowers, G., F., and Hedges, C., S., (1966), "*Dynamic Cone for Shallow In-Situ Penetration Testing*" Vane Shear and Cone Penetration Resistance Testing of Soil, Special Technical Publication 399, ASTM, Philadelphia, p 29.

Terzaghi, K., and Peck, R., B., (1967). "*Soil Mechanics in Engineering Practice*" John Wiley & Sons, New York.

Transport Research Laboratory (2004), "*Report 361-Dynamic Cone Penetrometer Tests and Analysis*" Berkshire, UK.

Uddin, W.(2002). "*In-Situ Evaluation of Seasonal Variability of Subgrade Modulus Using DCP And Falling Weight Deflectometer*", 6th International Conference on bearing Capacity of Roads, Railways and Airfields, Lisbon, Portugal.

Vanagas, C., Minasnu, B., and McBratney, A.,B.,(2004). "*The Dynamic Cone Penetrometers for Assessment of Soil Mechanical Resistance*" 3rd Australian, New Zealand Soils Conference, Sydney, Australia.

Van Vuuren, D., J., (1969). "*Rapid Determination of CBR with the Portable DCP*", The Rhodesian Engineer.

Vesic, A.S.(1973), "*Analysis of Ultimate Loads of Shallow Foundations*" Journal of the Soil Mechanics and Foundation Division, ASCE Vol. 99 No. SM pp. 45-73.

APPENDICES

- I TEST PIT LOG
- II NATURAL MOISTURE CONTENT
SPECIFIC GRAVITY
GRADING
ATTERBERG LIMITS
COMPACTION TEST
- III CALIBRATION CURVES
- IV LOADING TEST
- V DYNAMIC CONE PENETROMETER TEST
- VI UNCONSOLIDATED-UNDRAINED TRIAXIAL TEST
TRIAXIAL STRESS-STRAIN CURVES
MOHR CIRCLE

APPENDIX I

TEST PIT LOG





CIVIL ENGINEERING DEPARTMENT-KNUST
DCPT-ULTIMATE BEARING CAPACITY PROJECT
-TEST PIT LOG

Site Location: Near Engineering Snack Bar, KNUST

Date: 10/10/2006

Method of Excavation: Manual

Depth m	Strata Symbol	Strata Description	Natural Moisture Content (%)
0.30		Loose to medium dense, moist, dark brown silty <i>SAND</i> . Decayed organic matter in the matrix (Topsoil).	
0.80		Firm, moist, reddish brown, lateritic sandy <i>CLAY</i> with little silt, rich in muscovite mica. (Residual Soil)	20.50

END OF TEST PIT

APPENDIX II

NATURAL MOISTURE CONTENT

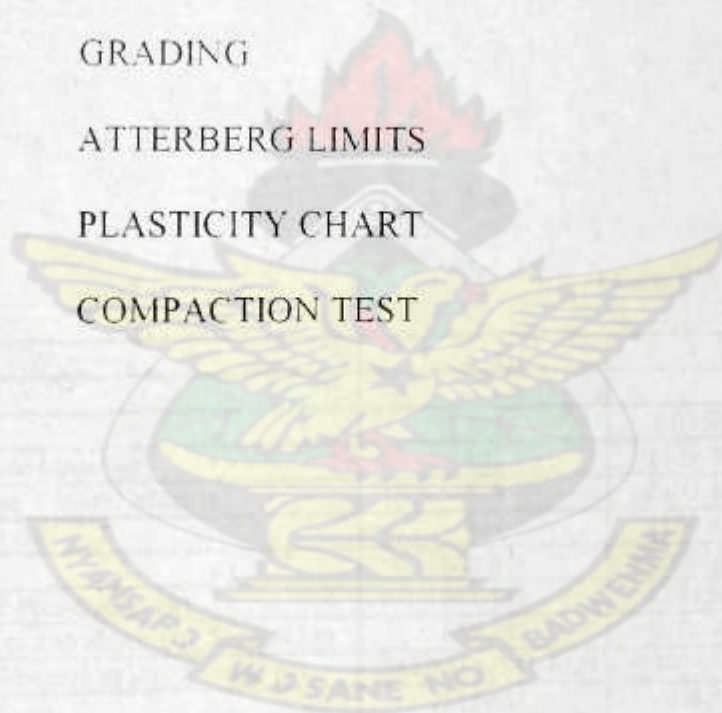
SPECIFIC GRAVITY

GRADING

ATTERBERG LIMITS

PLASTICITY CHART

COMPACTION TEST



CIVIL ENGINEERING DEPARTMENT-KNUST
DCPT-ULTIMATE BEARING CAPACITY PROJECT

Date: 10/10/2006

NATURAL MOISTURE CONTENT

Test Number	1	2
Container Number	B23	A33
Container Mass(g)	3.70	3.62
Container + Wet Sample Mass(g)	28.98	34.00
Container + Oven Dried Sample Mass(g)	24.71	28.78
Moisture Content Mass(g)	4.27	5.22
Dry Sample Mass (g)	21.01	25.16
Moisture Content (%)	20.3	20.7
Average Moisture Content %	20.5	

Date: 17/10/2006

SPECIFIC GRAVITY

Sample Number		A	B
Pycnometer Number		1	2
Empty Pycnometer Mass (g)	M1	846.20	843.10
Pycnometer + Oven Dried Sample Mass (g)	M2	1329.70	1322.10
Pycnometer + Oven Dried Sample + Water Mass (g)	M3	2401.10	2405.60
Pycnometer Full of Water Mass (g)	M4	2100.80	2106.60
Oven Dried Sample Mass (g)	M2-M1	483.50	479.00
Mass of Water Filling the Empty Pycnometer (g)	M4-M1	1254.60	1263.50
Mass of Water in Pycnometer over and above Dry Sample (g)	M3-M2	1071.40	1083.50
Mass of Water having the same Volume as Dry Sample (g)	(M4-M1)-(M3-M2)	183.20	180.00
Specific Gravity	(M2-M1)	2.64	2.66
	(M4-M1)-(M3-M2)		
Average Specific Gravity		2.65	

CIVIL ENGINEERING DEPARTMENT-KNUST
DCPT-ULTIMATE BEARING CAPACITY PROJECT
PARTICLE SIZE DISTRIBUTION

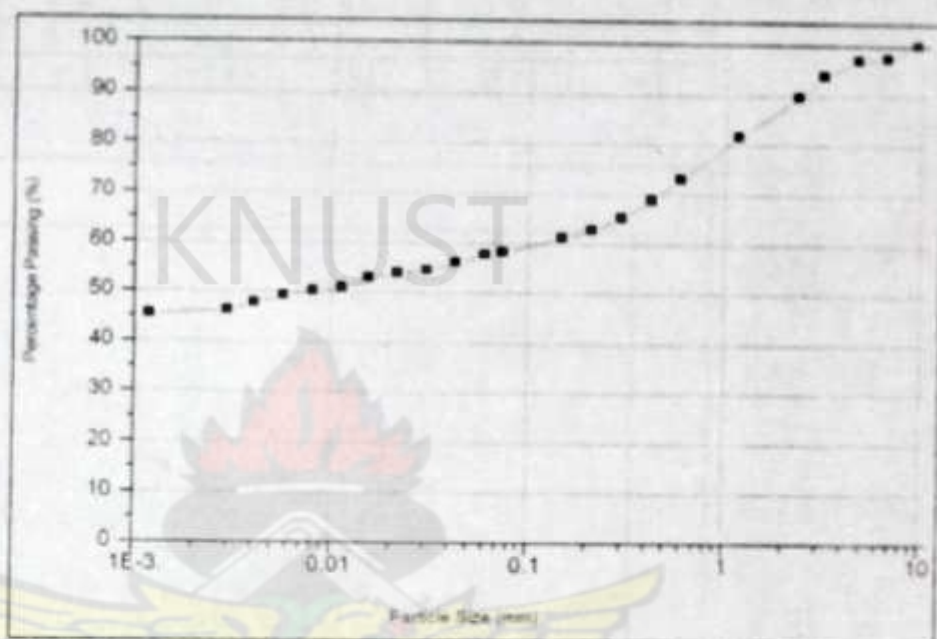
Sample Depth: 0.30-0.80m

Date 19/10/2006

WET SIEVING

Dry Mass (g) = 200

	Mass Retain (g)	% Retain	% Passing
		0.00	100.00
5.16	2.58	97.42	
0.84	0.42	97.00	
6.52	3.26	93.74	
8.36	4.18	89.56	
16.20	8.10	81.46	
16.88	8.44	73.02	
8.72	4.36	68.66	
6.96	3.48	65.18	
4.76	2.38	62.80	
3.28	1.64	61.16	
5.80	2.90	58.26	



HYDROMETER TEST

Total Dry Mass (g) = 50.0

G_s = 2.65

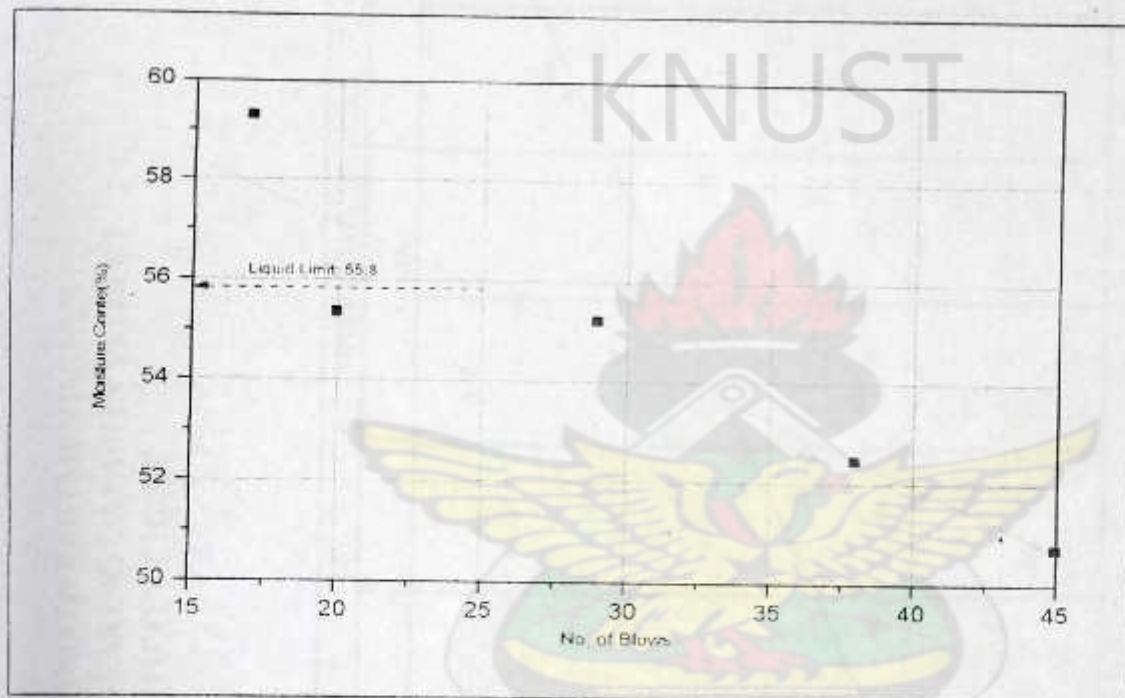
Time	Elapsed Time, t (min)	Temp. T (°C)	Direct Hydrometer Reading, R _H	Transformed Hydrometer Reading, R _H '	True Hydrometer Reading, R _H = R _H ' + C _m	Effective Depth, H _e (mm)	Viscosity, η (mPa.s)	Equivalent Diameter, D (mm)	Temp. Correction to Hydrometer Reading, ΔR	Modified Hydrometer Reading, R _H = R _H ' + ΔR	% of Particles $\geq D$ (K _s %)
9:39am	0.5	29.0	1.0190	19.0	19.5	123.58	0.809	0.0609	2.0591	17.96	57.69
9:40am	1.0	29.0	1.0185	18.5	19.0	125.55	0.809	0.0434	2.0591	17.46	56.08
9:41am	2.0	29.0	1.0180	18.0	18.5	127.53	0.809	0.0309	2.0591	16.96	54.47
9:43am	4.0	29.0	1.0178	17.8	18.3	128.32	0.81	0.0219	2.0591	16.76	53.83
9:47am	8.0	29.0	1.0175	17.5	18.0	129.50	0.81	0.0156	2.0591	16.46	52.87
9:54am	13.0	28.5	1.0170	17.0	17.5	131.48	0.82	0.0115	1.9218	15.82	50.82
10:09am	30.0	28.5	1.0168	16.8	17.3	132.27	0.82	0.0082	1.9218	15.62	50.18
10:39am	60.0	28.5	1.0165	16.5	17.0	133.45	0.82	0.0058	1.9218	15.32	49.22
11:39am	120	28.5	1.0160	16.0	16.5	135.43	0.82	0.0041	1.9218	14.82	47.61
1:39pm	240	28.0	1.0157	15.7	16.2	136.61	0.83	0.0030	1.7872	14.39	46.21
9:39pm	1440	29.5	1.0150	15.0	15.5	139.38	0.80	0.0012	2.1991	14.10	45.29

CIVIL ENGINEERING DEPARTMENT-KNUST
DCPT-ULTIMATE BEARING CAPACITY PROJECT
ATTERBERG LIMITS DETERMINATION

Date: 25/10/2006

Liquid Limit

Container Number	B29	A43	A7	A24	C4
Container Mass (g)	3.75	3.79	3.9	3.71	3.66
Number of Blows	45	38	29	20	17
Wet Sample+ Container Mass(g)	18.76	17.51	19.11	21.31	20.75
Dry Sample + Container Mass(g)	13.71	12.79	13.7	15.04	14.39
Dry Sample Mass(g)	9.96	9	9.8	11.33	10.73
Moisture Content Mass (g)	5.05	4.72	5.41	6.27	6.36
Moisture Content (%)	50.7	52.4	55.2	55.3	59.3



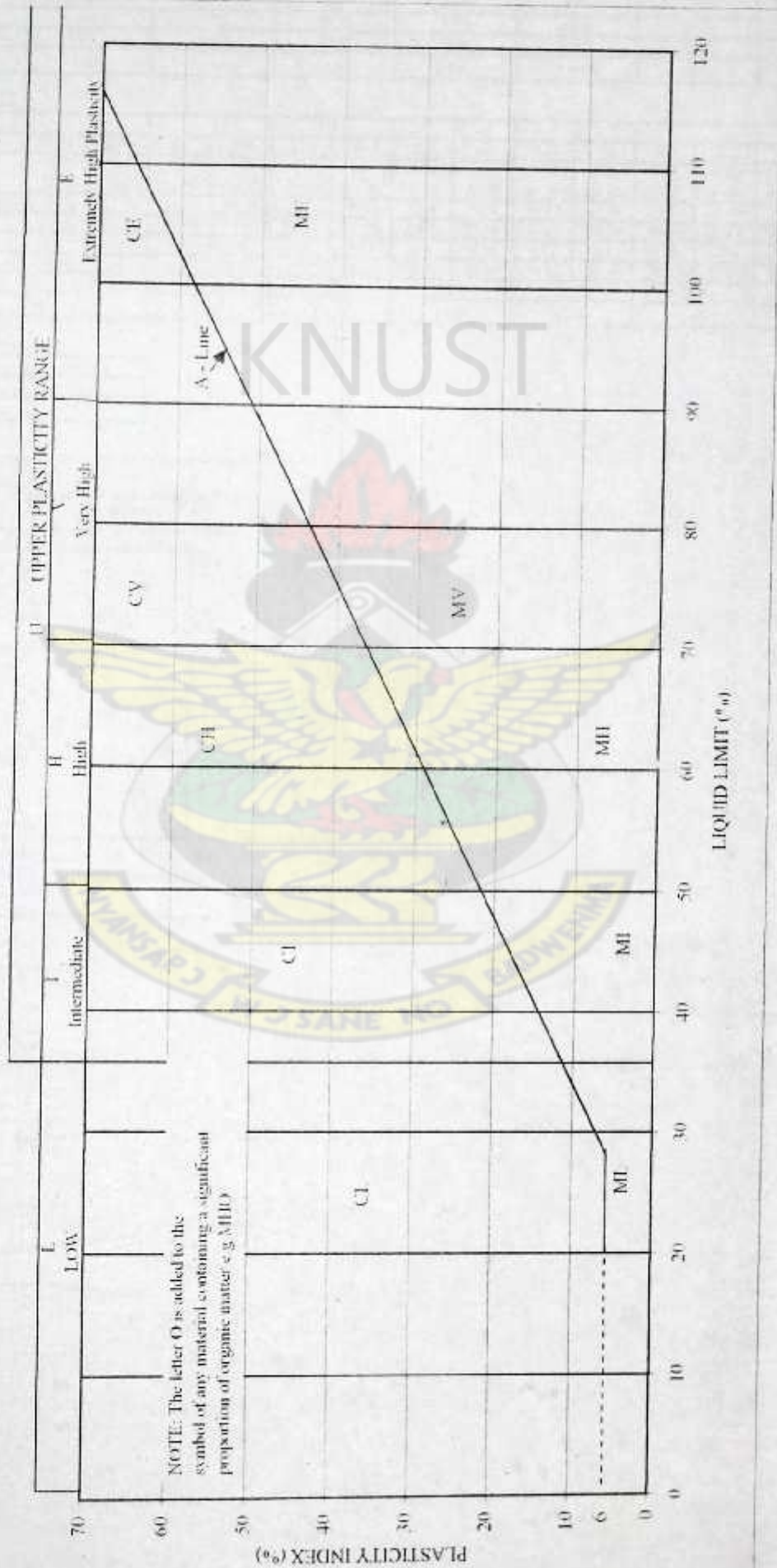
Plastic Limit

Container number	E3	101
Container mass (g)	3.57	3.62
Wet Sample+ Container Mass(g)	9.68	8.94
Dry Sample + Container Mass(g)	8.29	7.76
Dry Sample Mass(g)	4.72	4.14
Moisture Content Mass (g)	1.39	1.18
Moisture Content (%)	29.4	28.5
Average Moisture Content (%)	29.0	

Plastic Limit = 29%

Liquid Limit (%)	56
Plastic Limit (%)	29
Plasticity Index (%)	27

CIVIL ENGINEERING DEPARTMENT-KNUST
DCPT-ULTIMATE BEARING CAPACITY PROJECT
PLASTICITY CHART



CIVIL ENGINEERING DEPARTMENT-KNUST
DCPT-ULTIMATE BEARING CAPACITY PROJECT
COMPACTION TEST (STANDARD PROCTOR)

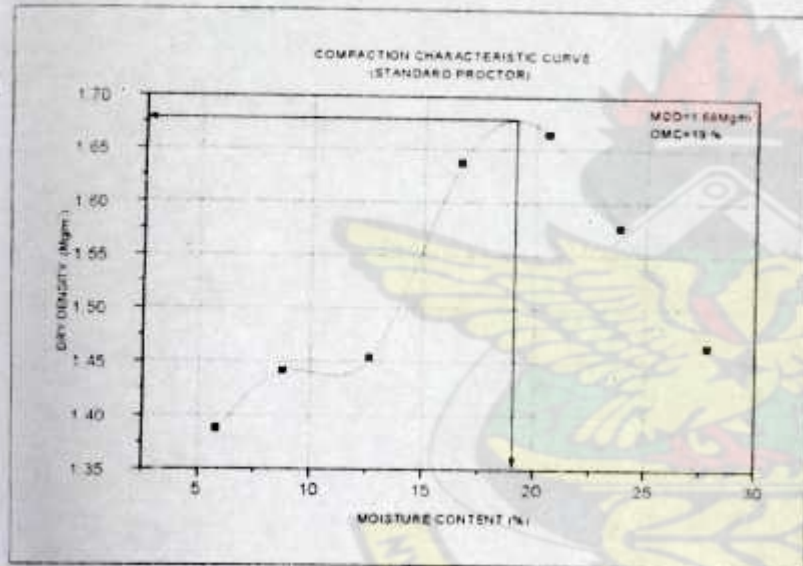
SAMPLE PREPARATION	1	2	3	4	5	6	7
Mould Mass(g)	4293	4293	4293	4293	4293	4293	4293
Mould + Wet Sample Mass(g)	5678	5771	5837	6004	6186	6134	6050
Wet Sample Mass(g)	1385	1478	1544	1701	1893	1841	1756
Wet Bulk Density ($Mg\ m^{-3}$)	1.4679	1.5665	1.6363	1.9088	2.0664	1.9512	1.8717

Moisture Content Determination

Test Number	1	2	3	4	5	6	7
Container Number	B23	A33	E3	B29	122	K6	A25
Container Mass(g)	3.7	3.62	3.57	3.73	3.7	3.66	3.73
Container + Wet Sample Mass(g)	25.98	34	36.94	34.27	32.64	31.96	37.6
Container + Dry Sample Mass(g)	24.71	32.58	34.29	31.78	29.24	28.94	32.8
Dry Sample Mass(g)	21.01	28.76	30.72	28.05	25.54	25.28	29.07
Moisture Content (%)	1.27	1.62	2.65	2.49	3.4	3.02	4.8
Average Moisture Content (%)	6.64	5.63	8.63	8.89	13.31	11.95	16.51
Average Moisture Content (%)	5.8	8.8	12.6	16.7	20.6	23.8	27.9
Dry Density ($Mg\ m^{-3}$)	1.387	1.449	1.453	1.636	1.694	1.576	1.464

Mould Characteristics

Mould Height (cm)	11.63
Mould Diameter (cm)	10.16
Mould Volume (cm^3)	943.8



APPENDIX III

PROVING RING CALIBRATION CURVES



CIVIL ENGINEERING DEPARTMENT-KNUST
DCPT-ULTIMATE BEARING CAPACITY PROJECT
CALIBRATION OF PROVING RING

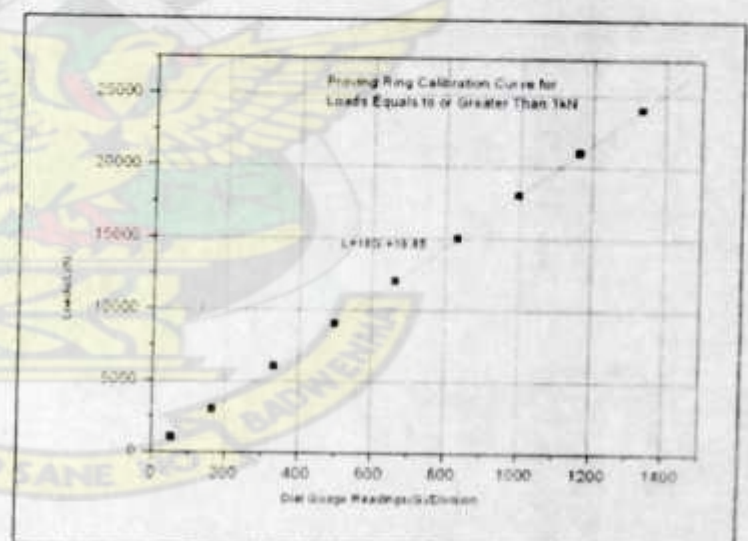
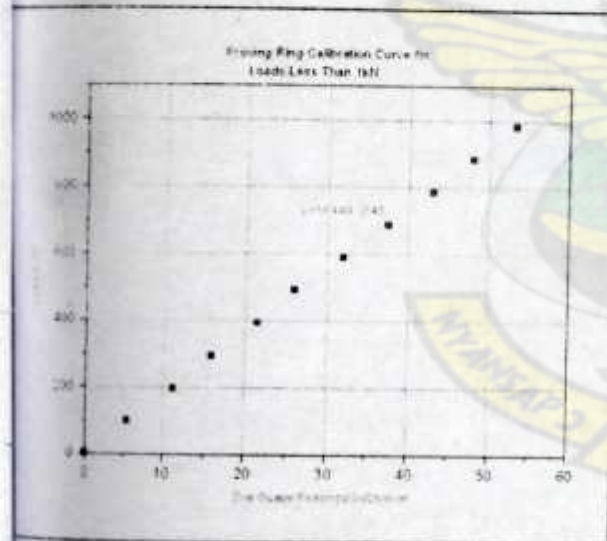
Date: 18/04/2007

For Loads Less Than 1kN

Dial Guage Readings(G)/Division			Load (L)/N
Reading 1	Reading 2	Average Reading	
0.0	0.0	0.0	0.0
5.5	5.5	5.5	98.1
11.0	11.5	11.3	196.2
16.0	16.0	16.0	294.3
21.5	21.5	21.5	392.4
26.0	26.0	26.0	490.5
32.0	32.0	32.0	588.6
37.5	37.5	37.5	686.7
43.0	43.0	43.0	784.8
48.0	48.0	48.0	882.9
53.0	53.5	53.3	981.0

For Loads Equals to or Greater Than 1kN

Dial Guage Readings(G)			Load (L)/N
Reading 1	Reading 2	Average Reading	
56.0	55.0	55.5	1000
166.0	166.0	166.0	3000.0
333.0	334.0	333.5	6000.0
499.0	499.0	499.0	9000.0
664.0	665.0	664.5	12000.0
833.0	832.0	832.5	15000.0
999.0	999.0	999.0	18000.0
1167.0	1165.0	1166.0	21000.0
1336.0	1335.0	1335.5	24000.0



APPENDIX IV

LOADING TEST



CIVIL ENGINEERING DEPARTMENT-KNUST
DCPT-ULTIMATE BEARING CAPACITY PROJECT
LOADING TEST

Test No.: BC-15/1

Date: 23/04/2007

Srl No.	Dial Gauge(div)	Proving Ring(div)	Force (N)	Penetration (mm)	Stress (kN/m ²)
1	0.0	0.0	0	0.0	0.0
2	50.0	2.0	34.5	0.5	0.8
3	100.0	8.0	145.2	1.0	3.2
4	150.0	15.0	274.2	1.5	6.1
5	200.0	24.0	440.2	2.0	9.8
6	250.0	33.0	606.2	2.5	13.5
7	300.0	41.0	753.7	3.0	16.7
8	350.0	49.0	901.2	3.5	20.0
9	400.0	57.0	1042.3	4.0	23.2
10	450.0	63.0	1150.2	4.5	25.6
11	500.0	70.0	1276.2	5.0	28.4
12	550.0	77.0	1402.1	5.5	31.2
13	600.0	82.0	1492.0	6.0	33.2
14	650.0	88.0	1600.0	6.5	35.6
15	700.0	93.0	1689.9	7.0	37.6
16	750.0	98.0	1779.9	7.5	39.6
17	800.0	102.5	1860.8	8.0	41.4
18	850.0	106.5	1932.8	8.5	43.0
19	900.0	111.0	2013.7	9.0	44.7
20	950.0	115.0	2085.7	9.5	46.3
21	1000.0	119.0	2157.7	10.0	47.9
22	1050.0	123.0	2229.6	10.5	49.5
23	1100.0	126.0	2283.6	11.0	50.7
24	1150.0	131.0	2373.5	11.5	52.7
25	1200.0	134.0	2427.5	12.0	53.9
26	1250.0	138.0	2499.5	12.5	55.5
27	1300.0	141.0	2553.4	13.0	56.7
28	1350.0	145.0	2625.4	13.5	58.3
29	1400.0	148.5	2688.4	14.0	59.7
30	1450.0	152.0	2751.3	14.5	61.1
31	1500.0	155.0	2805.3	15.0	62.3
32	1550.0	158.5	2868.3	15.5	63.7
33	1600.0	162.0	2931.2	16.0	65.1
34	1650.0	165.0	2985.2	16.5	66.3
35	1700.0	168.5	3048.2	17.0	67.7
36	1750.0	172.0	3111.1	17.5	69.1
37	1800.0	175.5	3174.1	18.0	70.5
38	1850.0	179.0	3237.1	18.5	71.9
39	1900.0	182.0	3291.0	19.0	73.1
40	1950.0	185.0	3345.0	19.5	74.3
41	2000.0	188.5	3408.0	20.0	75.7
42	2100.0	194.5	3515.9	21.0	78.1
43	2200.0	201.5	3641.8	22.0	80.9
44	2300.0	208.0	3758.8	23.0	83.5
45	2400.0	214.5	3875.7	24.0	86.1
46	2500.0	221.0	3992.6	25.0	88.7
47	2600.0	227.0	4100.6	26.0	91.1
48	2700.0	234.0	4226.5	27.0	93.9
49	2800.0	240.0	4334.5	28.0	96.3
50	2900.0	246.5	4451.4	29.0	98.9
51	3000.0	253.0	4568.3	30.0	101.5
52	3100.0	259.0	4676.3	31.0	103.9
53	3200.0	265.0	4784.2	32.0	106.3
54	3300.0	272.5	4919.1	33.0	109.3
55	3400.0	279.0	5036.1	34.0	111.9

Srl No.	Dial Gauge(div)	Proving Ring(div)	Force (N)	Penetration (mm)	Stress (kN/m ²)
56	3500.0	285.5	5153.0	35.0	114.5
57	3600.0	292.5	5278.9	36.0	117.3
58	3700.0	299.0	5395.9	37.0	119.9
59	3800.0	306.0	5521.8	38.0	122.7
60	3900.0	312.5	5638.7	39.0	125.3
61	4000.0	319.0	5755.7	40.0	127.9
62	4100.0	326.5	5890.6	41.0	130.9
63	4200.0	334.0	6025.5	42.0	133.9
64	4300.0	341.0	6151.4	43.0	136.7
65	4400.0	348.0	6277.4	44.0	139.5
66	4500.0	355.5	6412.3	45.0	142.5
67	4600.0	362.5	6538.2	46.0	145.3
68	4700.0	370.0	6673.2	47.0	148.3
69	4800.0	377.5	6808.1	48.0	151.3
70	4900.0	385.0	6943.0	49.0	154.3
71	5000.0	393.0	7086.9	50.0	157.5
72	5100.0	400.0	7212.9	51.0	160.3
73	5200.0	408.5	7365.8	52.0	163.7
74	5300.0	416.0	7500.7	53.0	166.7
75	5400.0	425.5	7671.6	54.0	170.5
76	5500.0	434.0	7824.5	55.0	173.9
77	5600.0	443.0	7986.4	56.0	177.5
78	5700.0	452.0	8148.3	57.0	181.1
79	5800.0	461.0	8310.2	58.0	184.7
80	5900.0	470.0	8472.2	59.0	188.3
81	6000.0	479.0	8634.1	60.0	191.9
82	6100.0	489.0	8814.0	61.0	195.9
83	6200.0	498.0	8975.9	62.0	199.5
84	6300.0	508.0	9155.8	63.0	203.5
85	6400.0	518.0	9335.7	64.0	207.5
86	6500.0	528.0	9515.6	65.0	211.5
87	6600.0	538.0	9695.5	66.0	215.5
88	6700.0	548.0	9875.4	67.0	219.5
89	6800.0	556.5	10028.3	68.0	222.9
90	6900.0	566.0	10199.2	69.0	226.6
91	7000.0	576.0	10379.1	70.0	230.6
92	7100.0	586.0	10559.0	71.0	234.6
93	7200.0	597.5	10765.9	72.0	239.2
94	7300.0	608.0	10954.8	73.0	243.4
95	7400.0	619.0	11152.7	74.0	247.8
96	7500.0	630.0	11350.6	75.0	252.2
97	7600.0	641.5	11557.4	76.0	256.8
98	7700.0	652.5	11755.3	77.0	261.2
99	7800.0	664.0	11962.2	78.0	265.8
100	7900.0	675.0	12160.1	79.0	270.2

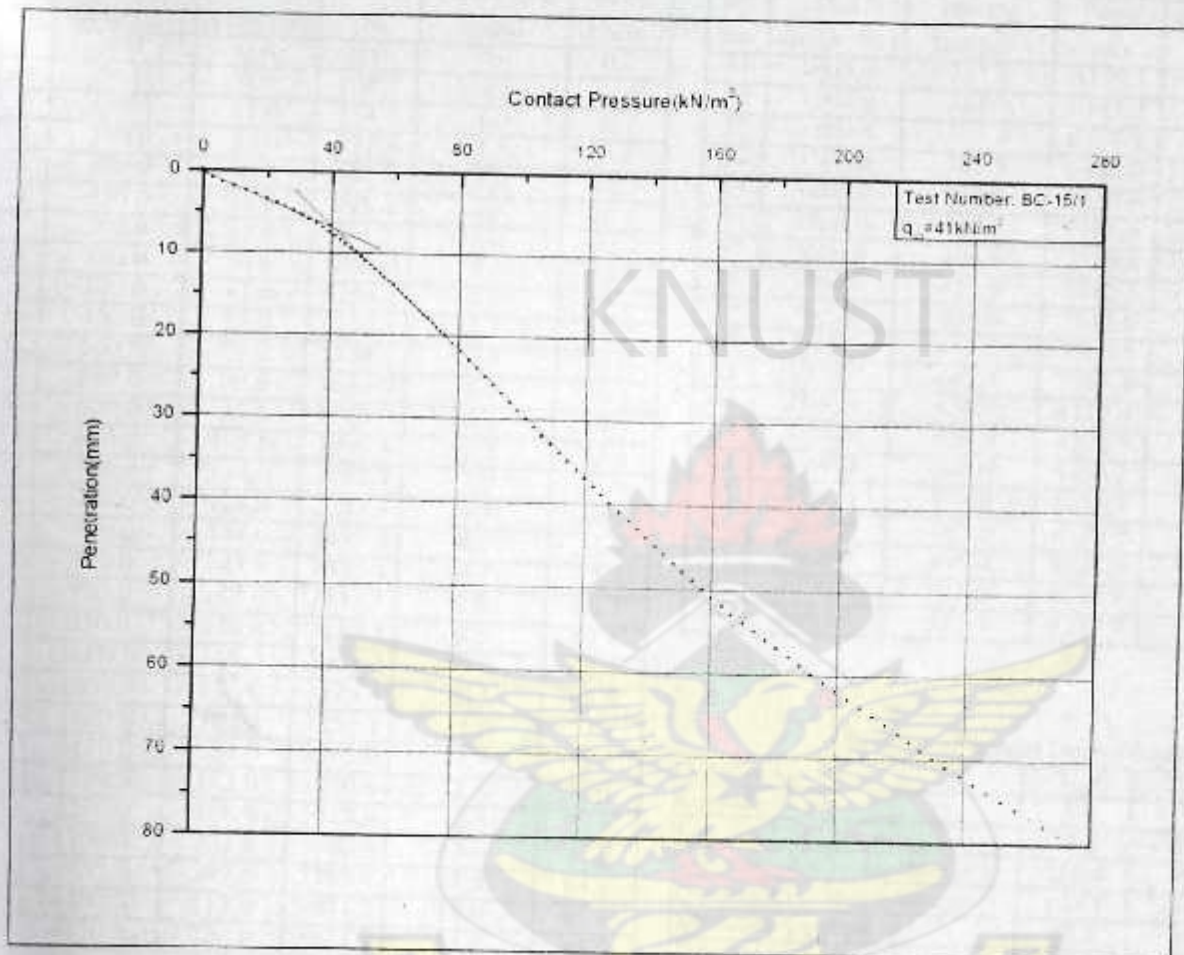
Moisture Content Determination

Sample Location	Top	Middle	Bottom
Container Number	X4	D9	C6
Container Mass (g)	18.17	18.1	17.8
Container + Wet Sample Mass (g)	122.11	102.5	112.2
Container + Dry Sample Mass (g)	107.14	89.3	97.2
Moisture Content (g)	14.97	13.14	15.09
Dry Sample Mass (g)	88.97	71.18	79.32
Moisture Content (%)	16.8	18.5	19.0
Average Moisture Content (%) =	18.1		

CIVIL ENGINEERING DEPARTMENT-KNUST
DCPT-ULTIMATE BEARING CAPACITY PROJECT
LOADING TEST GRAPH

Test No.: BC-15/1

Date: 23/04/2007



LIBRARY
KWAME NKRUMAH UNIVERSITY OF
SCIENCE AND TECHNOLOGY
KUMASI-GP

CIVIL ENGINEERING DEPARTMENT-KNUST
DCPT-ULTIMATE BEARING CAPACITY PROJECT
LOADING TEST

Test No.: BC-20/1

Date: 19/04/2007

Srl No.	Dial Gauge (div)	Proving Ring (div)	Force (N)	Penetration (mm)	Stress (kN/m ²)
1	0.0	0.0	0.0	0.0	0.0
2	50.0	6.0	108.3	0.5	2.4
3	100.0	15.0	274.2	1.0	6.1
4	150.0	23.0	421.8	1.5	9.4
5	200.0	30.0	550.8	2.0	12.2
6	250.0	38.0	698.4	2.5	15.5
7	300.0	49.0	901.2	3.0	20.0
8	350.0	56.0	1024.3	3.5	22.8
9	400.0	63.0	1150.2	4.0	25.6
10	450.0	72.0	1312.1	4.5	29.2
11	500.0	79.0	1438.1	5.0	32.0
12	550.0	90.0	1636.0	5.5	36.4
13	600.0	95.0	1725.9	6.0	38.4
14	650.0	105.0	1905.8	6.5	42.4
15	700.0	114.0	2067.7	7.0	45.9
16	750.0	124.0	2247.6	7.5	49.9
17	800.0	134.0	2427.5	8.0	53.9
18	850.0	143.0	2589.4	8.5	57.5
19	900.0	151.0	2733.3	9.0	60.7
20	950.0	158.0	2859.3	9.5	63.5
21	1000.0	166.0	3003.2	10.0	66.7
22	1050.0	173.0	3129.1	10.5	69.5
23	1100.0	180.0	3255.1	11.0	72.3
24	1150.0	186.0	3363.0	11.5	74.7
25	1200.0	192.0	3470.9	12.0	77.1
26	1250.0	198.0	3578.9	12.5	79.5
27	1300.0	204.0	3686.8	13.0	81.9
28	1350.0	209.5	3785.8	13.5	84.1
29	1400.0	215.0	3884.7	14.0	86.3
30	1450.0	220.0	3974.7	14.5	88.3
31	1500.0	225.5	4073.6	15.0	90.5
32	1550.0	230.0	4154.6	15.5	92.3
33	1600.0	235.0	4244.5	16.0	94.3
34	1650.0	240.0	4334.5	16.5	96.3
35	1700.0	245.0	4424.4	17.0	98.3
36	1750.0	249.5	4505.4	17.5	100.1
37	1800.0	254.0	4586.3	18.0	101.9
38	1850.0	258.0	4658.3	18.5	103.5
39	1900.0	263.0	4748.2	19.0	105.5
40	1950.0	267.0	4820.2	19.5	107.1
41	2000.0	272.0	4910.1	20.0	109.1
42	2100.0	280.5	5063.0	21.0	112.5
43	2200.0	289.0	5216.0	22.0	115.9
44	2300.0	298.0	5377.9	23.0	119.5
45	2400.0	306.5	5530.8	24.0	122.9
46	2500.0	315.0	5683.7	25.0	126.3
47	2600.0	323.5	5836.6	26.0	129.7
48	2700.0	331.5	5980.5	27.0	132.9
49	2800.0	340.0	6133.5	28.0	136.3
50	2900.0	348.5	6286.4	29.0	139.7

Srl No.	Dial Gauge (div)	Proving Ring (div)	Force (N)	Penetration (mm)	Stress (kN/m ²)
51	3000.0	357.0	6439.3	30.0	143.1
52	3100.0	365.0	6583.2	31.0	146.3
53	3200.0	373.0	6727.1	32.0	149.5
54	3300.0	381.5	6880.0	33.0	152.9
55	3400.0	390.0	7033.0	34.0	156.3
56	3500.0	398.5	7185.9	35.0	159.7
57	3600.0	406.0	7320.8	36.0	162.7
58	3700.0	415.0	7482.7	37.0	166.3
59	3800.0	424.0	7644.6	38.0	169.9
60	3900.0	433.0	7806.5	39.0	173.5
61	4000.0	442.0	7968.4	40.0	177.1
62	4100.0	450.0	8112.4	41.0	180.3
63	4200.0	459.0	8274.3	42.0	183.9
64	4300.0	468.0	8436.2	43.0	187.5
65	4400.0	478.0	8616.1	44.0	191.5
66	4500.0	487.0	8778.0	45.0	195.1
67	4600.0	495.0	8921.9	46.0	198.3
68	4700.0	505.0	9101.8	47.0	202.3
69	4800.0	512.0	9227.7	48.0	205.1

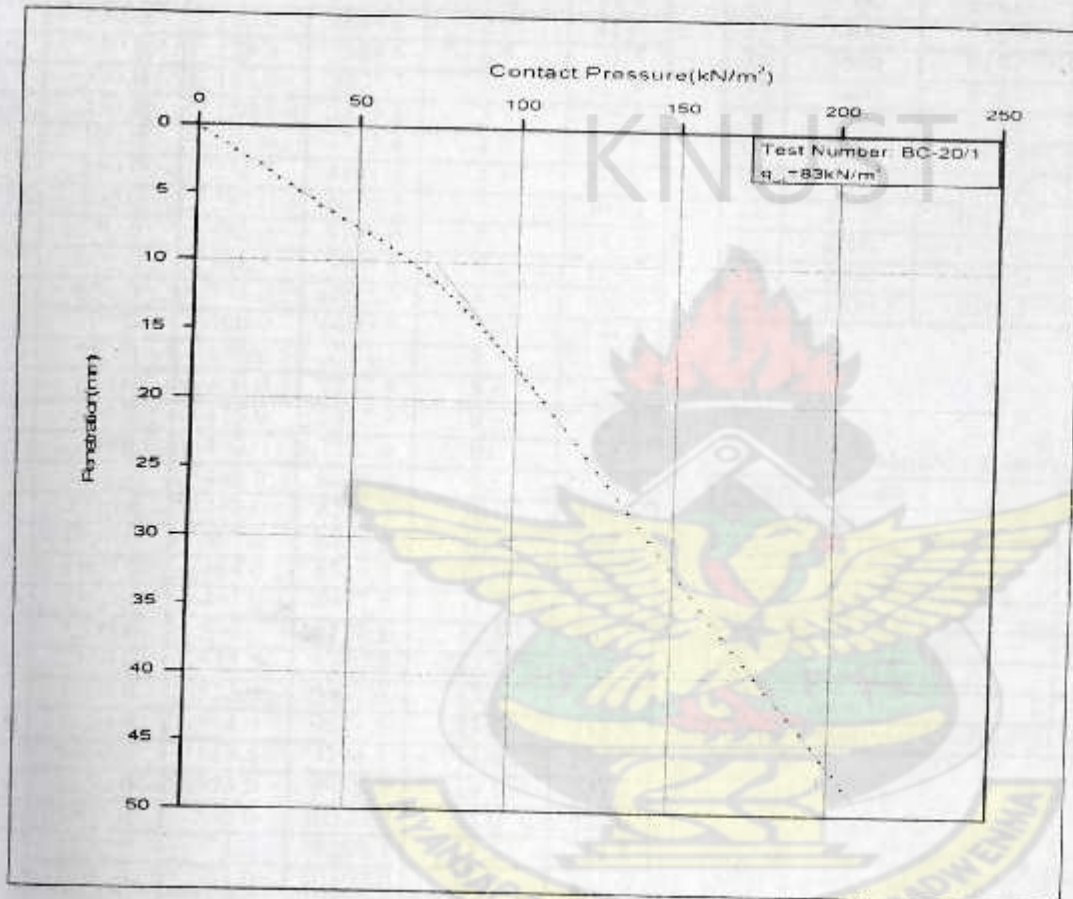
Moisture Content Determination

Sample Location	Top	Middle	Bottom
Container Number	X4	D9	C6
Container Mass (g)	18.2	18.1	17.8
Container + Wet Sample Mass (g)	126.4	103.5	105.2
Container + Dry Sample Mass (g)	109.1	89.3	91.9
Moisture Content (g)	17.3	14.3	13.3
Dry Sample Mass (g)	90.9	71.1	74.1
Moisture Content (%)	19.0	20.1	18.0
Average Moisture Content (%) =	19.0		

CIVIL ENGINEERING DEPARTMENT-KNUST
DCPT-ULTIMATE BEARING CAPACITY PROJECT
LOADING TEST GRAPH

Test No.: BC-20/1

Date: 19/04/2007



CIVIL ENGINEERING DEPARTMENT-KNUST
DCPT-ULTIMATE BEARING CAPACITY PROJECT
LOADING TEST

Test No.: BC-30/1

Date: 26/04/2007

Srl No	Dial Gauge(div)	Proving Ring(div)	Force (N)	Penetration (mm)	Stress (kN/m ²)
1	0.0	0.0	0	0.0	0.0
2	50.0	25.5	467.9	0.5	10.4
3	100.0	51.5	947.3	1.0	21.1
4	150.0	77.0	1402.1	1.5	31.2
5	200.0	103.0	1869.8	2.0	41.6
6	250.0	128.5	2328.6	2.5	51.7
7	300.0	155.0	2805.3	3.0	62.3
8	350.0	180.0	3255.1	3.5	72.3
9	400.0	206.0	3722.8	4.0	82.7
10	450.0	231.5	4181.5	4.5	92.9
11	500.0	257.0	4640.3	5.0	103.1
12	550.0	283.0	5108.0	5.5	113.5
13	600.0	308.5	5566.8	6.0	123.7
14	650.0	334.0	6025.5	6.5	133.9
15	700.0	360.0	6493.3	7.0	144.3
16	750.0	376.0	6781.1	7.5	150.7
17	800.0	400.0	7212.9	8.0	160.3
18	850.0	415.0	7482.7	8.5	166.3
19	900.0	430.0	7752.6	9.0	172.3
20	950.0	448.0	8076.4	9.5	179.5
21	1000.0	458.0	8256.3	10.0	183.5
22	1050.0	467.0	8418.2	10.5	187.1
23	1100.0	484.0	8724.0	11.0	193.9
24	1150.0	497.0	8957.9	11.5	199.1
25	1200.0	506.0	9119.8	12.0	202.7
26	1250.0	515.5	9290.7	12.5	206.5
27	1300.0	525.0	9461.6	13.0	210.3
28	1350.0	534.0	9623.5	13.5	213.9
29	1400.0	543.5	9794.4	14.0	217.7
30	1450.0	553.0	9965.3	14.5	221.5
31	1500.0	562.0	10127.2	15.0	225.0
32	1550.0	571.5	10298.1	15.5	228.8
33	1600.0	581.0	10469.0	16.0	232.6
34	1650.0	590.0	10631.0	16.5	236.2
35	1700.0	599.5	10801.9	17.0	240.0
36	1750.0	609.0	10972.8	17.5	243.8
37	1800.0	618.0	11134.7	18.0	247.4
38	1850.0	627.5	11305.6	18.5	251.2
39	1900.0	637.0	11476.5	19.0	255.0
40	1950.0	646.0	11638.4	19.5	258.6
41	2000.0	655.5	11809.3	20.0	262.4
42	2100.0	674.0	12142.1	21.0	269.8
43	2200.0	693.0	12483.9	22.0	277.4
44	2300.0	711.5	12816.7	23.0	284.8
45	2400.0	730.0	13149.6	24.0	292.2
46	2500.0	749.0	13491.4	25.0	299.8
47	2600.0	767.5	13824.2	26.0	307.2
48	2700.0	786.0	14157.0	27.0	314.6
49	2800.0	804.5	14489.8	28.0	322.0
50	2900.0	823.5	14831.6	29.0	329.6

Srl No	Dial Gauge(div)	Proving Ring(div)	Force (N)	Penetration (mm)	Stress (kN/m ²)
51	3000	842.0	15164.4	30.00	337.0
52	3100	860.5	15497.2	31.00	344.4
53	3200	879.5	15839.1	32.00	352.0
54	3300	898.0	16171.9	33.00	359.4
55	3400	916.5	16504.7	34.00	366.8
56	3500	935.5	16846.5	35.00	374.4
57	3600	954.0	17179.3	36.00	381.8
58	3700	972.5	17512.1	37.00	389.2
59	3800	991.5	17853.9	38.00	396.8
60	3900	1010.0	18186.8	39.00	404.2
61	4000	1028.5	18519.6	40.00	411.5
62	4100	1047.0	18852.4	41.00	418.9
63	4200	1066.0	19194.2	42.00	426.5
64	4300	1084.5	19527.0	43.00	433.9

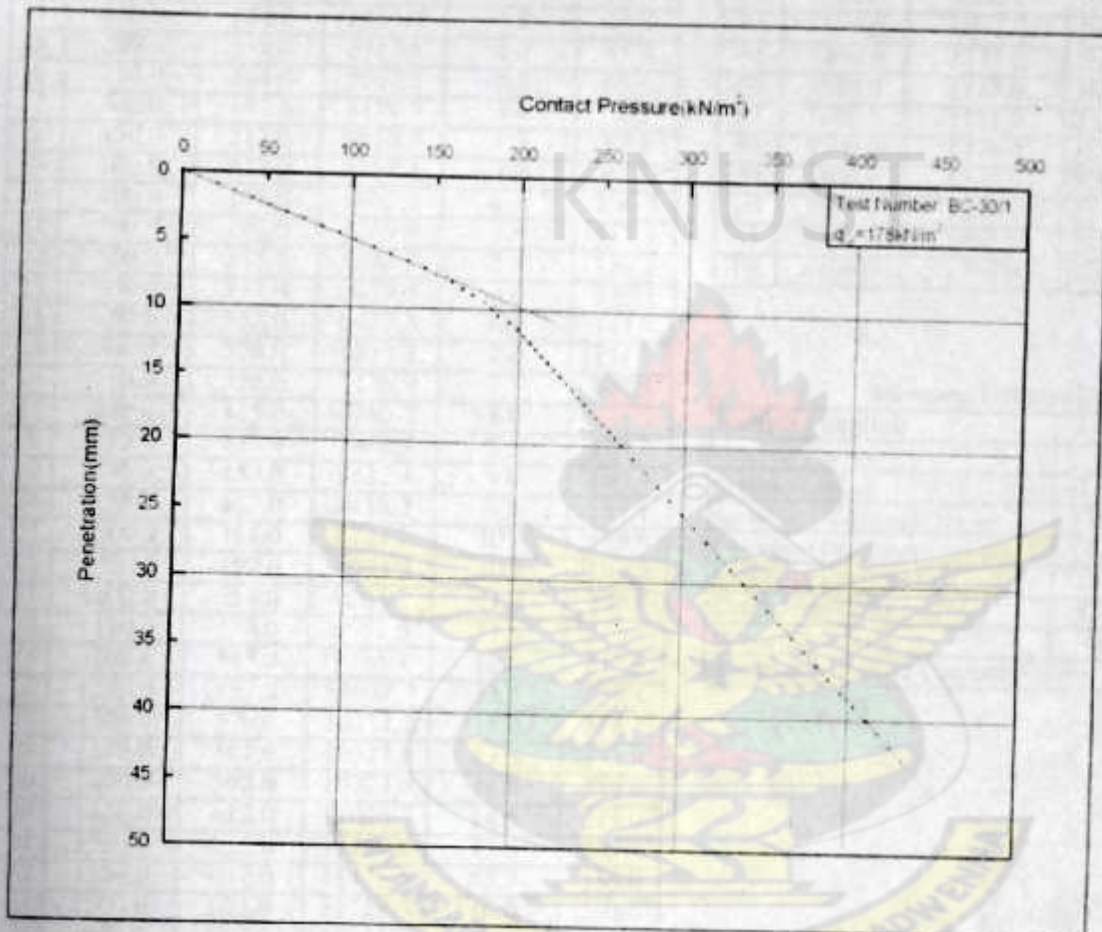
Moisture Content Determination

Sample Location	Top	Middle	Bottom
Container Number	X4	D9	C6
Container Mass (g)	18.17	18.13	17.8
Container + Wet Sample Mass(g)	107.67	108.52	119.1
Container + Dry Sample Mass (g)	94.63	93.77	104.2
Moisture Content (g)	13.04	14.75	14.95
Dry Sample Mass (g)	76.46	75.64	86.32
Moisture Content (%)	17.1	19.5	17.3
Average Moisture Content (%) =	18.0		

CIVIL ENGINEERING DEPARTMENT-KNUST
DCPT-ULTIMATE BEARING CAPACITY PROJECT
LOADING TEST GRAPH

Test No.: BC-30/1

Date: 26/04/20



CIVIL ENGINEERING DEPARTMENT-KNUST
DCPT-ULTIMATE BEARING CAPACITY PROJECT
LOADING TEST

Date: 1/05/2007

Test No.: BC-35/1

Srl No.	Dial Gauge (div)	Proving Ring (div)	Force (N)	Penetration (mm)	Stress (kN/m ²)
1	0.0	0.0	0	0.0	0.0
2	50.0	65.0	1186.2	0.5	26.4
3	100.0	90.0	1636.0	1.0	36.4
4	150.0	114.0	2067.7	1.5	45.9
5	200.0	139.0	2517.5	2.0	55.9
6	250.0	164.0	2967.2	2.5	65.9
7	300.0	192.0	3470.9	3.0	77.1
8	350.0	217.0	3920.7	3.5	87.1
9	400.0	243.0	4388.4	4.0	97.5
10	450.0	266.0	4802.2	4.5	106.7
11	500.0	292.0	5269.9	5.0	117.1
12	550.0	315.0	5683.7	5.5	126.3
13	600.0	337.0	6079.5	6.0	135.1
14	650.0	358.0	6457.3	6.5	143.5
15	700.0	378.0	6817.1	7.0	151.5
16	750.0	398.0	7176.9	7.5	159.5
17	800.0	415.0	7482.7	8.0	166.3
18	850.0	433.0	7806.5	8.5	173.5
19	900.0	450.0	8112.4	9.0	180.3
20	950.0	467.0	8418.2	9.5	187.1
21	1000.0	484.0	8724.0	10.0	193.9
22	1050.0	499.0	8993.9	10.5	199.9
23	1100.0	514.0	9263.7	11.0	205.9
24	1150.0	530.0	9551.6	11.5	212.3
25	1200.0	543.0	9785.4	12.0	217.5
26	1250.0	557.0	10037.3	12.5	223.4
27	1300.0	570.0	10271.2	13.0	228.2
28	1350.0	584.0	10523.0	13.5	233.8
29	1400.0	598.0	10774.9	14.0	239.4
30	1450.0	612.0	11026.7	14.5	245.0
31	1500.0	625.0	11260.6	15.0	250.2
32	1550.0	637.0	11476.5	15.5	255.0
33	1600.0	651.0	11728.3	16.0	260.6
34	1650.0	664.0	11962.2	16.5	265.8
35	1700.0	678.0	12214.1	17.0	271.4
36	1750.0	692.0	12465.9	17.5	277.0
37	1800.0	705.0	12699.8	18.0	282.2
38	1850.0	718.0	12933.7	18.5	287.4
39	1900.0	732.0	13185.5	19.0	293.0
40	1950.0	745.0	13419.4	19.5	298.2
41	2000.0	758.0	13653.3	20.0	303.4
42	2100.0	785.0	14139.0	21.0	314.2
43	2200.0	809.0	14570.8	22.0	323.8
44	2300.0	834.0	15020.5	23.0	333.8
45	2400.0	860.0	15488.3	24.0	344.2
46	2500.0	885.0	15938.0	25.0	354.2
47	2600.0	911.0	16405.7	26.0	364.6
48	2700.0	936.0	16855.5	27.0	374.6
49	2800.0	963.0	17341.2	28.0	385.4
50	2900.0	990.0	17827.0	29.0	396.2

Srl No.	Dial Gauge (div)	Proving Ring (div)	Force (N)	Penetration (mm)	Stress (kN/m ²)
51	3000.0	1015.0	18276.7	30.0	406.1
52	3100.0	1040.0	18726.5	31.0	416.1
53	3200.0	1066.0	19194.2	32.0	426.5
54	3300.0	1092.0	19661.9	33.0	436.9
55	3400.0	1117.0	20111.7	34.0	446.9
56	3500.0	1145.0	20615.4	35.0	458.1
57	3600.0	1171.0	21083.1	36.0	468.5
58	3700.0	1210.0	21784.8	37.0	484.1
59	3800.0	1227.0	22090.6	38.0	490.9
60	3900.0	1254.0	22576.3	39.0	501.7
61	4000.0	1282.0	23080.0	40.0	512.9
62	4100.0	1309.0	23565.8	41.0	523.7

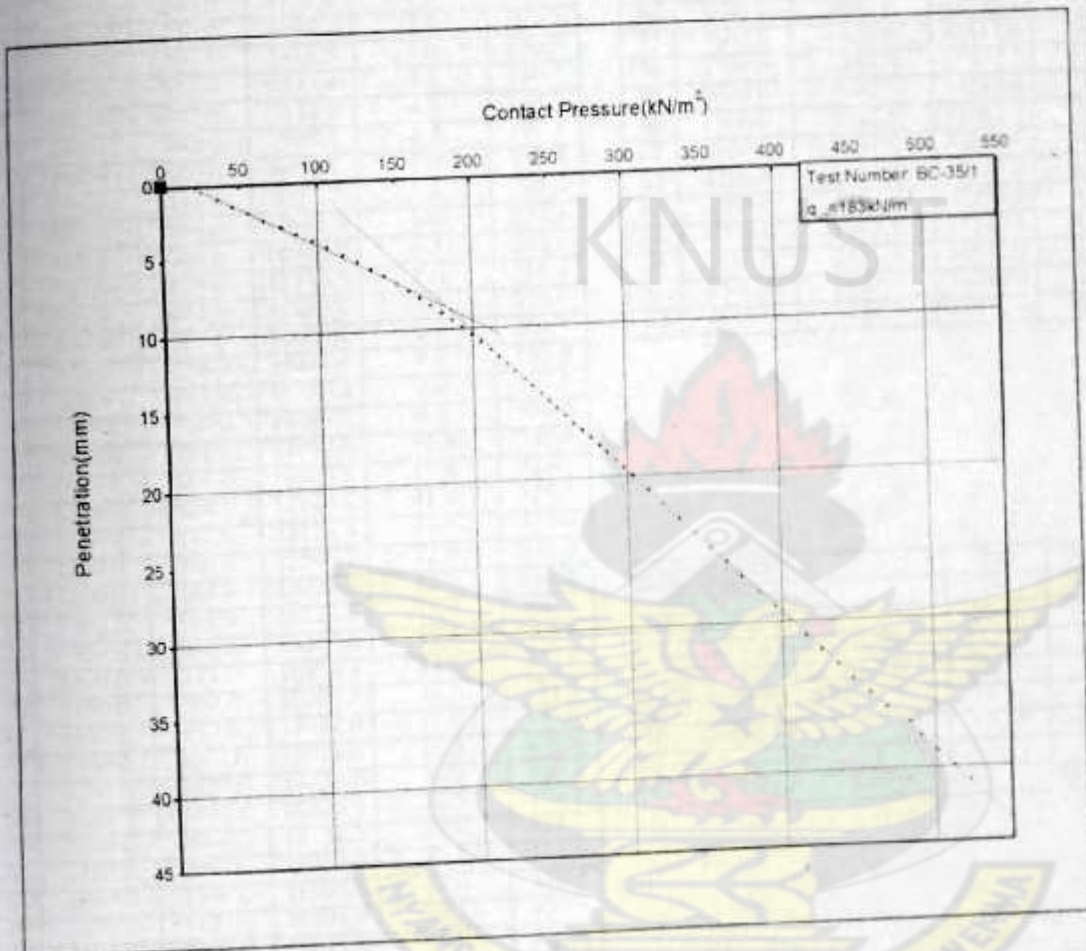
Moisture Content Determination

Sample Location	Top	Middle	Bottom
Container Number	X4	B3	C6
Container Mass (g)	18.17	14.2	17.8
Container + Wet Sample Mass (g)	133.44	88.1	149.8
Container + Dry Sample Mass (g)	115.19	76.4	129.7
Moisture Content (g)	18.25	11.73	20.09
Dry Sample Mass (g)	97.02	62.16	111.86
Moisture Content (%)	18.8	18.9	18.0
Average Moisture Content (%) =	18.5		

CIVIL ENGINEERING DEPARTMENT-KNUST
DCPT-ULTIMATE BEARING CAPACITY PROJECT
LOADING TEST GRAPH

Test No.: BC-35/1

Date: 1/05/2007



CIVIL ENGINEERING DEPARTMENT-KNUST
DCPT-ULTIMATE BEARING CAPACITY PROJECT
LOADING TEST

Test No.: BC-100/I

Date: 25/05/2007

Srl No.	Dial Gauge (div)	Proving Ring (div)	Force (N)	Penetration (mm)	Stress (kN/m ²)
1	0.0	0.0	0	0.0	0.0
2	50.0	68.0	1240.2	0.5	27.6
3	100.0	125.0	2265.6	1.0	50.3
4	150.0	164.0	2967.2	1.5	65.9
5	200.0	205.0	3704.8	2.0	82.3
6	250.0	250.0	4514.4	2.5	100.3
7	300.0	300.0	5413.9	3.0	120.3
8	350.0	350.0	6313.4	3.5	140.3
9	400.0	395.0	7122.9	4.0	158.3
10	450.0	442.0	7968.4	4.5	177.1
11	500.0	480.0	8652.1	5.0	192.3
12	550.0	512.0	9227.7	5.5	205.1
13	600.0	560.0	10091.3	6.0	224.3
14	650.0	606.0	10918.8	6.5	242.6
15	700.0	640.0	11530.5	7.0	256.2
16	750.0	682.0	12286.0	7.5	273.0
17	800.0	703.0	12663.8	8.0	281.4
18	850.0	724.0	13041.6	8.5	289.8
19	900.0	743.0	13383.4	9.0	297.4
20	950.0	766.0	13797.2	9.5	306.6
21	1000.0	781.0	14067.0	10.0	312.6
22	1050.0	805.0	14498.8	10.5	322.2
23	1100.0	824.0	14840.6	11.0	329.8
24	1150.0	847.0	15254.4	11.5	339.0
25	1200.0	866.0	15596.2	12.0	346.6
26	1250.0	884.0	15920.0	12.5	353.8
27	1300.0	901.0	16225.8	13.0	360.6
28	1350.0	922.0	16603.6	13.5	369.0
29	1400.0	944.0	16999.4	14.0	377.8
30	1450.0	960.0	17287.3	14.5	384.2
31	1500.0	982.0	17683.0	15.0	393.0
32	1550.0	1001.0	18024.8	15.5	400.6
33	1600.0	1025.0	18456.6	16.0	410.1
34	1650.0	1040.0	18726.5	16.5	416.1
35	1700.0	1064.0	19158.2	17.0	425.7
36	1750.0	1081.0	19464.0	17.5	432.5
37	1800.0	1100.0	19805.9	18.0	440.1
38	1850.0	1127.0	20291.6	18.5	450.9
39	1900.0	1145.0	20615.4	19.0	458.1
40	1950.0	1160.0	20885.3	19.5	464.1
41	2000.0	1185.0	21335.0	20.0	474.1
42	2100.0	1222.0	22000.6	21.0	488.9
43	2200.0	1266.0	22792.2	22.0	506.5
44	2300.0	1301.0	23421.8	23.0	520.5
45	2400.0	1342.0	24159.4	24.0	536.9
46	2500.0	1384.0	24915.0	25.0	553.7
47	2600.0	1420.0	25562.7	26.0	568.1
48	2700.0	1465.0	26372.2	27.0	586.0
49	2800.0	1500.0	27001.9	28.0	600.0
50	2900.0	1540.0	27721.5	29.0	616.0

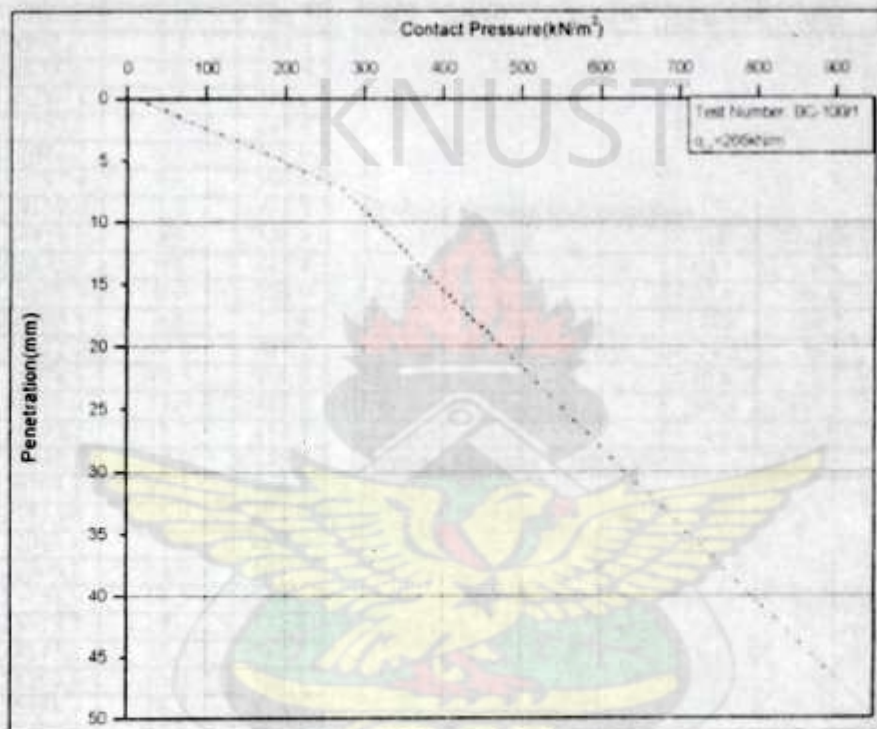
Srl No.	Dial Gauge (div)	Proving Ring (div)	Force (N)	Penetration (mm)	Stress (kN/m ²)
51	3000.0	1579.0	28423.1	30.0	631.6
52	3100.0	1620.0	29160.7	31.0	648.0
53	3200.0	1664.0	29952.2	32.0	665.6
54	3300.0	1704.0	30671.8	33.0	681.6
55	3400.0	1740.0	31319.5	34.0	696.0
56	3500.0	1780.0	32039.1	35.0	712.0
57	3600.0	1823.0	32812.6	36.0	729.2
58	3700.0	1863.0	33532.2	37.0	745.2
59	3800.0	1902.5	34242.8	38.0	761.0
60	3900.0	1942.5	34962.4	39.0	776.9
61	4000.0	1981.5	35664.0	40.0	792.5
62	4100.0	2022.0	36392.6	41.0	808.7
63	4200.0	2061.5	37103.2	42.0	824.5
64	4300.0	2102.5	37840.8	43.0	840.9
65	4400.0	2141.5	38542.4	44.0	856.5
66	4500.0	2182.5	39280.0	45.0	872.9
67	4600.0	2221.0	39972.6	46.0	888.3

Sample Location	Top	Middle	Bottom
Container Number	D1	N3	18.0
Container Mass (g)	18.32	17.9	17.7
Container + Wet Sample Mass (g)	132.89	144.9	150.4
Container + Dry Sample Mass (g)	114.05	124.2	129.2
Moisture Content (g)	18.84	20.69	21.25
Dry Sample Mass (g)	95.73	106.25	111.46
Moisture Content (%)	19.7	19.5	19.1
Average Moisture Content (%) =	19.4		

CIVIL ENGINEERING DEPARTMENT-KNUST
DCPT-ULTIMATE BEARING CAPACITY PROJECT
LOADING TEST GRAPH

Test No.: BC-100/1

Date: 25/05/2007



CIVIL ENGINEERING DEPARTMENT-KNUST
DCPT-ULTIMATE BEARING CAPACITY PROJECT
LOADING TEST

Test No.: BC-150/1

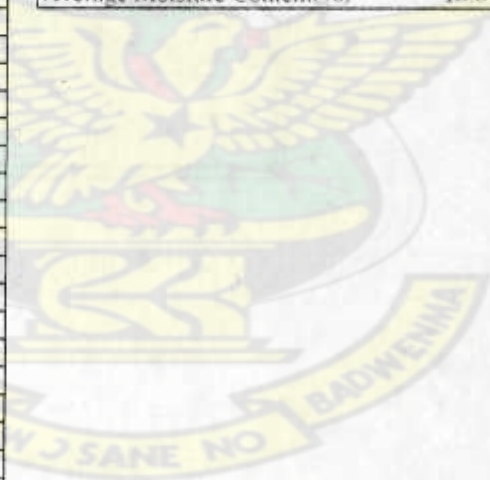
Date: 30/05/2007

Srl No	Dial Gauge (div)	Proving Ring (div)	Force (N)	Penetration (mm)	Stress (kN/m ²)
1	0.0	0.0	0	0.0	0.0
2	50.0	73.0	1330.1	0.5	29.6
3	100.0	130.0	2355.6	1.0	52.3
4	150.0	185.0	3345.0	1.5	74.3
5	200.0	238.0	4298.5	2.0	95.5
6	250.0	286.0	5162.0	2.5	114.7
7	300.0	334.0	6025.5	3.0	133.9
8	350.0	378.0	6817.1	3.5	151.5
9	400.0	421.0	7590.6	4.0	168.7
10	450.0	460.0	8292.3	4.5	184.3
11	500.0	498.0	8975.9	5.0	199.5
12	550.0	571.0	10289.1	5.5	228.6
13	600.0	619.0	11152.7	6.0	247.8
14	650.0	667.0	12016.2	6.5	267.0
15	700.0	741.0	13347.4	7.0	296.6
16	750.0	785.0	14139.0	7.5	314.2
17	800.0	821.5	14795.6	8.0	328.8
18	850.0	858.0	15452.3	8.5	343.4
19	900.0	894.5	16108.9	9.0	358.0
20	950.0	931.0	16765.5	9.5	372.6
21	1000.0	967.5	17422.2	10.0	387.2
22	1050.0	1004.0	18078.8	10.5	401.8
23	1100.0	1040.5	18735.4	11.0	416.3
24	1150.0	1077.0	19392.1	11.5	430.9
25	1200.0	1113.5	20048.7	12.0	445.5
26	1250.0	1150.0	20705.4	12.5	460.1
27	1300.0	1186.0	21353.0	13.0	474.5
28	1350.0	1223.0	22018.6	13.5	489.3
29	1400.0	1259.0	22666.3	14.0	503.7
30	1450.0	1296.0	23331.9	14.5	518.5
31	1500.0	1332.0	23979.5	15.0	532.9
32	1550.0	1369.0	24645.2	15.5	547.7
33	1600.0	1405.0	25292.8	16.0	562.1
34	1650.0	1442.0	25958.4	16.5	576.9
35	1700.0	1478.0	26606.1	17.0	591.2
36	1750.0	1514.5	27262.7	17.5	605.8
37	1800.0	1551.0	27919.3	18.0	620.4
38	1850.0	1587.5	28576.0	18.5	635.0
39	1900.0	1624.0	29232.6	19.0	649.6
40	1950.0	1660.5	29889.2	19.5	664.2
41	2000.0	1697.0	30545.9	20.0	678.8
42	2100.0	1770.0	31859.2	21.0	708.0
43	2200.0	1843.0	33172.4	22.0	737.2
44	2300.0	1916.0	34485.7	23.0	766.3
45	2400.0	1988.5	35790.0	24.0	795.3
46	2500.0	2061.5	37103.2	25.0	824.5
47	2600.0	2134.5	38416.5	26.0	853.7
48	2700.0	2207.5	39729.8	27.0	882.9
49	2800.0	2280.5	41043.0	28.0	912.1
50	2900.0	2353.0	42347.3	29.0	941.1

Srl No	Dial Gauge (div)	Proving Ring (div)	Force (N)	Penetration (mm)	Stress (kN/m ²)
51	3000.0	2426.0	43660.6	30.0	970.2
52	3100.0	2499.0	44973.9	31.0	999.4
53	3200.0	2572.0	46287.1	32.0	1028.6
54	3300.0	2645.0	47600.4	33.0	1057.8
55	3400.0	2718.0	48913.7	34.0	1087.0
56	3500.0	2791.0	50226.9	35.0	1116.2
57	3600.0	2864.0	51540.2	36.0	1145.3
58	3700.0	2937.0	52853.5	37.0	1174.5
59	3800.0	3010.0	54166.8	38.0	1203.7

Moisture Content Determination

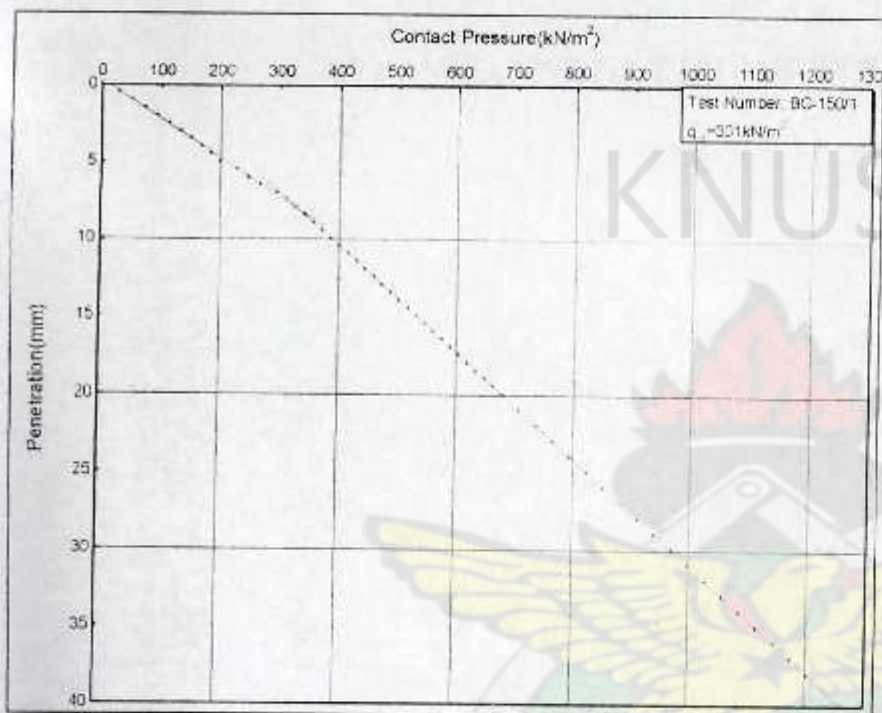
Sample Location	Top	Middle	Bottom
Container Number	C17	A9	Y3
Container Mass (g)	17.8	18.4	17.8
Container + Wet Sample Mass (g)	144.0	160.5	160.1
Container + Dry Sample Mass (g)	124.2	138.1	137.2
Moisture Content (g)	19.8	22.4	22.8
Dry Sample Mass (g)	106.4	119.8	119.5
Moisture Content (%)	18.6	18.7	19.1
Average Moisture Content (%) =	18.8		



CIVIL ENGINEERING DEPARTMENT-KNUST
DCPT-ULTIMATE BEARING CAPACITY PROJECT
LOADING TEST GRAPH

Test No.: BC-150/1

Date: 30/05/2007



LIBRARY
KWAME NKRUumah UNIVERSITY OF
SCIENCE AND TECHNOLOGY
KUMASI-GHANA

APPENDIX IV

DYNAMIC CONE PENETROMETER TEST

KNUST

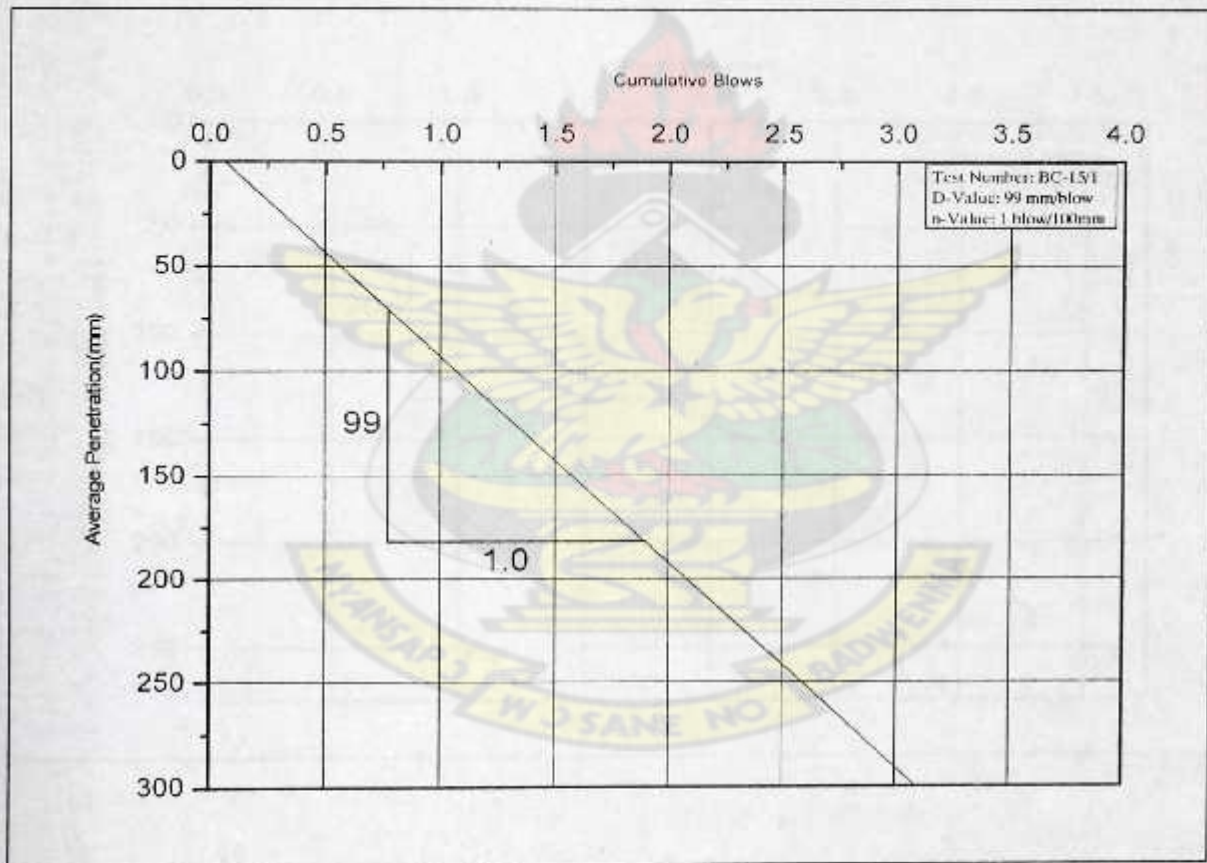


CIVIL ENGINEERING DEPARTMENT-KNUST
DCPT-ULTIMATE BEARING CAPACITY PROJECT
DYNAMIC CONE PENETROMETER TEST

Test No.: BC-15/1

Date: 23/04/2007

Cumulative Blows	Penetration(mm)		
	d_1	d_2	Aveg. $d = (d_1 + d_2)/2$
0	0	0	0
1	70	90	80
2	220	180	200
3	320	260	290

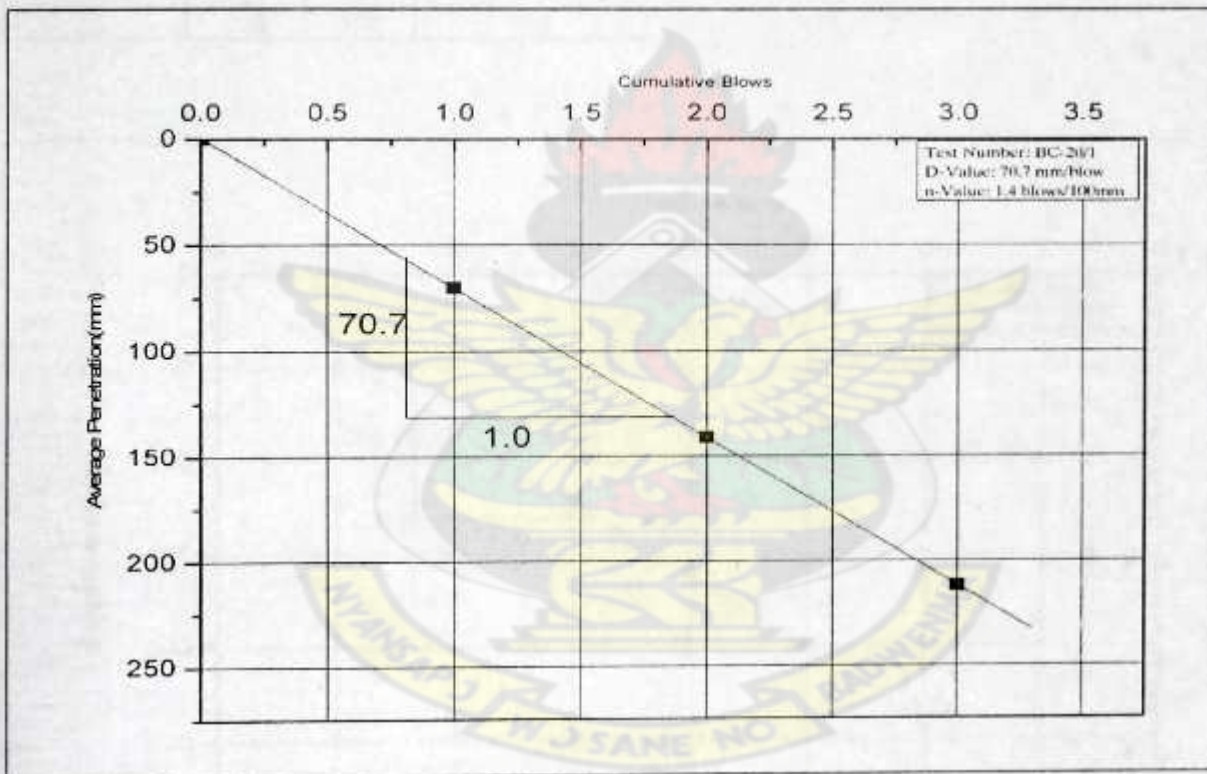


CIVIL ENGINEERING DEPARTMENT-KNUST
DCPT-ULTIMATE BEARING CAPACITY PROJECT
DYNAMIC CONE PENETROMETER TEST

Test No.:BC-20/1

Date: 19/04/2007

Cumulative Blows	Penetration(mm)		
	d_1	d_2	Aveg. $d=(d_1+d_2)/2$
0	0	0.0	0
1	50	90.0	70
2	112	170.0	141
3	180	244.0	212

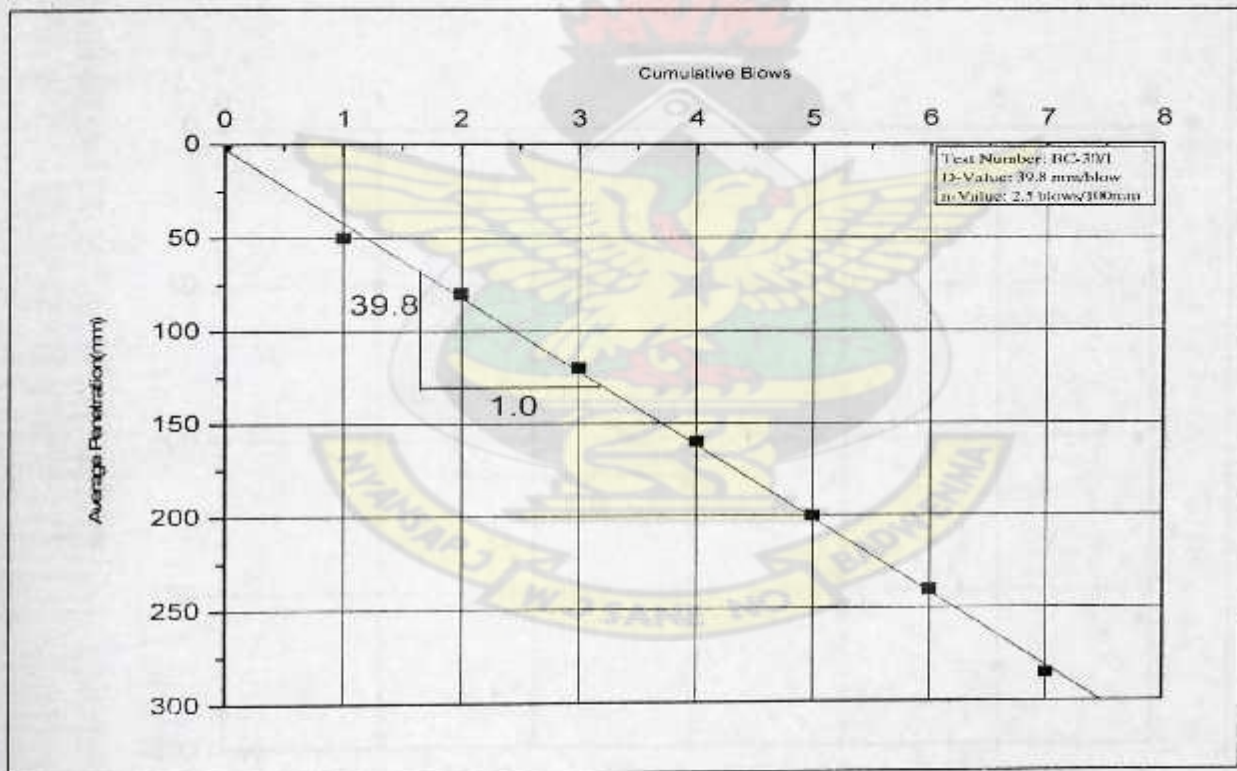


CIVIL ENGINEERING DEPARTMENT-KNUST
DCPT-ULTIMATE BEARING CAPACITY PROJECT
DYNAMIC CONE PENETROMETER TEST

Test No.: BC-30/1

Date: 26/04/2007

Cumulative Blows	Penetration(mm)		
	d_1	d_2	Aveg. $d = (d_1 + d_2)/2$
0	0	0	0
1	60	40	50
2	90	70	80
3	130	110	120
4	160	160	160
5	200	200	200
6	230	250	240
7	270	300	285

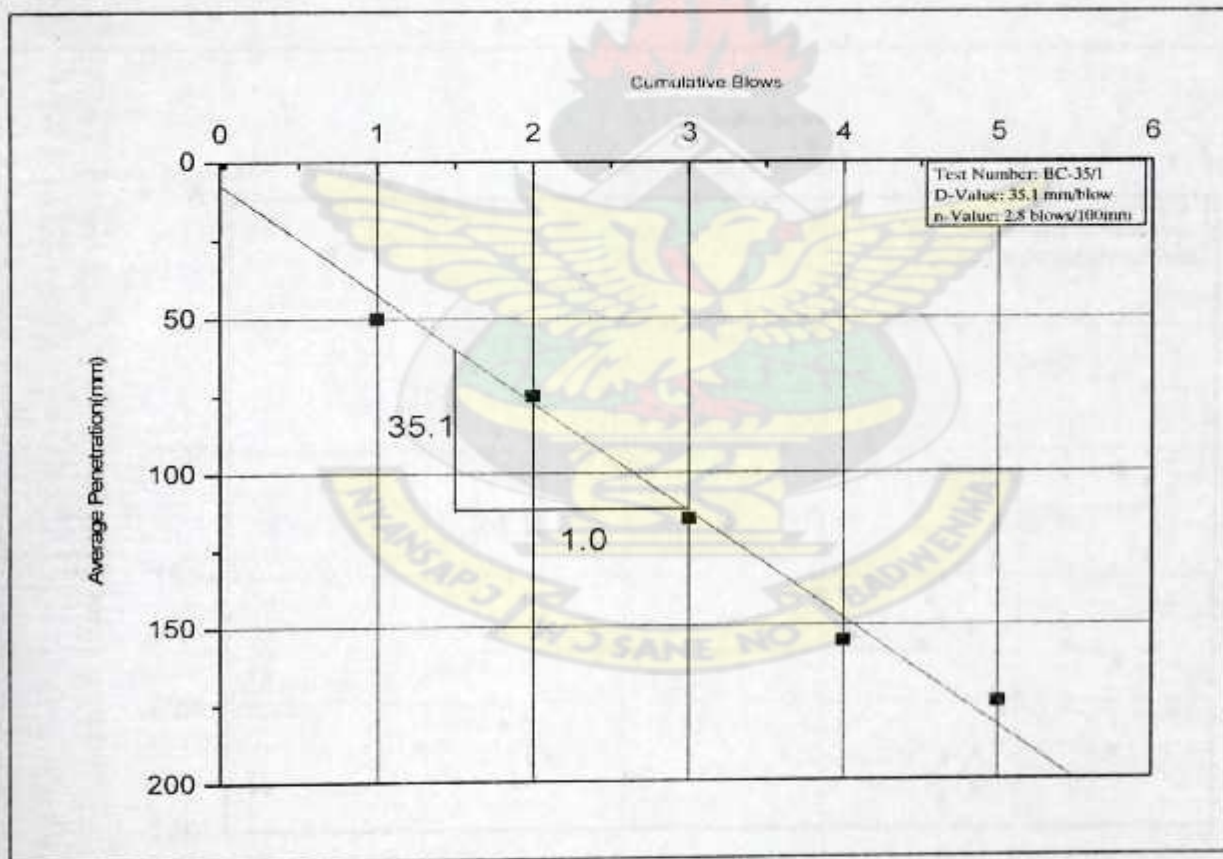


CIVIL ENGINEERING DEPARTMENT-KNUST
DCPT-ULTIMATE BEARING CAPACITY PROJECT
DYNAMIC CONE PENETROMETER TEST

Test No.: BC-35/1

Date: 1/05/2007

Cumulative Blows	Penetration(mm)		
	d_1	d_2	Aveg. $d = (d_1 + d_2)/2$
0	0	0	0
1	50	50	50
2	80	70	75
3	120	110	115
4	160	150	155
5	180	170	175

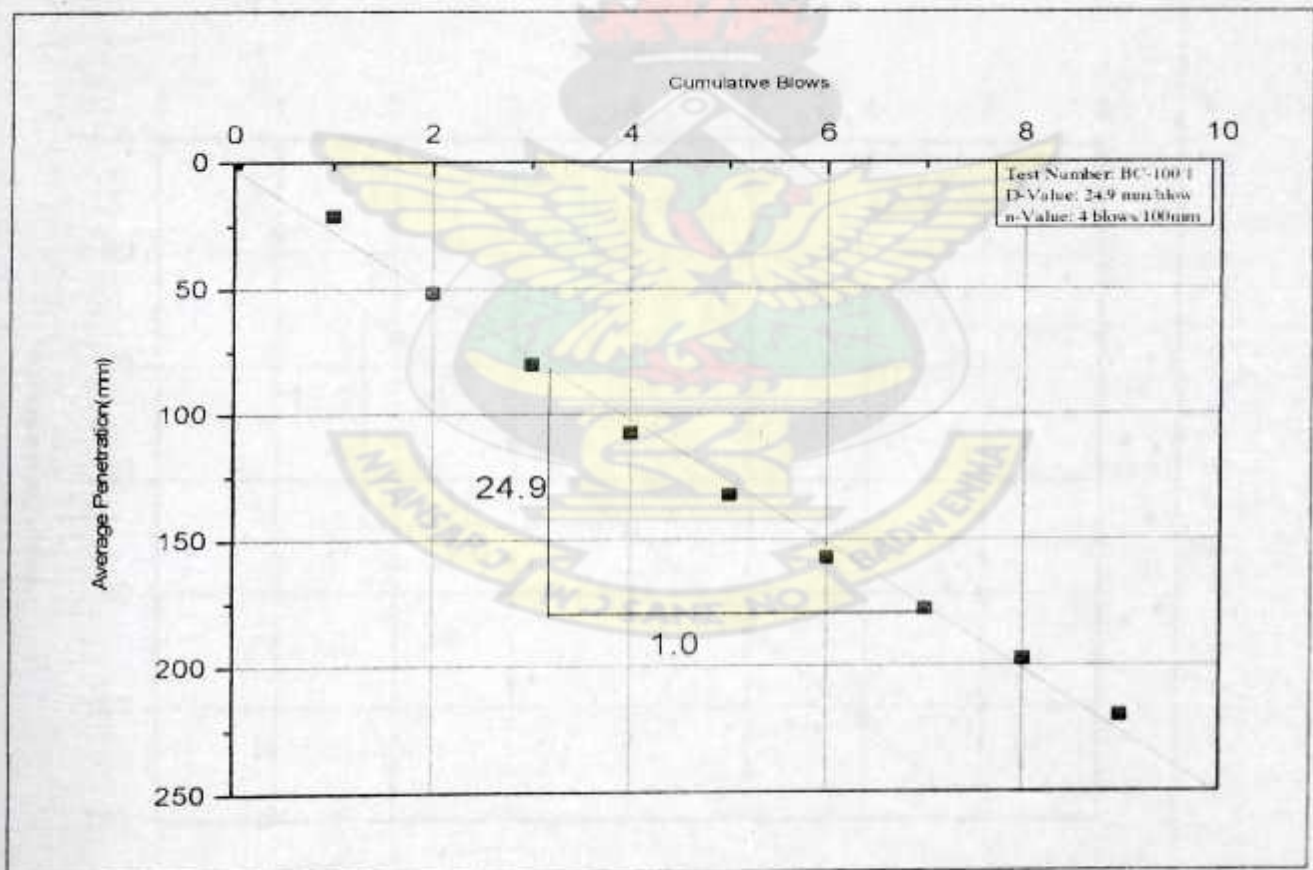


CIVIL ENGINEERING DEPARTMENT-KNUST
DCPT-ULTIMATE BEARING CAPACITY PROJECT
DYNAMIC CONE PENETROMETER TEST

Test No.: BC-100/1

Date: 25/05/2007

Cumulative Blows	Penetration(mm)		
	d_1	d_2	Aveg. $d = (d_1 + d_2) / 2$
0	0	0	0.0
1	20	22	21.0
2	55	48	51.5
3	80	80	80.0
4	110	105	107.5
5	135	130	132.5
6	160	155	157.5
7	185	170	177.5
8	200	195	197.5
9	220	220	220.0

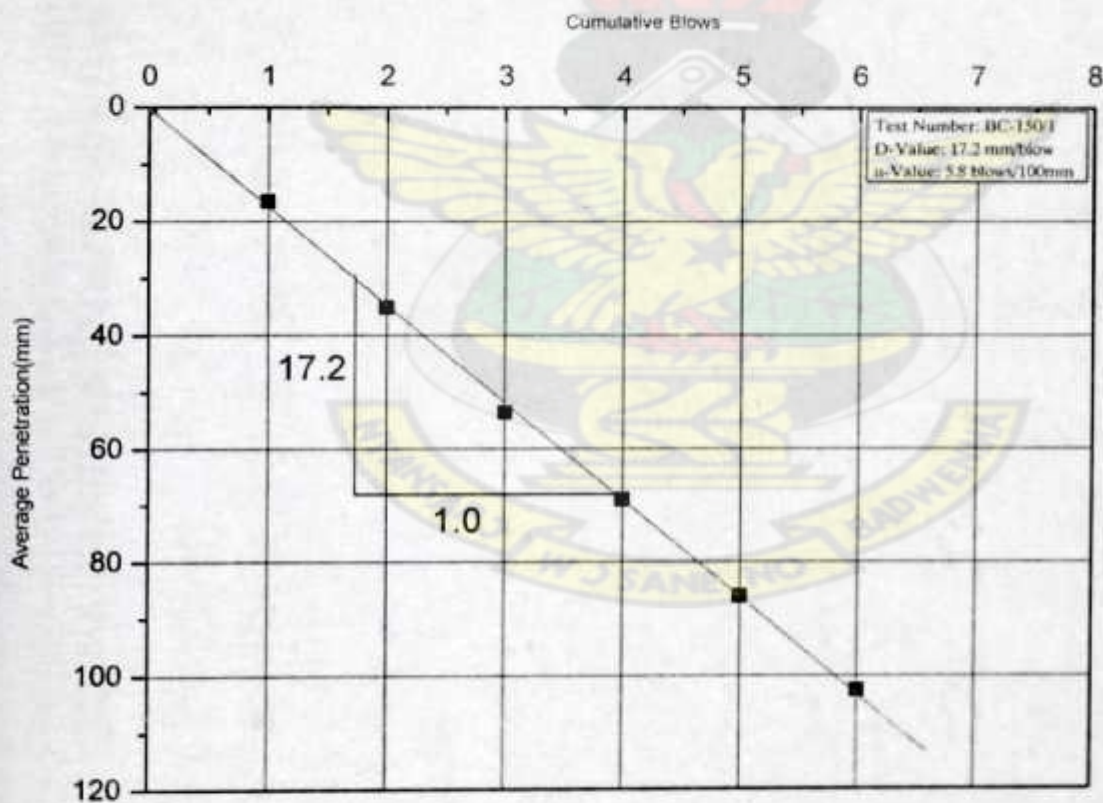


CIVIL ENGINEERING DEPARTMENT-KNUST
DCPT-ULTIMATE BEARING CAPACITY PROJECT
DYNAMIC CONE PENETROMETER TEST

Test No.: BC-150/1

Date: 30/05/2007

Cumulative Blows	Penetration(mm)		
	d_1	d_2	Aveg. $d = (d_1 + d_2)/2$
0	0	0	0
1	18	15	16.5
2	35	35	35
3	52	55	53.5
4	68	70	69
5	85	87	86
6	100	105	102.5



APPENDIX VI

UNCONSOLIDATED-UNDRAINED TRIAXIAL TEST

TRIAXIAL STRESS-STRAIN CURVES

MOHR CIRCLE



LIBRARY
KWAME NKUMAH UNIVERSITY OF
SCIENCE AND TECHNOLOGY
KUMASI-GHANA

CIVIL ENGINEERING DEPARTMENT-KNUST
DCPT-ULTIMATE BEARING CAPACITY PROJECT
UNCONSOLIDATED-UNDRAINED TRIAXIAL TEST ANALYSIS

Test No.: BC-15/1

Date :24/4/2007

SAMPLE CHARACTERISTICS

Sample Number	A	B	C	Averages
Initial Sample Height (cm)	7.60	7.60	7.60	
Initial Sample Diameter (cm)	3.80	3.80	3.80	
Initial Sample Volume(cm^3)	86.19	86.19	86.19	
Initial Wet Sample Mass (g)	132.60	133.21	132.85	
Wet Bulk Density (g/cm^3)	1.538	1.546	1.541	1.542
Container Number	5	D9	D19	
Container Mass (g)	16.45	16.01	18.24	
Cont. + Final Wet Sample Mass (g)	146.70	148.81	150.62	
Container + Dry Sample Mass (g)	128.67	129.99	132.13	
Moisture Content Mass (g)	18.03	18.82	18.49	
Dry Sample Mass (g)	112.22	113.98	113.89	
Moisture Content (%)	16.1	16.5	16.2	16.3
Dry Density (g/cm^3)	1.325	1.327	1.326	1.326

TEST CONDITION

Sample Number	A	B	C
Confining Pressure (kpa)	150	300	450
Proving Ring Constant	0.00816	0.00207	0.00199

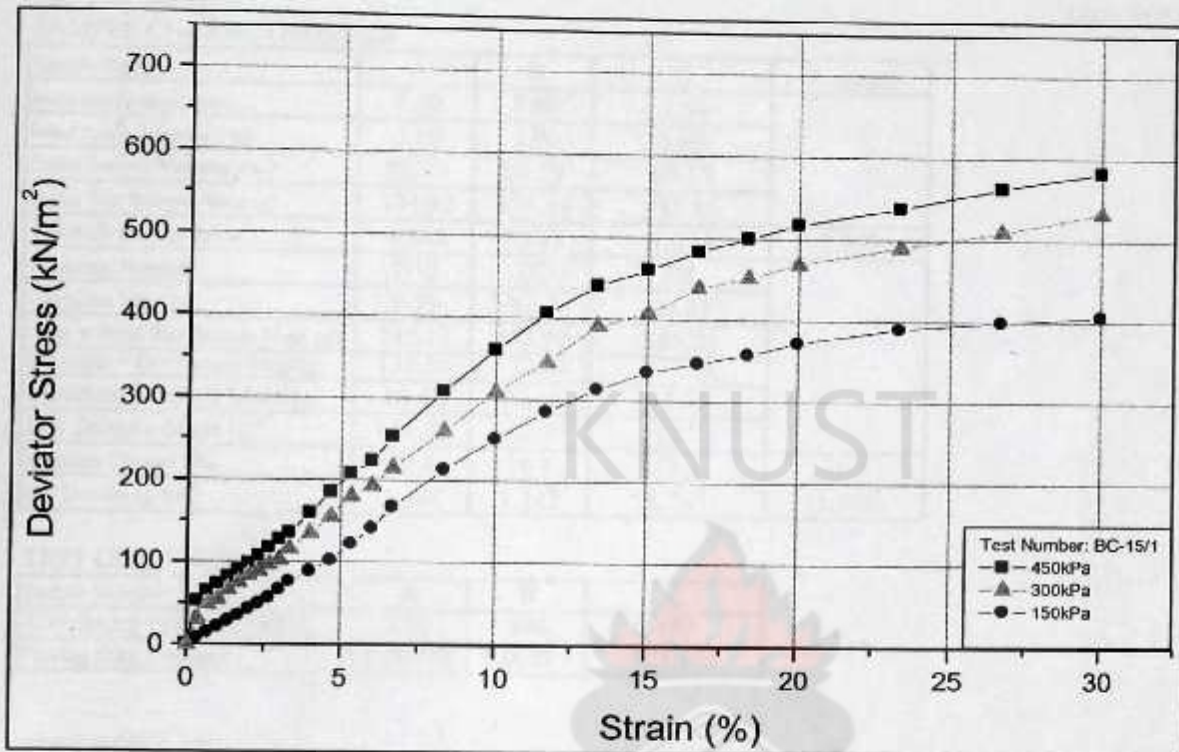
TEST RESULTS

			Sample Number A ($\sigma_3=150\text{kPa}$)		Sample Number B ($\sigma_3=300\text{kPa}$)		Sample Number C ($\sigma_3=450\text{kPa}$)	
Change in Length (mm)	Strain (%)	New area (mm^2)	Ring Reading (div)	Deviator Stress $q = \sigma_1 - \sigma_3$ (kPa)	Proving Ring Reading (div)	Deviator Stress $q = \sigma_1 - \sigma_3$ (kPa)	Proving Ring Reading (div)	Deviator Stress $q = \sigma_1 - \sigma_3$ (kPa)
0.00	0.00	1140.09	0.0	0	0.0	0	0.0	0
0.25	0.33	1143.91	1.0	7	17.0	31	30.0	52
0.51	0.67	1147.75	2.0	14	27.0	49	37.0	64
0.76	1.00	1151.61	3.0	21	30.0	54	42.0	73
1.02	1.33	1155.50	4.0	28	37.0	66	47.0	81
1.27	1.67	1159.42	5.0	35	42.0	75	52.0	89
1.52	2.00	1163.36	6.0	42	47.0	84	57.0	98
1.78	2.33	1167.33	7.0	49	50.0	89	63.0	107
2.03	2.67	1171.33	8.0	56	55.0	97	69.0	117
2.29	3.00	1175.36	9.5	66	58.0	102	75.0	127
2.54	3.33	1179.41	11.0	76	66.0	116	80.0	135
3.05	4.00	1187.60	13.0	89	77.5	135	95.0	159
3.56	4.67	1195.90	15.0	102	89.5	155	111.0	185
4.06	5.33	1204.33	18.0	122	105.0	180	126.0	208
4.57	6.00	1212.87	21.0	141	113.0	193	136.0	223
5.08	6.67	1221.53	25.0	167	127.0	215	155.0	253
6.35	8.33	1243.74	32.5	213	156.0	260	193.0	309
7.62	10.00	1266.77	39.0	251	189.0	309	229.0	360
8.89	11.67	1290.67	45.0	285	216.0	346	263.0	406
10.16	13.33	1315.49	50.5	313	248.5	391	291.0	440
11.43	15.00	1341.29	55.0	335	264.0	407	310.0	460
12.70	16.67	1368.11	58.0	346	289.5	438	332.0	483
13.97	18.33	1396.03	61.0	357	305.0	452	351.0	500
15.24	20.00	1425.12	65.0	372	323.0	469	370.0	517
17.78	23.33	1487.08	71.0	390	352.0	490	402.0	538
20.32	26.67	1554.67	76.0	399	383.0	510	440.0	563
22.85	30.00	1528.71	76.0	406	393.5	533	448.0	583

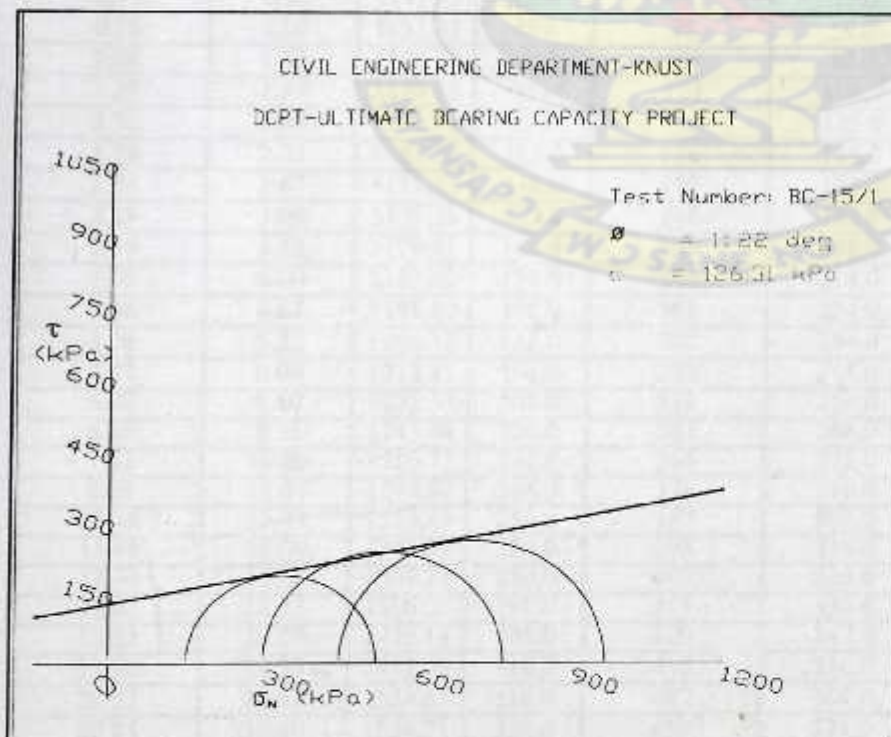
CIVIL ENGINEERING DEPARTMENT-KNUST
DCPT-ULTIMATE BEARING CAPACITY PROJECT
UNCONSOLIDATED-UNDRAINED TRIAXIAL TEST GRAPH

Test Number.: BC-15/1

Date :24/04/2007



σ_3 (kPa)	$(\sigma_1 - \sigma_3)$ kPa	(σ_1) kPa
150	372	522
300	469	769
450	517	967



CIVIL ENGINEERING DEPARTMENT-KNUST
DCPT-ULTIMATE BEARING CAPACITY PROJECT
UNCONSOLIDATED-UNDRAINED TRIAXIAL TEST ANALYSIS

Test No.: BC-20/1

Date :20/04/2007

SAMPLE CHARACTERISTICS

Sample Number	A	B	C	Averages
Initial Sample Height (cm)	7.60	7.60	7.60	
Initial Sample Diameter (cm)	3.80	3.80	3.80	
Initial Sample Volume(cm ³)	86.19	86.19	86.19	
Initial Wet Sample Mass (g)	134.92	135.14	135.66	
Wet Bulk Density (g/cm ³)	1.565	1.568	1.574	1.569
Container Number	D12	D2	D1	
Container Mass (g)	9.39	9.47	20.21	
Cont. + Final Wet Sample Mass (g)	142.11	152.90	155.74	
Container + Dry Sample Mass (g)	123.65	132.26	137.91	
Moisture Content Mass (g)	18.46	20.64	17.83	
Dry Sample Mass (g)	114.26	122.79	117.70	
Moisture Content (%)	16.2	16.8	15.1	
Dry Density (g/cm ³)	1.348	1.342	1.367	1.345

TEST CONDITION

Sample Number	A	B	C
Confining Pressure (kpa)	150	300	450
Proving Ring Constant	0.00816	0.00207	0.00199

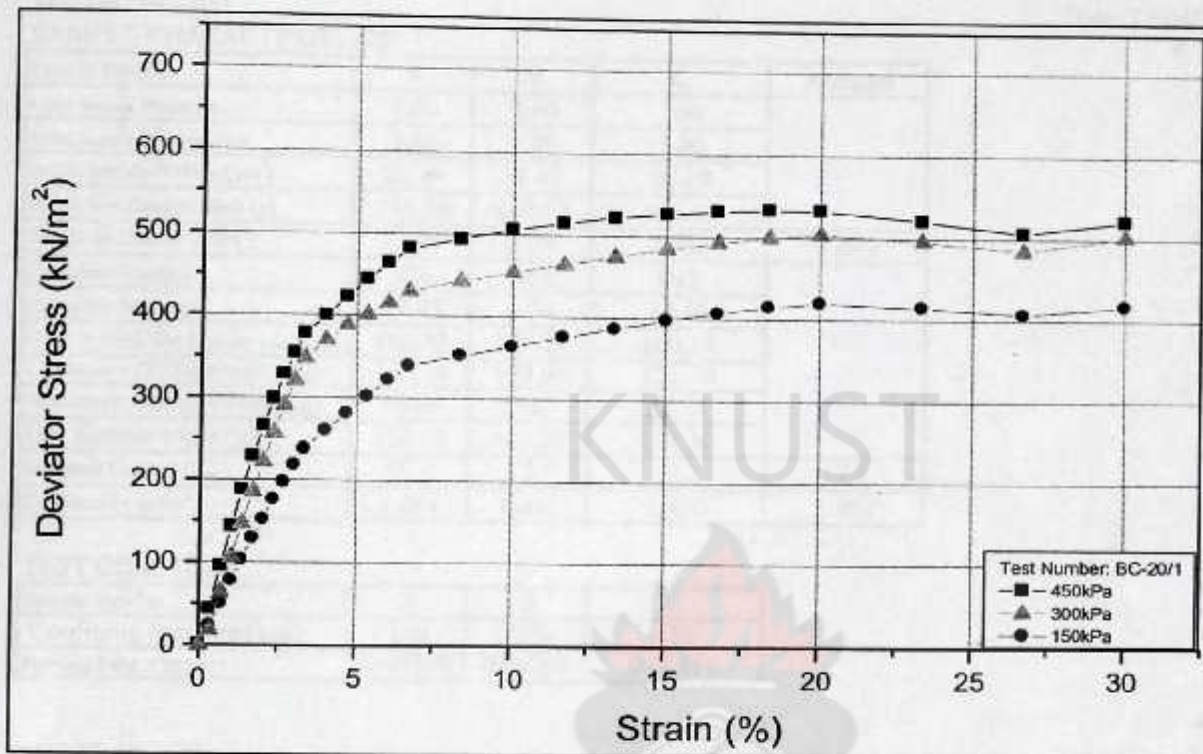
TEST RESULTS

			Sample Number A ($\sigma_3=150\text{kPa}$)		Sample Number B ($\sigma_3=300\text{kPa}$)		Sample Number C ($\sigma_3=450\text{kPa}$)	
Change in Length (mm)	Strain (%)	New area (mm ²)	Ring Reading (div)	Deviator Stress $q = \sigma_1 - \sigma_3$ (kPa)	Proving Ring Reading (div)	Deviator Stress $q = \sigma_1 - \sigma_3$ (kPa)	Proving Ring Reading (div)	Deviator Stress $q = \sigma_1 - \sigma_3$ (kPa)
0.00	0.00	1140.09	0.0	0	0.0	0	0.0	0
0.25	0.33	1143.91	13.0	23	10.0	18	25.0	43
0.51	0.67	1147.75	29.0	50	35.0	63	55.0	95
0.76	1.00	1151.61	45.0	78	59.0	106	83.0	143
1.02	1.33	1155.50	60.0	103	82.0	147	109.0	188
1.27	1.67	1159.42	75.0	129	104.0	186	133.0	228
1.52	2.00	1163.36	89.0	152	125.0	222	155.0	265
1.78	2.33	1167.33	103.0	176	145.0	257	175.0	298
2.03	2.67	1171.33	116.0	197	164.0	290	193.0	328
2.29	3.00	1175.36	129.0	218	182.0	321	209.0	354
2.54	3.33	1179.41	141.0	238	198.0	348	224.0	378
3.05	4.00	1187.60	155.0	260	212.0	370	239.0	400
3.56	4.67	1195.90	169.0	281	224.0	388	254.0	423
4.06	5.33	1204.33	183.0	302	234.0	402	269.0	444
4.57	6.00	1212.87	196.0	322	244.0	416	283.0	464
5.08	6.67	1221.53	208.0	339	254.0	430	296.0	482
6.35	8.33	1243.74	220.0	352	266.0	443	309.0	494
7.62	10.00	1266.77	232.0	364	278.0	454	322.0	506
8.89	11.67	1290.67	244.0	376	290.0	465	334.0	515
10.16	13.33	1315.49	256.0	387	302.0	475	345.0	522
11.43	15.00	1341.29	268.0	398	314.0	485	355.0	527
12.70	16.67	1368.11	280.0	407	326.0	493	365.0	531
13.97	18.33	1396.03	291.0	415	337.0	500	374.0	533
15.24	20.00	1425.12	301.0	420	347.0	504	382.0	533
17.78	23.33	1487.08	310.0	415	356.0	496	389.0	521
20.32	26.67	1554.67	318.0	407	364.0	485	395.0	506
22.85	30.00	1528.71	320.0	417	371.0	502	400.0	521

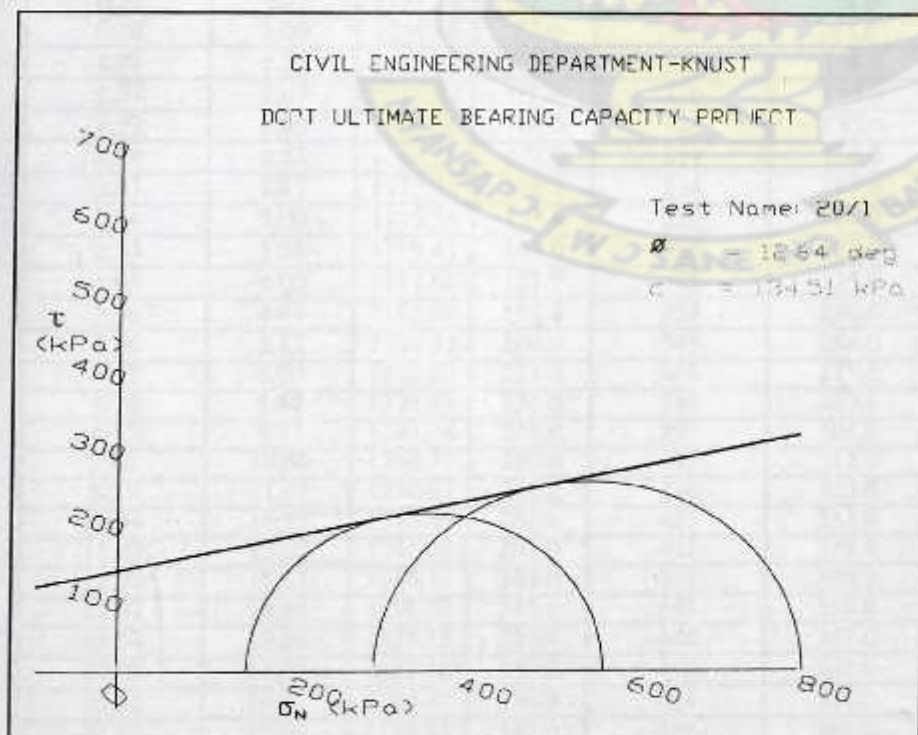
CIVIL ENGINEERING DEPARTMENT-KNUST
DCPT-ULTIMATE BEARING CAPACITY PROJECT
UNCONSOLIDATED-UNDRAINED TRIAXIAL TEST GRAPH

Test Number.: BC-20/1

Date :20/04/2007



σ_3 (kPa)	$(\sigma_1 - \sigma_3)$ kPa	(σ_1) kPa
150	420	570
300	504	804
450	533	983



CIVIL ENGINEERING DEPARTMENT-KNUST
DCPT-ULTIMATE BEARING CAPACITY PROJECT
UNCONSOLIDATED-UNDRAINED TRIAXIAL TEST ANALYSIS

Test No.: BC-30/1

Date :27/04/2007

SAMPLE CHARACTERISTICS

Sample Number	A	B	C	Averages
Initial Sample Height (cm)	7.60	7.60	7.60	
Initial Sample Diameter (cm)	3.80	3.80	3.80	
Initial Sample Volume(cm^3)	86.19	86.19	86.19	
Initial Wet Sample Mass (g)	146.08	146.52	146.65	
Wet Bulk Density (g/cm^3)	1.695	1.700	1.701	1.699
Container Number	K5	D15	D12	
Container Mass (g)	17.45	6.44	14.40	
Cont. + Final Wet Sample Mass (g)	162.33	175.27	160.24	
Container + Dry Sample Mass (g)	142.34	149.66	138.70	
Moisture Content Mass (g)	19.99	25.61	21.54	
Dry Sample Mass (g)	124.89	143.22	124.30	
Moisture Content (%)	16.0	17.9	17.3	17.1
Dry Density (g/cm^3)	1.461	1.442	1.450	1.451

TEST CONDITION

Sample Number	A	B	C
Confining Pressure (kpa)	150	300	450
Proving Ring Constant	0.00199	0.00207	0.00816

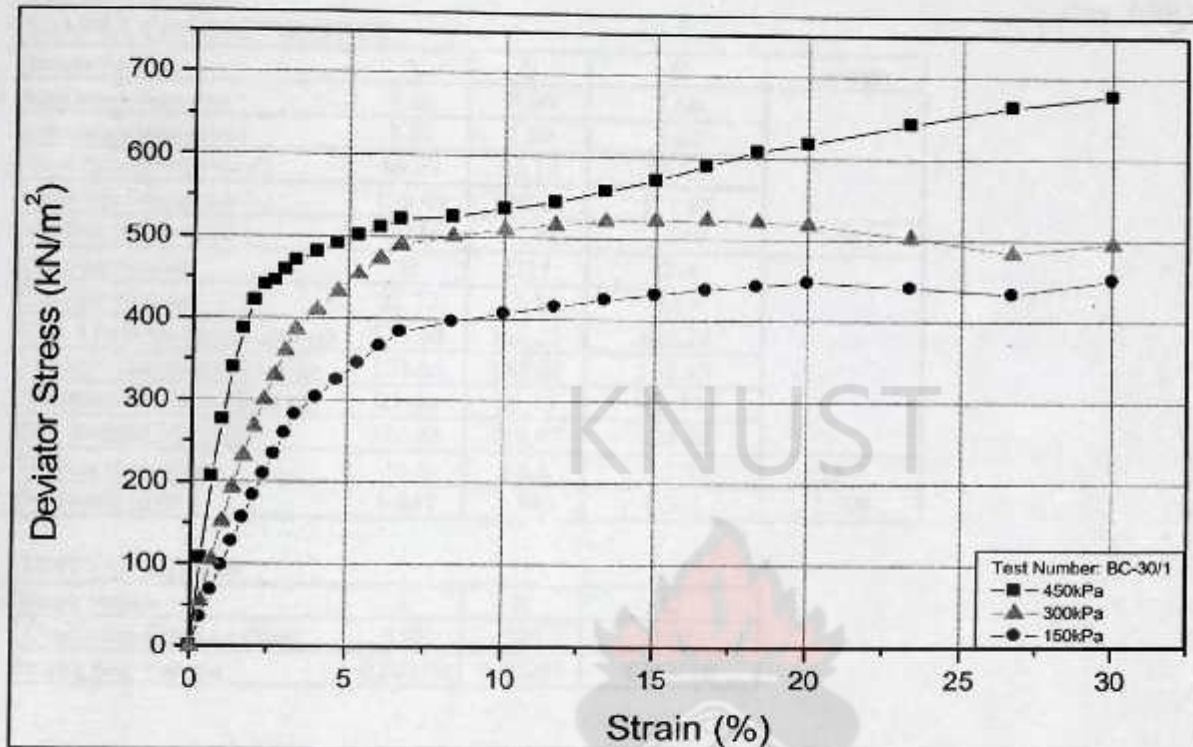
TEST RESULTS

			Sample Number A ($\sigma_3=150\text{kPa}$)		Sample Number B ($\sigma_3=300\text{kPa}$)		Sample Number C ($\sigma_3=450\text{kPa}$)	
Change in Length (mm)	Strain (%)	New area (mm^2)	Ring Reading (div)	Deviator Stress $q = \sigma_1 - \sigma_3$ (kPa)	Proving Ring Reading (div)	Deviator Stress $q = \sigma_1 - \sigma_3$ (kPa)	Proving Ring Reading (div)	Deviator Stress $q = \sigma_1 - \sigma_3$ (kPa)
0.00	0.00	1140.09	0.0	0	0.0	0	0.0	0
0.25	0.33	1143.91	20.0	35	30.0	54	15.0	107
0.51	0.67	1147.75	39.0	68	58.0	105	29.0	206
0.76	1.00	1151.61	57.0	98	84.0	151	39.0	276
1.02	1.33	1155.50	74.0	127	108.0	193	48.0	339
1.27	1.67	1159.42	91.0	156	130.0	232	55.0	387
1.52	2.00	1163.36	107.0	183	150.0	267	60.0	421
1.78	2.33	1167.33	123.0	210	169.0	300	63.0	440
2.03	2.67	1171.33	138.0	234	187.0	330	64.0	446
2.29	3.00	1175.36	153.0	259	204.0	359	66.0	458
2.54	3.33	1179.41	167.0	282	220.0	386	68.0	470
3.05	4.00	1187.60	181.0	303	235.0	410	70.0	481
3.56	4.67	1195.90	195.0	324	250.0	433	72.0	491
4.06	5.33	1204.33	209.0	345	264.0	454	74.0	501
4.57	6.00	1212.87	223.0	366	277.0	473	76.0	511
5.08	6.67	1221.53	236.0	384	289.0	490	78.0	521
6.35	8.33	1243.74	248.0	397	301.0	501	80.0	525
7.62	10.00	1266.77	259.0	407	312.0	510	83.0	535
8.89	11.67	1290.67	270.0	416	322.0	516	86.0	544
10.16	13.33	1315.49	281.0	425	331.0	521	90.0	558
11.43	15.00	1341.29	291.0	432	339.0	523	94.0	572
12.70	16.67	1368.11	301.0	438	346.0	524	99.0	590
13.97	18.33	1396.03	311.0	443	352.0	522	104.0	608
15.24	20.00	1425.12	321.0	448	357.0	519	108.0	618
17.78	23.33	1487.08	330.0	442	361.0	503	117.0	642
20.32	26.67	1554.67	339.0	434	364.0	485	126.5	664
22.85	30.00	1528.71	347.0	452	366.0	496	127.0	678

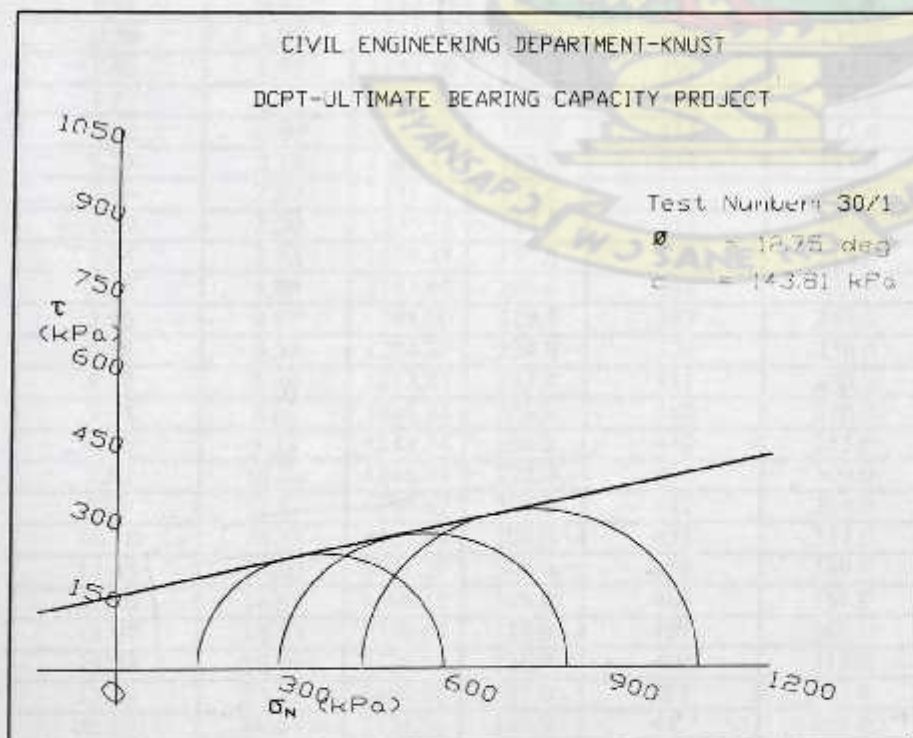
CIVIL ENGINEERING DEPARTMENT-KNUST
DCPT-ULTIMATE BEARING CAPACITY PROJECT
UNCONSOLIDATED-UNDRAINED TRIAXIAL TEST GRAPH

Test Number: BC-30/1

Date: 27/04/2007



σ_3 kPa	$\sigma_1 - \sigma_3$ kPa	σ_1 kPa
150	448	598
300	524	824
450	618	1068



CIVIL ENGINEERING DEPARTMENT-KNUST
DCPT-ULTIMATE BEARING CAPACITY PROJECT
UNCONSOLIDATED-UNDRAINED TRIAXIAL TEST ANALYSIS

Test No.: BC-35/1

Date :2/05/2007

SAMPLE CHARACTERISTICS

Sample Number	A	B	C	Averages
Initial Sample Height (cm)	7.60	7.60	7.60	
Initial Sample Diameter (cm)	3.80	3.80	3.80	
Initial Sample Volume(cm^3)	86.19	86.19	86.19	
Initial Wet Sample Mass (g)	150.49	150.66	151.61	
Wet Bulk Density (g/cm^3)	1.746	1.748	1.759	1.751
Container Number	B	D21	D14	
Container Mass (g)	22.72	15.59	9.67	
Cont. + Final Wet Sample Mass (g)	173.04	166.21	160.24	
Container + Dry Sample Mass (g)	151.60	145.06	138.13	
Moisture Content Mass (g)	21.44	21.15	22.11	
Dry Sample Mass (g)	128.88	129.47	128.46	
Moisture Content (%)	16.6	16.3	17.2	16.7
Dry Density (g/cm^3)	1.497	1.503	1.501	1.500

TEST CONDITION

Sample Number	A	B	C
Confining Pressure (kpa)	150	300	450
Proving Ring Constant	0.00199	0.00207	0.00816

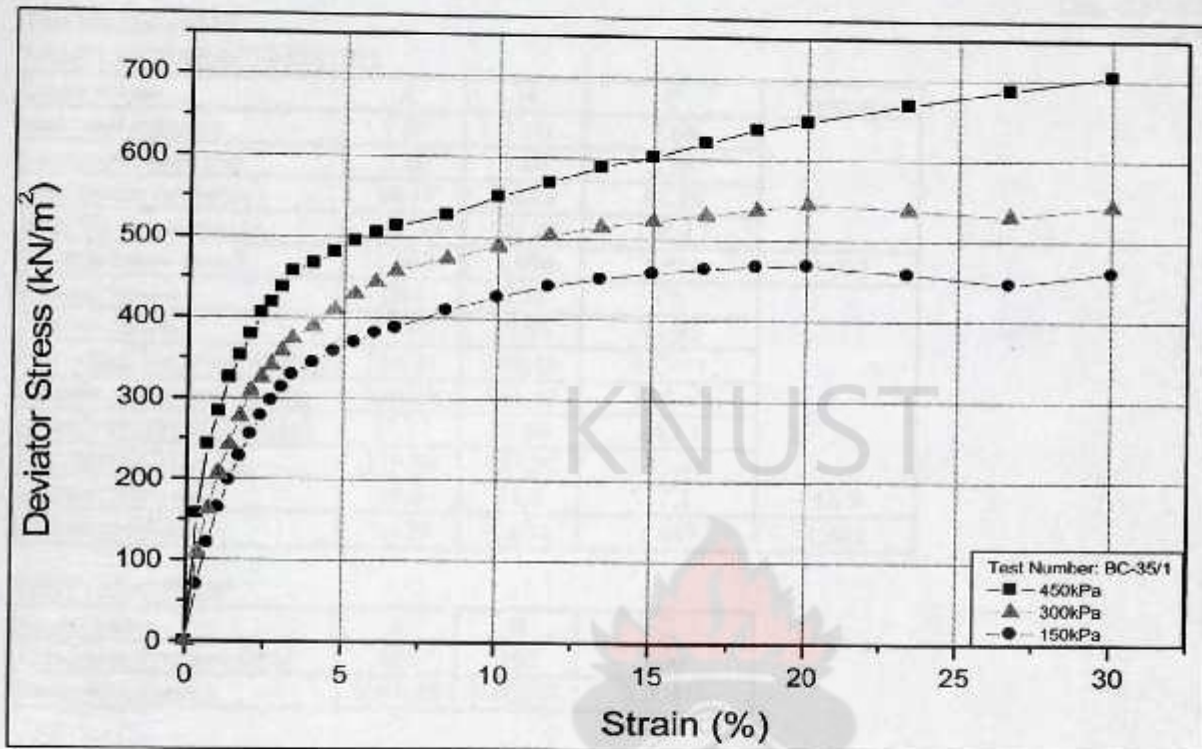
TEST RESULTS

			Sample Number A ($\sigma_3=150\text{kPa}$)		Sample Number B ($\sigma_3=300\text{kPa}$)		Sample Number C ($\sigma_3=450\text{kPa}$)	
Change in Length (mm)	Strain (%)	New area (mm^2)	Proving Ring Reading	Deviator Stress $q = \sigma_1 - \sigma_3$ (kPa)	Proving Ring Reading (div)	Deviator Stress $q = \sigma_1 - \sigma_3$ (kPa)	Proving Ring Reading (div)	Deviator Stress $q = \sigma_1 - \sigma_3$ (kPa)
0.00	0.00	1140.09	0.0	0	0.0	0	0.0	0
0.25	0.33	1143.91	40.0	70	60.0	109	22.0	157
0.51	0.67	1147.75	70.0	121	90.0	162	34.0	242
0.76	1.00	1151.61	95.0	164	115.0	207	40.0	283
1.02	1.33	1155.50	115.0	198	135.0	242	46.0	325
1.27	1.67	1159.42	133.0	228	155.0	277	50.0	352
1.52	2.00	1163.36	149.0	255	173.0	308	54.0	379
1.78	2.33	1167.33	163.0	278	183.0	325	58.0	405
2.03	2.67	1171.33	175.0	297	193.0	341	60.0	418
2.29	3.00	1175.36	185.0	313	203.0	358	63.0	437
2.54	3.33	1179.41	195.0	329	213.0	374	66.0	457
3.05	4.00	1187.60	205.0	344	223.0	389	68.0	467
3.56	4.67	1195.90	215.0	358	237.0	410	70.5	481
4.06	5.33	1204.33	224.0	370	250.0	430	73.0	495
4.57	6.00	1212.87	232.0	381	260.0	444	75.0	505
5.08	6.67	1221.53	238.0	388	270.0	458	77.0	514
6.35	8.33	1243.74	256.0	410	285.0	474	80.5	528
7.62	10.00	1266.77	272.0	427	300.0	490	85.5	551
8.89	11.67	1290.67	286.0	441	314.0	504	90.0	569
10.16	13.33	1315.49	298.0	451	327.0	515	95.0	589
11.43	15.00	1341.29	309.0	458	339.0	523	99.0	602
12.70	16.67	1368.11	319.0	464	351.0	531	104.0	620
13.97	18.33	1396.03	328.0	468	363.0	538	109.0	637
15.24	20.00	1425.12	336.0	469	375.0	545	113.0	647
17.78	23.33	1487.08	343.0	459	387.0	539	122.0	669
20.32	26.67	1554.67	349.0	447	399.0	531	131.0	688
22.85	30.00	1528.71	354.0	461	402.0	544	132.0	705

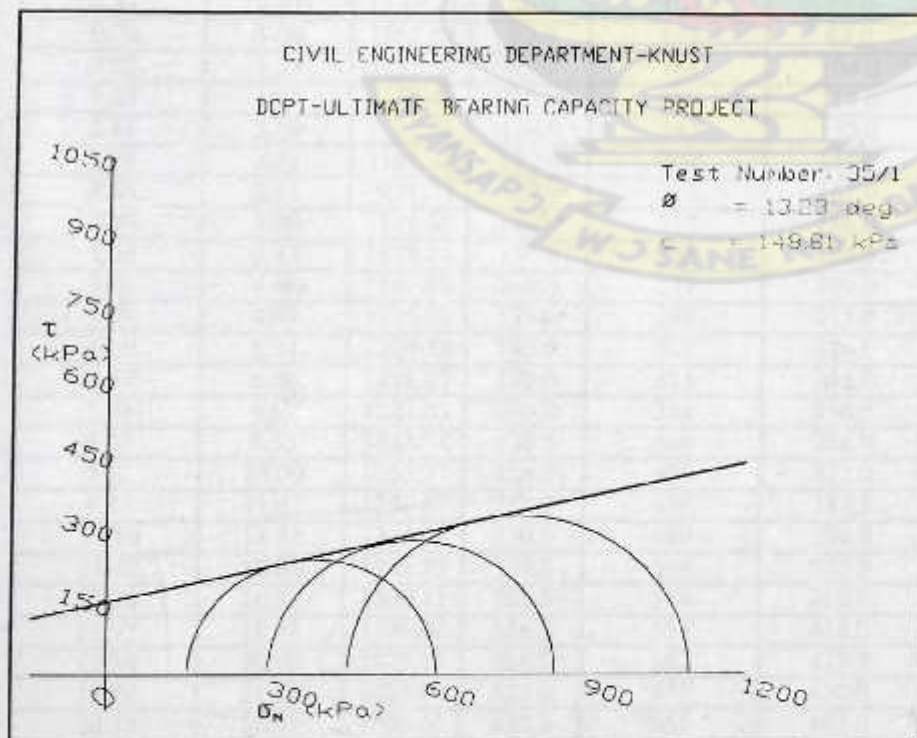
CIVIL ENGINEERING DEPARTMENT-KNUST
DCPT-ULTIMATE BEARING CAPACITY PROJECT
UNCONSOLIDATED-UNDRAINED TRIAXIAL TEST GRAPH

Test Number: BC-35/1

Date :2/05/2007



σ_3 kPa	$\sigma_1 - \sigma_3$ kPa	σ_1 kPa
150	469	619
300	545	845
450	647	1097



CIVIL ENGINEERING DEPARTMENT-KNUST
DCPT-ULTIMATE BEARING CAPACITY PROJECT
UNCONSOLIDATED-UNDRAINED TRIAXIAL TEST ANALYSIS

Date :28/05/2007

Test No.: BC-100/1

SAMPLE CHARACTERISTICS

Sample Number	A	B	C	Averages
Initial Sample Height (cm)	7.60	7.60	7.60	
Initial Sample Diameter (cm)	3.80	3.80	3.80	
Initial Sample Volume(cm^3)	86.19	86.19	86.19	
Initial Wet Sample Mass (g)	167.33	171.48	166.17	
Wet Bulk Density (g/cm^3)	1.941	1.990	1.928	1.953
Container Number	D11	X10	C9	
Container Mass (g)	17.90	17.58	17.92	
Cont. + Final Wet Sample Mass (g)	184.25	188.21	183.54	
Container + Dry Sample Mass (g)	156.98	161.15	159.40	
Moisture Content Mass (g)	27.27	27.06	24.14	
Dry Sample Mass (g)	139.08	143.57	141.48	
Moisture Content (%)	19.6	18.8	17.1	18.5
Dry Density (g/cm^3)	1.623	1.674	1.647	1.648

TEST CONDITION

Sample Number	A	B	C
Confining Pressure (kpa)	100	250	400
Proving Ring Constant	0.00199	0.00207	0.00816

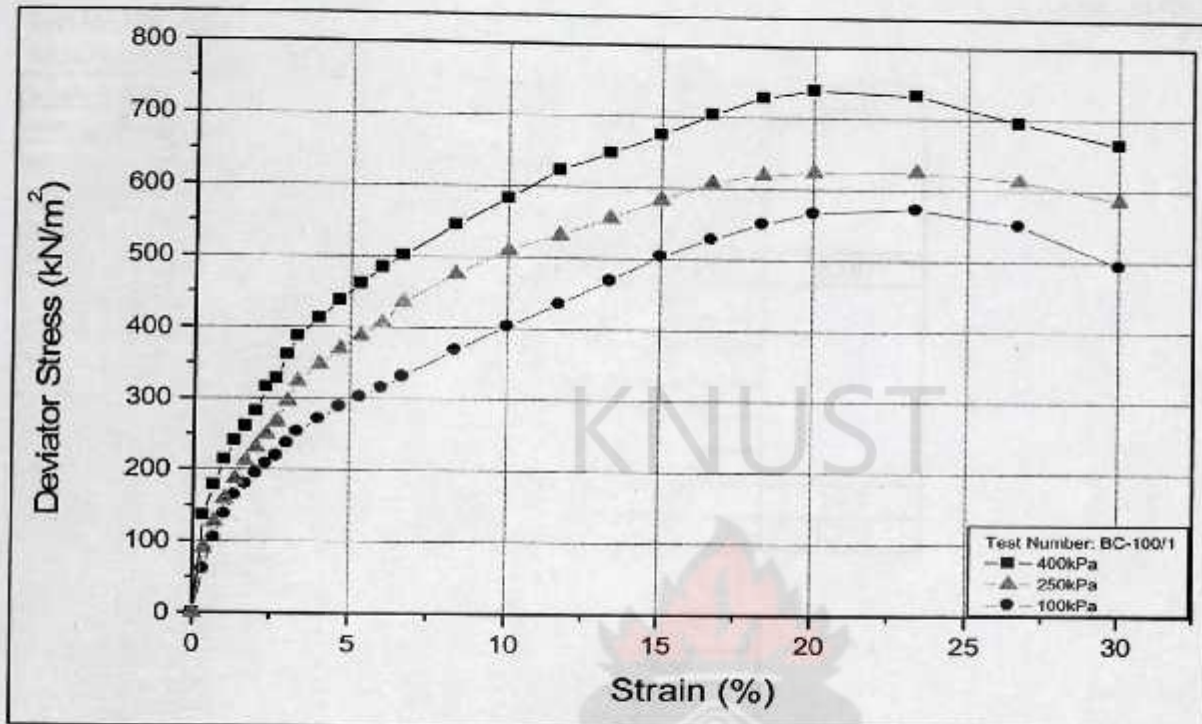
TEST RESULTS

			Sample Number A ($\sigma_3=100\text{kPa}$)		Sample Number B ($\sigma_3=250\text{kPa}$)		Sample Number C ($\sigma_3=400\text{kPa}$)	
Change in Length (mm)	Strain (%)	New area (mm^2)	Proving Ring Reading	Deviator Stress $q = \sigma_1 - \sigma_3$ (kPa)	Proving Ring Reading (div)	Deviator Stress $q = \sigma_1 - \sigma_3$ (kPa)	Proving Ring Reading (div)	Deviator Stress $q = \sigma_1 - \sigma_3$ (kPa)
0.00	0.00	1140.09	0.0	0	0.0	0	0.0	0
0.25	0.33	1143.91	35.0	61	50.0	90	19.0	136
0.51	0.67	1147.75	60.0	104	70.0	126	25.0	178
0.76	1.00	1151.61	80.0	138	88.0	158	30.0	213
1.02	1.33	1155.50	95.0	164	104.0	186	34.0	240
1.27	1.67	1159.42	105.0	180	118.0	211	37.0	260
1.52	2.00	1163.36	114.0	195	130.0	231	40.0	281
1.78	2.33	1167.33	122.0	208	141.0	250	45.0	315
2.03	2.67	1171.33	129.0	219	151.0	267	47.0	327
2.29	3.00	1175.36	140.0	237	168.0	296	52.0	361
2.54	3.33	1179.41	150.0	253	184.0	323	56.0	387
3.05	4.00	1187.60	162.0	271	199.0	347	60.0	412
3.56	4.67	1195.90	173.0	288	213.0	369	64.0	437
4.06	5.33	1204.33	183.0	302	226.0	388	68.0	461
4.57	6.00	1212.87	192.0	315	238.0	406	72.0	484
5.08	6.67	1221.53	203.0	331	256.5	435	75.0	501
6.35	8.33	1243.74	230.5	369	286.0	476	83.0	545
7.62	10.00	1266.77	256.5	403	312.0	510	90.5	583
8.89	11.67	1290.67	282.0	435	331.5	532	98.5	623
10.16	13.33	1315.49	310.0	469	354.0	557	104.5	648
11.43	15.00	1341.29	339.5	504	377.5	583	111.0	675
12.70	16.67	1368.11	363.5	529	402.0	608	118.0	704
13.97	18.33	1396.03	386.5	551	418.0	620	124.5	728
15.24	20.00	1425.12	406.0	567	429.5	624	129.0	739
17.78	23.33	1487.08	428.0	573	450.0	626	133.5	733
20.32	26.67	1554.67	430.5	551	461.0	614	132.5	695
22.85	30.00	1528.71	379.5	494	432.5	586	124.5	665

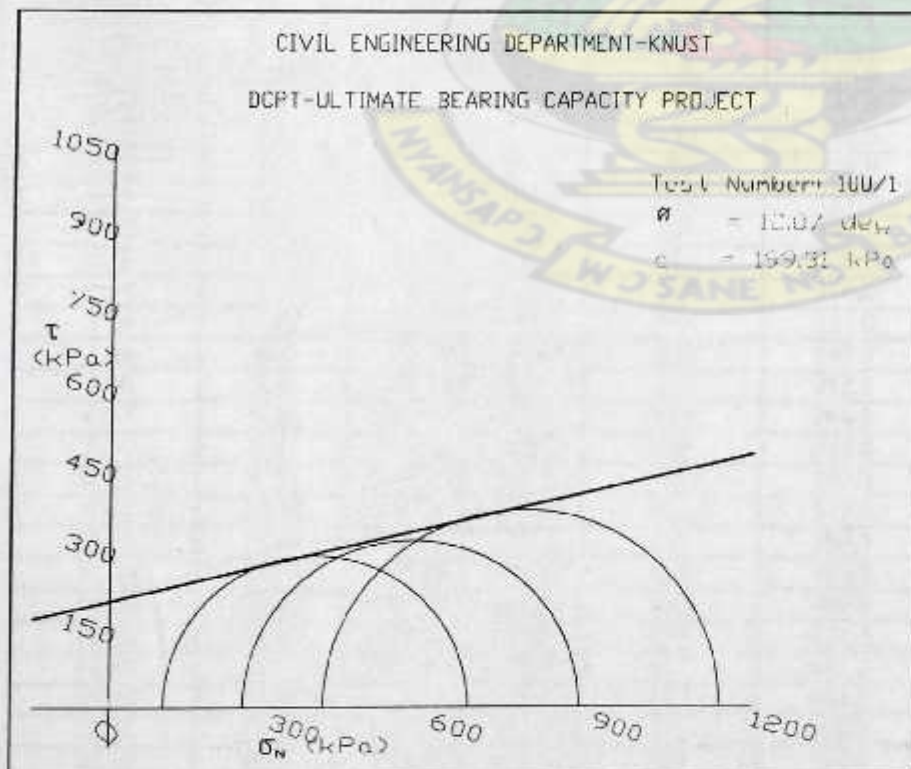
CIVIL ENGINEERING DEPARTMENT-KNUST
DCPT-ULTIMATE BEARING CAPACITY PROJECT
UNCONSOLIDATED-UNDRAINED TRIAXIAL TEST GRAPH

Test Number: BC-100/1

Date :28/05/2007



σ_3 kPa	$\sigma_1 - \sigma_3$ kPa	σ_1 kPa
100	567	667
250	624	874
400	739	1139



CIVIL ENGINEERING DEPARTMENT-KNUST
DCPT-ULTIMATE BEARING CAPACITY PROJECT
UNCONSOLIDATED-UNDRAINED TRIAXIAL TEST ANALYSIS

Test No.: BC-150/1

Date :31/05/2007

SAMPLE CHARACTERISTICS

Sample Number	A	B	C	Averages
Initial Sample Height (cm)	7.60	7.60	7.60	
Initial Sample Diameter (cm)	3.80	3.80	3.80	
Initial Sample Volume(cm^3)	86.19	86.19	86.19	
Initial Wet Sample Mass (g)	181.28	181.46	182.00	
Wet Bulk Density (g/cm^3)	2.103	2.105	2.112	2.107
Container Number	D8	D6	X7	
Container Mass (g)	18.02	18.60	18.14	
Cont. + Final Wet Sample Mass (g)	197.62	196.32	198.11	
Container + Dry Sample Mass (g)	169.67	168.07	169.80	
Moisture Content Mass (g)	27.95	28.25	28.31	
Dry Sample Mass (g)	151.65	149.47	151.66	
Moisture Content (%)	18.4	18.9	18.7	18.7
Dry Density (g/cm^3)	1.776	1.771	1.779	1.775

TEST CONDITION

Sample Number	A	B	C
Confining Pressure (kpa)	100	250	400
Proving Ring Constant	0.00199	0.00207	0.00816

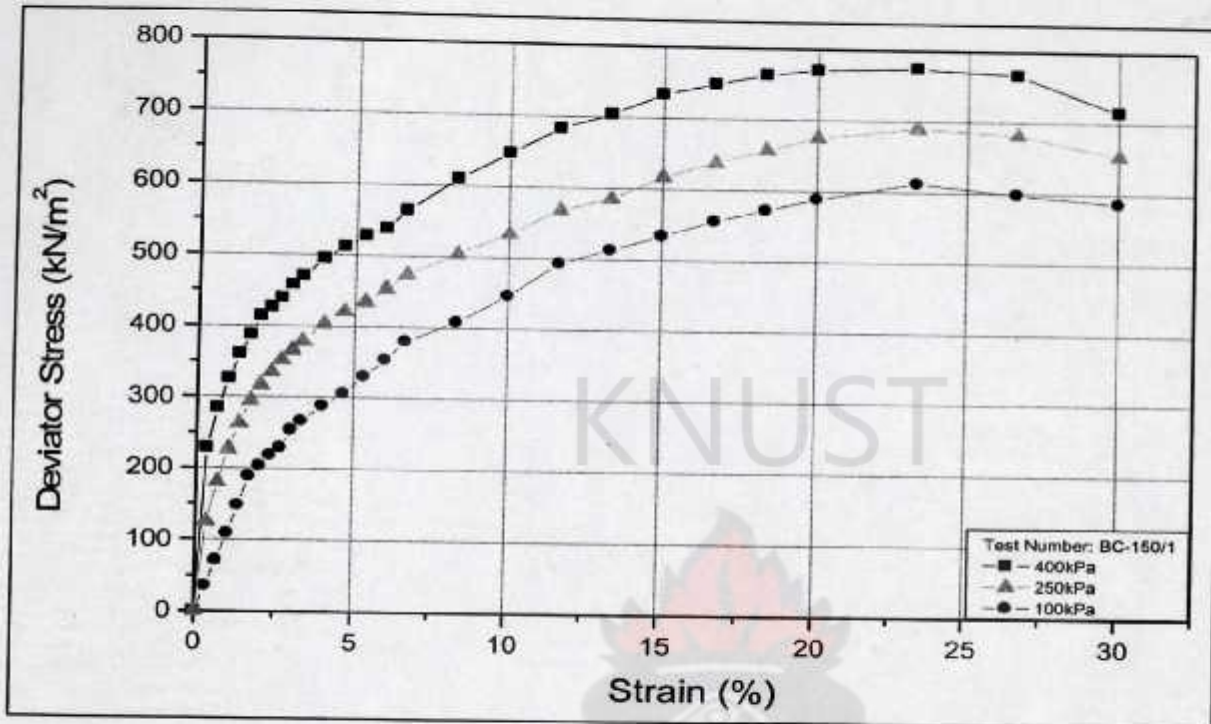
TEST RESULTS

			Sample Number A ($\sigma_3=100\text{kPa}$)		Sample Number B ($\sigma_3=250\text{kPa}$)		Sample Number C ($\sigma_3=400\text{kPa}$)	
Change in Length (mm)	Strain (%)	New area (mm^2)	Proving Ring Reading	Deviator Stress $q = \sigma_1 - \sigma_3$ (kPa)	Proving Ring Reading (div)	Deviator Stress $q = \sigma_1 - \sigma_3$ (kPa)	Proving Ring Reading (div)	Deviator Stress $q = \sigma_1 - \sigma_3$ (kPa)
0.00	0.00	1140.09	0.0	0	0.0	0	0.0	0
0.25	0.33	1143.91	20.0	35	69.0	125	32.0	228
0.51	0.67	1147.75	41.0	71	100.0	180	40.0	284
0.76	1.00	1151.61	63.0	109	126.0	226	46.0	326
1.02	1.33	1155.50	86.0	148	147.0	263	51.0	360
1.27	1.67	1159.42	110.0	189	165.0	295	55.0	387
1.52	2.00	1163.36	118.5	203	178.0	317	59.0	414
1.78	2.33	1167.33	128.0	218	189.0	335	61.0	426
2.03	2.67	1171.33	135.0	229	199.0	352	63.0	439
2.29	3.00	1175.36	150.0	254	208.0	366	66.0	458
2.54	3.33	1179.41	158.0	267	216.0	379	68.0	470
3.05	4.00	1187.60	172.0	288	231.0	403	72.0	495
3.56	4.67	1195.90	184.0	306	243.0	421	75.0	512
4.06	5.33	1204.33	200.0	330	253.0	435	78.0	528
4.57	6.00	1212.87	216.0	354	266.0	454	80.0	538
5.08	6.67	1221.53	233.0	380	280.0	474	84.5	564
6.35	8.33	1243.74	255.0	408	303.0	504	93.0	610
7.62	10.00	1266.77	284.0	446	327.0	534	100.5	647
8.89	11.67	1290.67	320.0	493	354.0	568	108.0	683
10.16	13.33	1315.49	339.0	513	372.0	585	113.5	704
11.43	15.00	1341.29	360.0	534	400.0	617	120.5	733
12.70	16.67	1368.11	382.0	556	421.5	638	125.5	749
13.97	18.33	1396.03	401.0	572	443.0	657	130.5	763
15.24	20.00	1425.12	422.0	589	464.5	675	134.5	770
17.78	23.33	1487.08	457.0	612	496.0	690	141.0	774
20.32	26.67	1554.67	467.0	598	512.0	682	146.0	766
22.85	30.00	1528.71	450.0	586	482.0	653	134.0	715

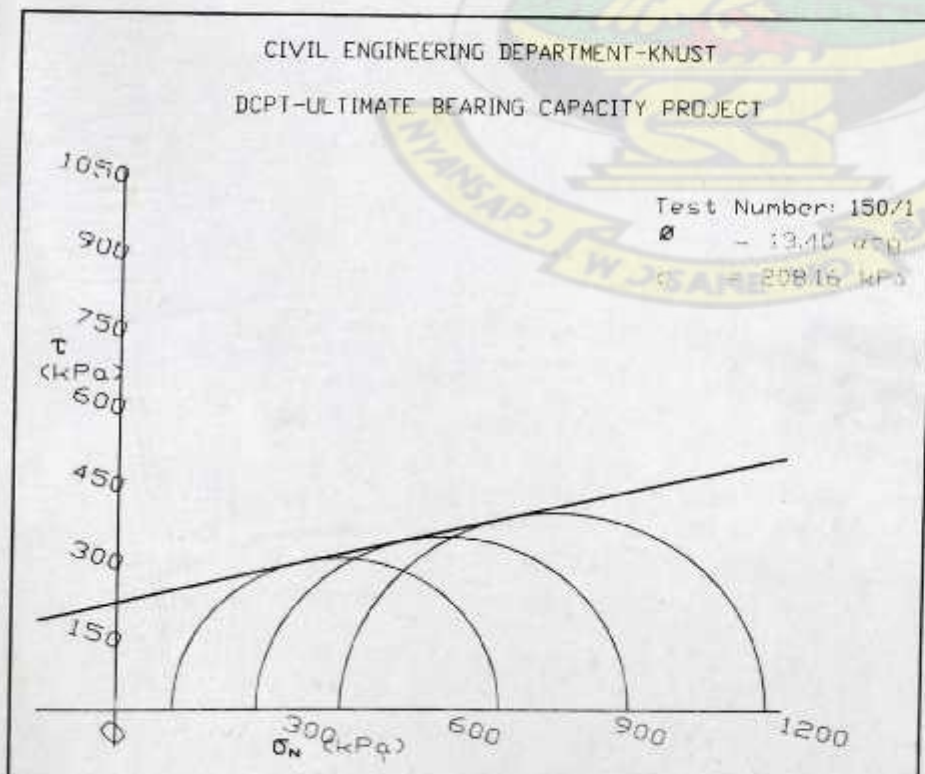
CIVIL ENGINEERING DEPARTMENT-KNUST
DCPT-ULTIMATE BEARING CAPACITY PROJECT
UNCONSOLIDATED-UNDRAINED TRIAXIAL TEST GRAPH

Test Number: BC-150/1

Date :31/05/2007



σ_3 kPa	$\sigma_1 - \sigma_3$ kPa	σ_1 kPa
100	589	689
250	675	925
400	770	1170



KNUST

